Deformation-Induced Crystallization In Rubber-Like Materials

Vom Fachbereich Mechanik der
Technischen Universität Darmstadt
zur Erlangung des akademischen Grades eines
DOKTORS DER INGENIEURWISSENSCHAFTEN
genehmigte
DISSERTATION

von

Chem. Eng. Motasem Saidan

aus Jordanien

Referent: Prof. Dr. T. Alts
Korreferent: Prof. K. Hutter, Ph. D./ Cornell University

Tag der Einreichung: 1. Dez. 2004
Tag der mündlichen Prüfung: 21. Jan. 2005

Darmstadt 2005
D 17

To my beloved brother, Khaled,
who passed away on 18th Apr 2003.
God bless you my brother,
you are always in my heart, Khaled.

Acknowledgment

Most of all, I would like to express my thanks to God, in him alone I put my trust. His mercy and blessing saved, guided and enabled me to run towards my ambitions. Also, I would like to express my sincere gratitude and heartfelt appreciations to my doctor-father, Prof. Thorsten Alts, for his guidance, encouragement, and support during my graduate studies. His impressive knowledge, technical skill, and creative thinking have been an invaluable help throughout the course of this work. The expertise that he shared me will remain a tremendous source of professional growth to me. I am really sure that I can not be here without him.

I am profoundly grateful to Prof. K. Hutter. His insight, kindness, and genuine concern for his students made staying in his group a memorable experience. I also wish to thank my committee members, Prof. Dr.-Ing. Ch. Tsakmakis, Prof. (jun.) Dr.-Ing. R. Müller, and Prof. Dr. M. Wilhelm, for their time, counsel, and valuable contributions to this work.

I owe much gratitude to DFG (German research foundation) for providing the financial support throughout my study.

I wish to thank Dr. Eisele, *Bayer AG, Leverkusen* for the polyisoprene rubber samples that he has provided for this work. Also, I would like to express my sincere thanks to Prof. Dr. Rolf Hosemann, *Bundesanstalt für Materialprüfung BAM-Berlin* for performing the tensile loading-unloading experiments for polyisoprene rubber samples and providing us with the Wide Angle X-ray Diffraction (WAXD) data.

We are indebted to *Rieter* Automative Germany GmbH for providing us with Ethylene-butene copolymers materials. Finally, I would like to express my gratitude to the German Polymer Institute *DKI*-Darmstadt. Especially, Dr. -Ing. M. Moneke, PD Dr. G. P. Hellmann, Dr. Reza Ghahary, and Reinhold Damko for their highly appreciated cooperation and help including the preparations of samples and running the tensile loading-unloading tests of ethylene-butene copolymers.

I would like to acknowledge mechanic AG3 staff for providing an enjoyable educational atmosphere. Getting international friends in our group and professional discussion with them made my work more valuable. Especially, I would like to thank Dr. habil. Yongqi Wang, Dr. Shiva Prasad Pudasaini, and Dr. Bernd Müge for their appreciated help with LINUX system and LaTex software. I wish

to thank Mahmoud Reza Maneshkarimi, M. Eng., Dr. Luca Placcidi, Dr. habil. Ralf Greve, Dipl.-Phys. Angelika Humbert, Dr. Sergio Faria, Chung Fang, M. Sc., Min-Ching Chiou, M. Sc., Dr. Ana Ursescu, for their endless friendship. I will never forget their supportive encouragement and sympathies when my brother passed away last year. I have more friends whom I wish to thank: Dr. Hazim Rahahleh, Dr.-Ing. Muhanned Hararah, Dr.-Ing. Muhanned Marashdeh, Dr.-Ing. Imad Mosallam.

Foremost, my parents, sisters, and brothers have always encouraged me to follow my dreams and believed in me, I dedicate this work to them. I wish to thank them who always provided me with invaluable guidance and without their support my dream of PhD degree would not have come true and my academic endeavors would not have been fulfilling. This dissertation is their accomplishment as much as it is mine.

Contents

List of Figures

List of Tables

Zusammenfassung

Deformations-induzierte Kristallisation ist entscheidend für die Vorherbestimmung der endgültigen mechanischen Eigenschaften von Elastomeren und Gummi. Elastomere Netzwerke zeigen einen steilen Anstieg in der Spannungs-Dehnungs Kurve mit bedeutenden Hysteresis-Effekten, beides wird dem Phänomen der deformations-induzierten Kristallisation zugeordnet.

Die Thermodynamik von gummi-ähnlichen Polymeren ist untersucht worden; und uni-axiale Dehnungen mit einigen Approximationen werden diskutiert, um einen Überblick über die vorgeschlagene thermodynamische Materialtheorie zu erhalten.

Ein thermodynamisch statistisches Modell wird vorgeschlagen zum Studium des Spannungs-Dehnungs Verhaltens von elastomeren Netzwerken und die Abhängigkeit der Spannungskoeffizienten vom Kristallisationsgrad wird berechnet. Dies beruht auf einer modifizierten Verteilungsfunktion von Kettensegmenten für Ketten von endlicher Länge.

Die Berechnung der Kristallisation basiert auf Gleichungen aus der Thermodynamik der irreversible Prozesse; hierbei werden Deformationsgeschwindigkeit und Temperatur berücksichtigt.

Mooney Darstellungen der Spannungs-Dehnungs Kurven werden eingeführt, um die starke Abhängigkeit der Spannungskoeffizenten vom Kristallisationsgrad zu zeigen.

Uni-axiale Belastungsprozesse mit anschliessender Entlastung werden untersucht für mehrere Deformationsgeschwindigkeiten und Temperaturen, um die Effekte der molekularen Orientierung und der dehnungs-induzierten Kristallisation zu zeigen in Polyisopren Gummi und in Ethylen-Butan Kopolymeren (thermoplastische Elastomere, TPE). Der Einfluss des Relaxationsprozesses und der Deformationsgeschwindigkeit auf die Kristallisation wird illustriert.

Die Hysteresis der Spannungs-Dehnungs Relation und das inelastische Deformationsverhalten wird der dehnungs-induzierten Kristallisation und ihrer Umwandlung zugeordnet; dies wird insbesondere evident für grosse Deformationsgeschwindigkeiten und tiefe Temperaturen (d.h. oberhalb der Glasübergangstemperatur).

Die Modell-Ergebnisse zeigen gute Übereinstimmung mit Experimenten, die in dieser Studie durchgeführt worden sind.

Abstract

Deformation induced crystallization is crucial for determining the final mechanical properties of elastomers-rubber. Elastomeric networks show high upturn in the stress-strain curves with a significant hysteresis, this is attributed to the deformation induced crystallization phenomenon.

Thermodynamics of rubber-like high polymers have been studied, and uniaxial extension with some approximations is discussed to obtain an overview of the proposed thermodynamic constitutive theory.

A thermodynamical statistical model is presented for studying the stress-strain behaviour of elastomeric networks, and the dependence of the stress coefficients on the degree of crystallinity. This is based on the modified distribution of chains of finite length.

A crystallization formulation based on irreversible thermodynamics is adopted to describe the crystallization taking into account the effects of strain rate and temperature.

Mooney representation curves are introduced in this study to show the strong dependence of stress coefficients on the degree of crystallinity.

Both uniaxial loading and unloading are investigated for a range of strain rates and temperatures, to explain the effect of molecular orientation and strain induced crystallization in polyisoprene rubber and ethylene-butene copolymers (thermoplastic elastomers). The effect of relaxation process, and the rate of deformation on crystallization has been illustrated.

The hysteresis of the stress-strain relation and inelastic deformation behaviour is attributed to the deformation induced crystallites and their transformation; this is clearly shown at high strain rates and low temperatures (i.e. above the glass transition temperature).

The model results show good agreement with experimental data that have been determined in this study.

Chapter 1

Introduction

1.1 Introduction

Of all the materials known to man, no material can match the remarkable behaviour of rubber and rubberlike materials (i.e. thermoplastic elastomers). They are capable of sustaining large deformations without rupture; a maximum extension of five to ten times the undeformed lengths is a common property of them. When a rubber-elastomeric material is stretched, it achieves its highest modulus of elasticity at maximum deformations. It possesses the capacity to recover spontaneously its original dimensions, with little appreciable fraction of pseudo-plastic residual deformation.

A wide spectrum of polymeric materials have been developed to replace the naturally occuring materials. Therefore, thermoplastic elastomers (TPEs) are widely used, due to the ease of processing; they behave like a cross-linked rubber under ambient conditions. TPEs differ from cross-linked rubber inso far as the cross-links are not covalent bonds but physical links, e.g. consisting of crystallized chain segments. These can be molten by heating, thus allowing thermoplastic processing.

Elastomeric polymers are commonly used in everyday life. In order to successfully manipulate their applicability, it is indispensable to completely understand the relationship between the structure and the properties of the polymer. The mechanical behaviour is closely related to the morphology and consequently depends on the thermal and deformation histories experienced by the polymer during the process.

A number of polymers including natural and synthetic rubbers and thermoplastic elastomers have the tendency to crystallize both mechanically and ther-

mally. In many applications, the formation of highly oriented or extended crystals has a beneficial impact on the mechanical behaviour of the polymer. This can be noticed in film blowing, injection molding and, drastically, in fiber spinning as shown in figure.

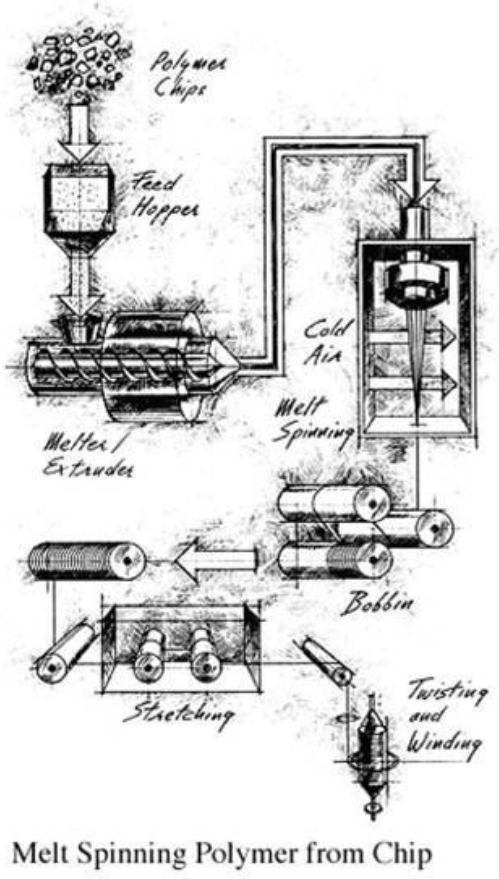

Figure 1.1: Schematic of fiber spinning process (This picture is from the website: www.fibersource.com/f-tutor/techpag.htm).

In fibers, the formation of the extended crystalline phase in the direction of extension greatly reinforces and increases the strength of the fiber.

The phenomenon of orientation in polymers is shown by the larvae of silk moth, and by spiders. The former weave their heads about inside of cocoon, so that as they spin their silk, it is pulled and oriented. The latter, by suddenly dropping on their drag line, produce a highly oriented and very strong fiber.

Recent fields of research on elastomeric networks have focused on mechanical properties under deformation. It has been frequently observed that some networks show rapid upturn in stress-strain isotherm. Many considerable views

have been proposed to interprete the cause of the upturn. It was interpreted mainly as a result of limited chain extensibility as being due to approximation inherent in the Gaussian theory. The other considerable view of this behaviour is attributed to deformation-induced-crystallization.

It is therefore indispensable to provide a qualitative understanding of the behaviour of the elastomeric network, and to completely predict the crystallization from macroscopic deformation during drawing.

1.2 Objectives and Justification

The foregoing discussion of polymer crystallization morphology, with its emphasis on the importance of deformation-induced crystallization would not be complete without a brief mention of the statistical approach to predict crystallization of elastomeric networks. According to this approach, a polymer is treated as a network of freely-jointed chains crosslinked at junction points, whose motions are affine to the macroscopic deformation.

Stress-strain dependence of crosslinked networks was first described by the classical Gaussian rubber elasticity theory in the pioneering work of Kuhn [41],[42]. A thermodynamic theory of strain-induced crystallization was first developed by Flory [21]. Both theories do not describe the real behaviour of physically or chemically crosslinked networks.

The goals of the present study may be summarized as follows:

(1) Gain a better understanding of the mechanism of deformation-induced-crystalization.

(2) Develop a model to simulate crystallization taking place at different strain rates and temperatures for uniaxial loading-unloading processes of elastomeric network chains.

(3) Modify the Gaussian distribution for chains of finite lengths to describe the end-to-end vector distribution function and the contribution of chain to crystallinity.

(4) Based on the results of the above mentioned objectives, to propose a statistical model for stress-strain-crystallinity prediction.

(5) Perform tensile experiments for both amorphous and semi-crystalline elastomeric network chains, to validate the modeled results of the 4 above points.

1.3 Summary of Contents

The dissertation is organized in the following way.

Chapter 2 deals with thermodynamics of rubber-like high polymers. An overview of the thermodynamic constitutive theory is obtained by discussing uniaxial extension at certain constant conditions (mainly temperature and external pressure). Approximations and internal constraints have been employed to simplify the theory [8].

In chapter 3, a review of the fundamental aspects of polymer crystallization is given, including various explanations of rubber as well as thermoplastic copolymer crystallization. The main section of this chapter is to develop the mathematical model and to simulate stress-induced crystallization taking place at different parameters. This model is given according to irreversible thermodynamics. It is capable to calculate the degree of crystallinity for both the uniaxial stretching loading and retraction unloading processes for a range of strain rates and temperatures. In this model, hysteresis loops and inelastic deformation behaviour (pseudo-plastic residual strain) is discussed in detail.

In chapter 4, a modified Gaussian distribution, based on affine deformation, is employed for chains of finite lengths to describe the end-to-end vector distribution function and the contribution of that chain to crystallinity. Stress-strain-crystallinity relations are then derived from conformational entropy. This is done in the context of statistical thermodynamics.

Chapter 5 is a discussion of the model results as well as experimental results. The experimental results of uniaxial loading-unloading extension are fully discussed and compared with those predicted for validation. The different polymeric elastomers (i.e. with different values of reference degree of crystallinity) that have been used in these experiments were obtained from Rieter Automotive system company-Gundernhausen. The experimental part has been performed in the laboratories of the German Polymer Institute-Darmstadt. Observed hysteresis loops and residual strain (pseudo-plastic effect) have been investigated for rubber and thermoplastic elastomer experiments at different ranges of the deformation ratios, temperatures, and strain rates. Model parameters and fittings are discussed in this section as well.

Chapter 6 gives the general conclusions and recommendations for potential future work.

Chapter 2

Thermodynamics of Rubber-Like High Polymers

2.1 Thermodynamic Constitutive Theory

The goal of thermodynamics of rubber-like high polymers is the determination of the fields of density $\rho(\mathbf{x},t)$, of the motion $x_i = \chi_i(X_\alpha,t)$, of the temperature $T(\mathbf{x},t)$ and the degree of crystallisation $\xi(\mathbf{x},t)$. Thus, the equations for the determination are the balance equations for mass, linear momentum, moment of momentum, internal energy and degree of crystallinity:

$$\begin{aligned} \dot{\rho} &= -\rho v_{i,i}\,, \qquad \rho\dot{v}_i = t_{ij,j}\,, \\ t_{ij} &= t_{ji}\,, \qquad \rho\dot{u} = -q_{j,j} + t_{ij}v_{i,j}\,, \\ \rho\dot{\xi} &= -\psi_{j,j} + A\,, \end{aligned} \tag{2.1}$$

where $v_i,\ t_{ij},\ q_j,\ \psi_j$ are components of the velocity $\mathbf{v}$, the Cauchy-stress $\mathbf{t}$, the heat flux $\mathbf{q}$ and the flux of crystallinity $\boldsymbol{\psi}$ (through a material surface, moving with material velocity $\mathbf{v}$) with respect to a Cartesian co-ordinate system (observer-system), which is rigidly connected to an inertial system. u denotes the specific internal energy and A has the meaning of a transformation rate (per unit volume and time) of chain segments from the amorphous into the crystalline state. The gravitation is neglected. The symbols $_{,i}$ and $\dot{}$ denote partial derivatives with respect to spatial co-ordinates and the material time derivative, respectively. Hence, for a function $f(\mathbf{x},t)$

$$f_{,i} := \frac{\partial f}{\partial x_i}\,, \qquad \dot{f} := \frac{\partial f}{\partial t} + v_l\frac{\partial f}{\partial x_l}\,. \tag{2.2}$$

According to Einstein's summation convention, doubly repeated co-ordinate indices denote summation from 1 to 3. The symmetry of the stress tensor $\mathbf{t}$ is

a consequence of conservation of moment of momentum in non-polar materials. The velocity v_i and the deformation gradient $F_{i\alpha}$ are obtained by partial derivatives of the material motion $\chi_i(X_\alpha, t)$:

$$v_i := \frac{\partial \chi_i(X_\alpha, t)}{\partial t}\,, \qquad F_{i\alpha} := \frac{\partial \chi_i(X_\alpha, t)}{\partial X_\alpha}\,. \tag{2.3}$$

X_α denotes the co-ordinates of a material element in some reference configuration, which we want to identify with some undeformed equilibrium state of the material with fixed values $T = T_R$ of temperature, $p = p_R$ of pressure and $\xi = \bar{\xi_R}$ of degree of crystallinity. In this reference state $F_{i\alpha_{|_R}} = \delta_{i\alpha}$, the unit tensor.

We now assume, that the material does not fracture during deformation. Then, due to $det\ \mathbf{F} > 0$, the inverse deformation $X_\alpha = \bar{X}_\alpha(x_i, t)$ exists. Consequently the inverse deformation gradient

$$(\mathbf{F}^{-1})_{\alpha i} := \frac{\partial \bar{X}_\alpha(x_i, t)}{\partial x_i} \tag{2.4}$$

is well defined. It holds

$$(\mathbf{F}^{-1})_{\alpha i} F_{i\beta} = \delta_{\alpha\beta}\,, \qquad F_{i\alpha}(\mathbf{F}^{-1})_{\alpha j} = \delta_{ij}\,, \tag{2.5}$$

where $\delta_{\alpha\beta}$ and δ_{ij} are Cartesian components of the unit tensor [71].

The mass balance $(2.1)_1$ can be integrated using (2.3), the result being

$$det\ \mathbf{F} = \frac{\rho_{_R}}{\rho} = \frac{v}{v_{_R}}\,, \tag{2.6}$$

where $v = 1/\rho$ is the specific volume, and $\rho_{_R}$, and $v_R = 1/\rho_{_R}$,respectively, are the density and the specific volume in the reference state.

With (2.6) one can introduce a new deformation measure

$$G_{i\alpha} := (\frac{v}{v_{_R}})^{-1/3} F_{i\alpha}\,, \qquad det\,\mathbf{G} = 1\,. \tag{2.7}$$

This measure has the special property, that it does not contain volume changes. Pure volume changes and isochoric deformations can be treated separately.

The decomposition (2.7) is rather important for the treatment of rubber-like high polymers, since the total deformation can be separated into inelastic and elastic contributions. The inelastic deformation -thermal volume expansion and a change of the volume by a change of the internal structure- is contained in the volume change $(\frac{v}{v_{_R}})$, while the elastic deformation is described by $G_{i\alpha}$. The last one is isochoric by definition. With this all deformations which are due to volume

changes are explicity separated. This is of crucial importance for the constitutive theory of rubber-like high polymers.

To come to the main goal of thermodynamics - which means to transform the balance equations to a set of field equations for the determination of the fields $\rho(\mathbf{x},t)$, $x_i = \chi_i(X_\alpha,t)$, $T(\mathbf{x},t)$, and $\xi(\mathbf{x},t)$- the fields of stress $t_{ij}(\mathbf{x},t)$, heat flux $q_i(\mathbf{x},t)$, internal energy $u(\mathbf{x},t)$, crystallization flux $\psi_i(\mathbf{x},t)$ and crystallization rate $A(\mathbf{x},t)$ must be related in a materially dependent manner to the independent fields ρ, χ_i, T, ξ. Such relations are called constitutive equations.

For rubber-like high polymers we make the following assumptions:

$$\begin{aligned} t_{ij}(\mathbf{x},t) &= \mathtt{t}_{ij}(v,T,\xi,G_{i\alpha},T_{,i})\,, \\ q_i(\mathbf{x},t) &= \mathtt{q}_i(v,T,\xi,G_{i\alpha},T_{,i})\,, \\ \psi_i(\mathbf{x},t) &= 0\,, \\ u(\mathbf{x},t) &= \mathtt{u}(v,T,\xi,G_{i\alpha},T_{,i})\,, \\ A(\mathbf{x},t) &= \mathtt{A}(v,T,\xi,G_{i\alpha},T_{,i})\,. \end{aligned} \tag{2.8}$$

Herein the hypothesis of equipresence has been applied, according to which it is assumed that a variable which appears in one constitutive equation can appear in all of them. In this way one avoids prejudices in the formulation of constitutive equations.

The constitutive equation $(2.8)_3$ about the flux of crystallization means, that the crystallites move with material velocity and do not diffuse against this velocity. This relates to the microscopic view, that crystallites inside their amorphous surroundings are just transformed during deformation, but cannot move relative to their amorphous surroundings.

We now introduce by the definition

$$p := -\frac{1}{3}t_{ll} = p(v,T,\xi,G_{i\alpha},T_{,i})\,, \tag{2.9}$$

an internal pressure $p(\mathbf{x},t)$. Since rubber-like high polymers are compressible, $\partial p/\partial v \neq 0$, the constitutive equation (2.9) can be inverted with respect to the specific volume

$$v(\mathbf{x},t) = \hat{v}(p,T,\xi,G_{i\alpha},T_{,i})\,; \tag{2.10}$$

instead of the specific volume the internal pressure can be chosen as an indepen-

dent field variable. Hence, we obtain

$$\begin{aligned} t_{ij}(\mathbf{x},t) &= -p(\mathbf{x},t)\delta_{ij} + \hat{t_{ij}}(p,T,\xi,G_{i\alpha},T_{,i}) \quad \text{with } \hat{t}_{ll}=0 \ , \\ q_i(\mathbf{x},t) &= \hat{q}_i(p,T,\xi,G_{i\alpha},T_{,i}) \, , \\ \psi_i(\mathbf{x},t) &= 0 \, , \\ u(\mathbf{x},t) &= \hat{u}(p,T,\xi,G_{i\alpha},T_{,i}) \, , \\ A(\mathbf{x},t) &= \hat{A}(p,T,\xi,G_{i\alpha},T_{,i}) \, . \end{aligned} \tag{2.11}$$

The constitutive equations (2.10) and (2.11) are equivalent to (2.8). The form of (2.10) and (2.11) is better suited for the description of the material behaviour of rubber-like high polymers, as we shall see later. Therefore we choose this formulation, [5].

If one inserts the constitutive equations (2.8) or (2.10) and (2.11) into the balance equations (2.1), these become field equations for the independent fields. Every solution of the field equations to a Cauchy-problem (Boundary-value and/or initial value problem) is called a thermodynamic process.

If the constitutive equations would be known, the exercise of thermodynamics would be to solve the field equations, and this is a purely mathematical problem. The constitutive equations, however, are in reality not known for no material, so neither for high polymers. For this reason the main exercise of thermodynamics is first of all to restrict the dependence of constitutive equations (on their variables) by general requirements. This is the content of the thermodynamic constitutive theory, which we shall formulate now.

There exist three generally valid requirements for the restriction of constitutive equations. These are the principle of material symmetry [71], The principle of material observer invariance, and the entropy principle [5, 54].

The principle of material symmetry states, that the constitutive equations are form invariant with respect to symmetry transformations in the undeformed state. For the isotropic high polymers considered here (with inversion symmetry) this means, that the constitutive equations can depend on $G_{i\alpha}$ only via the left Cauchy-Green deformation tensor

$$\beta_{ij} := G_{i\alpha}G_{j\alpha} \ . \tag{2.12}$$

The principle of material observer invariance states, that the constitutive equations which are measured by an observer in an inertial frame, are the same as for another observer in a frame, which is translated and rotated against the inertial frame. Then, the constitutive equations are form invariant under Euclidean transformations. From this one concludes, that the constitutive functions

are isotropic functions of $T_{,i}$ and β_{ij} and possess the following irreducible representations [64]:

$$\begin{aligned} u &= u(p,T,\xi,I_\alpha,H_\alpha) \quad , \quad A = A(p,T,\xi,I_\alpha,H_\alpha) \quad , \quad v = v(p,T,I_\alpha,H_\alpha)\,, \\ q_i &= -[\kappa_1\delta_{ij} + \kappa_2\beta_{ij} + \kappa_3(\boldsymbol{\beta}^2)_{ij}]T_{,j} \quad , \\ t_{ij} &= -p\delta_{ij} - \frac{2}{3}(C_1I_1 + 2C_2I_2)\delta_{ij} + 2(C_1 + C_2I_1)\beta_{ij} - 2C_2(\boldsymbol{\beta}^2)_{ij} \\ &\quad +\alpha_1\left[(\mathbf{T}\otimes\mathbf{T})_{ij} - \frac{H_1}{3}\delta_{ij}\right] + \alpha_2\left[\frac{1}{2}\left(\mathbf{T}\otimes\boldsymbol{\beta}\cdot\mathbf{T} + \boldsymbol{\beta}\mathbf{T}\otimes\mathbf{T}\right)_{ij} - H_2\delta_{ij}\right] \\ &\quad +\alpha_3\left[\frac{1}{2}\left(\mathbf{T}\otimes\boldsymbol{\beta}^2\mathbf{T} + \boldsymbol{\beta}^2\mathbf{T}\otimes\mathbf{T}\right)_{ij} - H_3\delta_{ij}\right]. \end{aligned} \tag{2.13}$$

Here $I_\alpha(\alpha = 1,2)$ are

$$I_1 := tr\boldsymbol{\beta} = \beta_{ll} \quad , \quad I_2 := \frac{1}{2}[(tr\boldsymbol{\beta})^2 - tr\boldsymbol{\beta}^2]\,, \tag{2.14}$$

the principal invariants of the elastic deformation ($I_3 := det\boldsymbol{\beta} = 1$),

$$H_a := \mathbf{T}\cdot(\boldsymbol{\beta}^{a-1}\mathbf{T}) = T_{,i}(\boldsymbol{\beta}^{a-1})_{ij}T_{,j} \quad (a = 1,2,3)\,. \tag{2.15}$$

H_a are the irreducible invariants, which can be formed with the temperature gradient.

The scalar coefficients $\kappa_1,\kappa_2,\kappa_3$ in the heat flux and C_1, C_2 and $\alpha_1,\alpha_2,\alpha_3$ in the stress tensor are in general functions of p, T, ξ, I_α, H_a . The terms in the stress tensor are trace free, except for the pressure part, e.g. $tr(\mathbf{t} + p\mathbf{1}) = t_{ll} + 3p = 0$. One can easily prove this with the help of the Hamilton-Cayley-Theorem :

$$(\boldsymbol{\beta}^3)_{ij} = I_1(\boldsymbol{\beta}^2)_{ij} - I_2\beta_{ij} + \delta_{ij}\ . \tag{2.16}$$

As a third general principle for the restrictions on constitutive equations serves the entropy principle . We postulate it in the form given by Müller [54].

i) There exists a mass - proportional entropy. This satisfies a balance equation of the form:

$$\rho\dot{s} = -\phi_{i,i} + \pi_s\ . \tag{2.17}$$

ii) The specific entropy s and the (non-convective) entropy flux ϕ_i are given by constitutive equations, which satisfy the principle of material symmetry and the principle of material observer invariance. For rubber-like isotropic high polymers we then have

$$\begin{aligned} s(\mathbf{x},t) &= \hat{s}(p,T,\xi,G_{i\alpha},T_{,i}) = s(p,T,\xi,I_\alpha,H_a)\,, \\ \phi_j(\mathbf{x},t) &= \hat{\phi}_j(p,T,\xi,G_{i\alpha},T_{,i}) = -[\varphi_1\delta_{ij} + \varphi_2\beta_{ij} + \varphi_3(\boldsymbol{\beta}^2)_{ij}]T_{,j} \quad , \end{aligned} \tag{2.18}$$

where $\varphi_1, \varphi_2, \varphi_3$ are scalar functions of p, T, ξ, I_α, H_a.

iii) At heat conducting material walls with continuous temperature, the normal component of the entropy flux is continuous,

$$[[\phi_j]]e_j = 0 \quad for \quad [[T]] = 0\,, \tag{2.19}$$

$[[\psi]] := \psi^+ - \psi^-$ means the difference of single sided limiting values when approaching the wall from either side, $\boldsymbol{e}$ is the unit normal vector of the heat conducting wall.

iv) The entropy production density is non-negative for all thermodynamic processes,

$$\pi_s \geq 0 \quad \forall \text{ thermodynamic processes } . \tag{2.20}$$

The key for drawing inferences from the entropy principle is inequality (2.20). It doesn't hold for arbitrary fields ρ, χ_i, T, ξ, but only for thermodynamic processes. The inequality is therefore valid for all solutions of the fields equations, which follow from the balance laws. These field equations formulate restrictions for the independent fields. One can account for these restrictions by the introduction of Lagrangian parameters. One then obtains an inequality that is equivalent to (2.20) and (2.17) of the following form:

$$\begin{aligned} \rho\dot{s} \;&+\; \phi_{i,i} - \wedge^\rho(\dot{\rho} + \rho v_{i,j}) - \wedge^v_i(\rho\dot{v}_i - t_{ij,j}) \\ &-\; \wedge^u(\rho\dot{u} + q_{j,j} - t_{ij}v_{i,j}) - \wedge^\xi(\rho\dot{\xi} + \psi_{j,j} - A) \geq 0\,, \end{aligned} \tag{2.21}$$

which is valid for arbitrary (unrestricted) fields ρ, χ_i, T and ξ [43].

According to (2.3), (2.4), and (2.7) the velocity gradient may be written as

$$v_{i,j} = \dot{F}_{i\alpha}(\mathbf{F}^{-1})_{\alpha j} = \frac{1}{3}\frac{\dot{v}}{v}\delta_{ij} + \dot{G}_{i\alpha}(\mathbf{G}^{-1})_{\alpha j}\,. \tag{2.22}$$

Now, one inserts into (2.21) the constitutive equations (2.18), (2.10) and (2.11)

and performs the differentiations. One obtains thus with $v = 1/\rho$ and (2.22)

$$
\begin{aligned}
& \rho\left[\frac{\partial\hat{s}}{\partial p} - \wedge^u\left(\frac{\partial\hat{u}}{\partial p} + p\frac{\partial\hat{v}}{\partial p}\right)\right]\dot{p} + \rho\left[\frac{\partial\hat{s}}{\partial T} - \wedge^u\left(\frac{\partial\hat{u}}{\partial T} + p\frac{\partial\hat{v}}{\partial T}\right)\right]\dot{T} \\
+ \quad & \rho\left[\frac{\partial\hat{s}}{\partial\xi} - \wedge^u\left(\frac{\partial\hat{u}}{\partial\xi} + p\frac{\partial\hat{v}}{\partial\xi}\right) - \wedge^\xi\right]\dot{\xi} \\
+ \quad & \rho\left[\frac{\partial\hat{s}}{\partial G_{i\alpha}} - \wedge^u\left(\frac{\partial\hat{u}}{\partial G_{i\alpha}} + p\frac{\partial\hat{v}}{\partial G_{i\alpha}} - \hat{v}\hat{t}_{ij}(\mathbf{G}^{-1})_{\alpha j}\right) - \wedge^\rho(\mathbf{G}^{-1})_{\alpha i}\right]\dot{G}_{i\alpha} \\
+ \quad & \rho\left[\frac{\partial\hat{s}}{\partial T_{,i}} - \wedge^u\left(\frac{\partial\hat{u}}{\partial T_{,i}} + p\frac{\partial\hat{v}}{\partial T_{,i}}\right)\right]\dot{(T_{,i})} - \rho\wedge_i^v\,\dot{v}_i + \wedge^\xi\hat{A} \qquad (2.23) \\
+ \quad & \left[\frac{\partial\hat{\phi}_j}{\partial p} - \wedge^u\frac{\partial\hat{q}_j}{\partial p} - \wedge_j^v + \wedge_k^v\frac{\partial\hat{t}_{kj}}{\partial p}\right]p_{,j} \\
+ \quad & \left[\frac{\partial\hat{\phi}_j}{\partial T} - \wedge^u\frac{\partial\hat{q}_j}{\partial T} + \wedge_k^v\frac{\partial\hat{t}_{kj}}{\partial T}\right]T_{,j} + \left[\frac{\partial\hat{\phi}_j}{\partial\xi} - \wedge^u\frac{\partial\hat{q}_j}{\partial\xi} + \wedge_k^v\frac{\partial\hat{t}_{kj}}{\partial\xi}\right]\xi_{,j} \\
+ \quad & \left[\frac{\partial\hat{\phi}_j}{\partial G_{i\alpha}} - \wedge^u\frac{\partial\hat{q}_j}{\partial G_{i\alpha}} + \wedge_k^v\frac{\partial\hat{t}_{kj}}{\partial G_{i\alpha}}\right]G_{i\alpha,j} \\
+ \quad & \left[\frac{\partial\hat{\phi}_j}{\partial T_{,i}} - \wedge^u\frac{\partial\hat{q}_j}{\partial T_{,i}} + \wedge_k^v\frac{\partial\hat{t}_{kj}}{\partial T_{,i}}\right]T_{,ij} \;\geq\; 0 \qquad .
\end{aligned}
$$

This inequality is valid for arbitrary variations of the (independent) fields. Without restriction of generality one can choose the Lagrange parameters $\wedge^u, \wedge^\xi, \wedge^\rho$ in such a way, that the expressions in the brackets in front of $\dot{T}$, $\dot{\xi}$ and $\dot{G}_{i\alpha}$ disappear. Then these Lagrange parameters are functions of the variables $p, T, \xi, G_{i\alpha}, T_{,i}$ of the constitutive equations. Further, the Lagrange parameter $\wedge_i^v$ can be chosen such, that it is independent of $\dot{v}_i$. Then $\wedge_i^v = 0$ must vanish, since otherwise the inequality can be contradicted. Now it follows, that the inequality (2.23) is linear in $\dot{p}$, $\dot{(T_{,j})}$, $p_{,j}$, $\xi_{,j}$, $G_{i\alpha,j}$ and $T_{,ij}$. It could, consequently, be violated for arbitrary variations of these fields, except if the corresponding forefactors vanish. This gives

$$
\begin{aligned}
\frac{\partial\hat{s}}{\partial T} &= \wedge^u\left(\frac{\partial\hat{u}}{\partial T} + p\frac{\partial\hat{v}}{\partial T}\right), \\
\frac{\partial\hat{s}}{\partial p} &= \wedge^u\left(\frac{\partial\hat{u}}{\partial p} + p\frac{\partial\hat{v}}{\partial p}\right), \qquad (2.24) \\
\frac{\partial\hat{s}}{\partial\xi} &= \wedge^u\left(\frac{\partial\hat{u}}{\partial\xi} + p\frac{\partial\hat{v}}{\partial\xi}\right) + \wedge^\xi, \\
\frac{\partial\hat{s}}{\partial G_{i\alpha}} &= \wedge^u\left(\frac{\partial\hat{u}}{\partial G_{i\alpha}} + p\frac{\partial\hat{v}}{\partial G_{i\alpha}} - \hat{v}\hat{t}_{ij}(\mathbf{G}^{-1})_{\alpha j}\right) + \wedge^\rho(\mathbf{G}^{-1})_{\alpha j}, \\
\frac{\partial\hat{s}}{\partial T_{,i}} &= \wedge^u\left(\frac{\partial\hat{u}}{\partial T_{,i}} + p\frac{\partial\hat{v}}{\partial T_{,i}}\right);
\end{aligned}
$$

$$\wedge_i^v = 0\,, \tag{2.25}$$

$$\begin{aligned}
\frac{\partial\hat{\phi}_j}{\partial p} &= \wedge^u \frac{\partial\hat{q}_j}{\partial p}\,,\\
\frac{\partial\hat{\phi}_j}{\partial \xi} &= \wedge^u \frac{\partial\hat{q}_j}{\partial \xi}\,,\\
\frac{\partial\hat{\phi}_j}{\partial G_{i\alpha}} &= \wedge^u \frac{\partial\hat{q}_j}{\partial G_{i\alpha}}\,,\\
\frac{\partial\hat{\phi}_{(j}}{\partial T_{,ij)}} &= \wedge^u \frac{\partial\hat{q}_{(j}}{\partial T_{,ij)}}\,.
\end{aligned} \tag{2.26}$$

There remains the residual inequality

$$\pi_s = \left(\frac{\partial\hat{\phi}_j}{\partial T} - \wedge^u\frac{\partial\hat{q}_j}{\partial T}\right) T_{,j} + \wedge^\xi \hat{A} \geq 0\,, \tag{2.27}$$

which holds for unrestricted processes.

It seems, that we do not come closer to our wanted goal, namely to find restrictions on the constitutive equations for $\hat{v}, \hat{u}, \hat{t}_{ij}, \hat{q}_j, \hat{A}$, because we introduced new unknown constitutive functions $\hat{s}, \hat{\phi}_j$ and unknown Lagrangean parameters $\wedge^u, \wedge^\xi, \wedge^\rho$. But this only seems so, because the new constitutive functions can be eliminated. First we recognise, that the " Ansatz" $\hat{\phi}_j = \wedge^u\hat{q}_j$ satisfies the relations (2.26), provided $\wedge^u$ is only a function of T,

$$\hat{\phi}_j = \wedge^u(T)\,\hat{q}_j\,. \tag{2.28}$$

This is a sufficient solution of (2.26). That it is also necessary, can be proven with the help of the representations $(2.18)_2$ for the entropy flux and $(2.13)_4$ for the heat flux after lengthly calculations. The entropy flux is therefore proportional to the heat flux with a factor of proportionality $\wedge^u(T)$, which is only a function of temperature. To determine this factor we use the requirement (iii) of the entropy principle on heat conducting material walls. At these walls, as a consequence of the energy law, the normal component of the heat flux must be continuous:

$$[[q_i]]\,e_i = 0\,. \tag{2.29}$$

If the heat conducting wall is nothing else but the interface between two heat conducting rubber-like high polymers + and −, the temperature is continuous and it follows from (2.29) and (2.19)

$$\wedge^u_+(T) = \wedge^u_-(T)\,. \tag{2.30}$$

The Lagrange parameter $\wedge^u(T)$ is continuous on heat conducting interfaces. Consequently, it is a universal function of temperature for all heat conducting rubber-like high polymers.

For an ideal gas the Lagrange parameter $\wedge^u_g(T) = 1/T$ is identified with (1 over the absolute ideal gas temperature). If one contacts the high polymer via a heat conducting interface with an ideal gas, one has

$$\wedge^u(T) = \frac{1}{T}\,. \tag{2.31}$$

The Lagrange parameter $\wedge^u(T)$ for high polymers is identified with the reciprocal (absolute) temperature.

Now we use this result and insert it in (2.24). With the specific enthalpy

$$\hat{h} := \hat{u} + p\hat{v}\,, \tag{2.32}$$

we obtain

$$\begin{aligned}
\frac{\partial \hat{s}}{\partial T} &= \frac{1}{T}\frac{\partial \hat{h}}{\partial T}\,,\\
\frac{\partial \hat{s}}{\partial p} &= \frac{1}{T}(\frac{\partial \hat{h}}{\partial p} - \hat{v})\,,\\
\frac{\partial \hat{s}}{\partial \xi} &= \frac{1}{T}\frac{\partial \hat{h}}{\partial \xi} + \wedge^\xi\,,\\
\frac{\partial \hat{s}}{\partial G_{i\alpha}} &= \frac{1}{T}\left(\frac{\partial \hat{h}}{\partial G_{i\alpha}} - \hat{v}\hat{t}_{ij}(\mathbf{G}^{-1})_{\alpha j}\right) - \wedge^\rho(\mathbf{G}^{-1})_{\alpha i}\,,\\
\frac{\partial \hat{s}}{\partial T_{,i}} &= \frac{1}{T}\frac{\partial \hat{h}}{\partial T_{,i}}\,.
\end{aligned} \tag{2.33}$$

We assume, that the entropy is twice continuously differentiable. From the interchangement of the second derivatives one concludes, among other things,

$$\frac{\partial \hat{h}}{\partial T_{,i}} = 0 \quad , \quad \frac{\partial \hat{v}}{\partial T_{,i}} = 0 \quad , \quad \frac{\partial \wedge^\xi}{\partial T_{,i}} = 0 \quad , \quad \frac{\partial \wedge^\rho}{\partial T_{,i}} = 0 \quad , \quad \frac{\partial \hat{t}_{kj}}{\partial T_{,i}} = 0\,. \tag{2.34}$$

The specific enthalpy, the specific volume, the trace-free contribution of the Cauchy-stress and the Lagrange parameters $\wedge^\xi$ and $\wedge^\rho$ are independent of the temperature gradient. The same result holds according to $(2.33)_5$ and (2.32) for the entropy and the internal energy

$$\frac{\partial \hat{s}}{\partial T_{,i}} = 0 \quad , \quad \frac{\partial \hat{u}}{\partial T_{,i}} = 0\,. \tag{2.35}$$

This implies important simplifications in the representations (2.13) and (2.18) of the constitutive functions: The specific volume, the internal energy, the entropy, the enthalpy and the coefficients C_1 and C_2 of the stress tensor are independent of the invariants H_a $(a = 1, 2, 3)$. Further, the coefficients of the stress tensor

$$\alpha_1 = \alpha_2 = \alpha_3 = 0 \tag{2.36}$$

vanish. The chemical production density A, and the coefficients $\kappa_1, \kappa_2, \kappa_3$ in the heat flux may, however, further depend on H_a $(a = 1, 2, 3)$.

We insert now the representations (2.13) under the use of (2.36) and (2.33) and obtain with (2.12), (2.14) and (2.16), using the following mathematical expressions

$$\begin{aligned} \frac{\partial s}{\partial G_{i\alpha}} &= \frac{\partial s}{\partial I_1} \times \frac{\partial I_1}{\partial G_{i\alpha}} + \frac{\partial s}{\partial I_2} \times \frac{\partial I_2}{\partial G_{i\alpha}}\,, \\ \frac{\partial h}{\partial G_{i\alpha}} &= \frac{\partial h}{\partial I_1} \times \frac{\partial I_1}{\partial G_{i\alpha}} + \frac{\partial h}{\partial I_2} \times \frac{\partial I_2}{\partial G_{i\alpha}}\,, \end{aligned}$$

after lengthy calculations[1]:

$$\wedge^{\rho} = \frac{v}{T}\frac{2}{3}(C_1 I_1 + 2C_2 I_2) \tag{2.37}$$

and

$$\begin{aligned} \frac{\partial s}{\partial T} &= \frac{1}{T}\frac{\partial h}{\partial T}\,, \\ \frac{\partial s}{\partial p} &= \frac{1}{T}(\frac{\partial h}{\partial p} - v)\,, \\ \frac{\partial s}{\partial \xi} &= \frac{1}{T}\frac{\partial h}{\partial \xi} + \wedge^{\xi}\,, \\ \frac{\partial s}{\partial I_\alpha} &= \frac{1}{T}(\frac{\partial h}{\partial I_\alpha} - vC_\alpha)\,, \qquad (\alpha = 1, 2)\,. \end{aligned} \tag{2.38}$$

To simplify notation, the hats $\hat{}$ above the constitutive functions have been dropped.

The Cauchy stress tensor can be somewhat simplified using the Hamilton-Cayley Theorem (2.16) and (2.36):

$$t_{ij} = -p\delta_{ij} - \frac{2}{3}(C_1 I_1 - C_2 I_2)\delta_{ij} + 2C_1\beta_{ij} - 2C_2(\boldsymbol{\beta}^{-1})_{ij}\,. \tag{2.39}$$

If one introduces the specific free enthalpy

$$g := h - Ts\,, \tag{2.40}$$

[1]These calculations are available upon request.

then relations (2.38) simplify formally to

$$\frac{\partial g}{\partial T} = -s \;\;,\;\; \frac{\partial g}{\partial p} = v \;\;,\;\; \frac{\partial g}{\partial \xi} = -T\wedge^{\xi} \;\;,\;\; \frac{\partial g}{\partial I_\alpha} = vC_\alpha \;\; (\alpha = 1,2)\,. \tag{2.41}$$

With these, the Lagrangean parameter $\wedge^{\xi}$ has finally been identified. It is given by the derivative of the free enthalpy with respect to the degree of crystallinity.

The integrability conditions for the free enthalpy are

$$\begin{aligned}
&\frac{\partial s}{\partial p} = -\frac{\partial v}{\partial T} \;\;,\;\; \frac{\partial s}{\partial \xi} = \frac{\partial (T\wedge^{\xi})}{\partial T} \;\;,\;\; \frac{\partial s}{\partial I_\alpha} = -\frac{\partial (vC_\alpha)}{\partial T} \;\;, \\
&\frac{\partial v}{\partial \xi} = -T\frac{\partial \wedge^{\xi}}{\partial P} \;\;,\;\; \frac{\partial v}{\partial I_\alpha} = \frac{\partial (vC_\alpha)}{\partial P} \;\;,\;\; T\frac{\partial \wedge^{\xi}}{\partial I_\alpha} = -\frac{\partial (vC_\alpha)}{\partial \xi} \;\;, \\
&\frac{\partial (vC_1)}{\partial I_2} = \frac{\partial (vC_2)}{\partial I_1} \;\;.
\end{aligned} \tag{2.42}$$

We shall produce some further relations. We introduce by $c_p := \frac{\partial h}{\partial T}$ the specific heat capacity at constant pressure. From (2.38) we conclude with (2.42)

$$\begin{aligned}
\frac{\partial h}{\partial T} &= c_p \;=\; T\,\frac{\partial s}{\partial T}\,, \\
\frac{\partial h}{\partial p} &= v - T\,\frac{\partial v}{\partial T}\,, \\
\frac{\partial h}{\partial \xi} &= T^2\,\frac{\partial \wedge^{\xi}}{\partial T}\,, \\
\frac{\partial h}{\partial I_\alpha} &= vC_\alpha - T\,\frac{\partial (vC_\alpha)}{\partial T}\,.
\end{aligned} \tag{2.43}$$

These relations imply the integrabitlity conditions

$$\frac{\partial c_p}{\partial p} = -T\,\frac{\partial^2 v}{\partial T} \;\;,\;\; \frac{\partial c_p}{\partial \xi} = \frac{\partial}{\partial T}(T^2\frac{\partial \wedge^{\xi}}{\partial T}) \;\;,\;\; \frac{\partial c_p}{\partial I_\alpha} = -T\frac{\partial^2 (vC_\alpha)}{\partial T^2}\,. \tag{2.44}$$

For the internal energy $u = h - pv$ we obtain with (2.43)

$$\begin{aligned}
\frac{\partial u}{\partial T} &= c_p - p\,\frac{\partial v}{\partial T}\,, \quad \frac{\partial u}{\partial p} = -T\,\frac{\partial v}{\partial T} - p\,\frac{\partial v}{\partial p} \;\;, \\
\frac{\partial u}{\partial \xi} &= T^2\,\frac{\partial \wedge^{\xi}}{\partial T} - p\frac{\partial v}{\partial \xi}\,, \quad \frac{\partial u}{\partial I_\alpha} = vC_\alpha - T\,\frac{\partial (vC_\alpha)}{\partial T} - p\,\frac{\partial v}{\partial I_\alpha}\,.
\end{aligned} \tag{2.45}$$

With this all general relations for rubber-like high polymers are derived.

There remains to draw conclusions from the residual-inequality (2.27). This simplifies with (2.28) and (2.31) to

$$\Pi_s = -\frac{1}{T^2}\, q_j\, T_{,j} + \wedge^{\xi} A \geq 0\,. \tag{2.46}$$

We define thermostatic equilibrium as a state with spatially and temporarily constant temperature T, with temporarily constant deformation $G_{i\alpha}$, temporarily constant pressure p and temporarily constant degree of crystallization ξ. According to (2.1) and $(2.11)_3$ the chemical production density $A = 0$. We denote this thermostatic equilibrium state by $|_E$ (equilibrium).

The entropy production assumes in equilibrium its minimum value zero. Necessary conditions are

$$\frac{\partial \Pi_s}{\partial T_{,j}}|_E = 0\,, \qquad \frac{\partial \Pi_s}{\partial A}|_E = 0\,, \tag{2.47}$$

$$\left\| \begin{array}{cc} \frac{\partial^2 \Pi_s}{\partial T_{,i} T_{,j}}|_E & \frac{\partial^2 \Pi_s}{\partial T_{,i}\, \partial A}|_E \\ \frac{\partial^2 \Pi_s}{\partial A\, \partial T_{,j}}|_E & \frac{\partial^2 \Pi_s}{\partial A^2}|_E \end{array} \right\| \sim \text{non} - \text{negative definite} \tag{2.48}$$

Relations (2.47) give

$$q_i|_E = 0 \quad , \quad \wedge^{\xi}|_E = 0\,. \tag{2.49}$$

According to $(2.13)_4$, $(2.49)_1$ is satisfied automatically, $(2.49)_2$ means according to $(2.41)_3$

$$\wedge^{\xi}|_E = -\frac{1}{T}\ \frac{\partial g}{\partial \xi}|_E = 0\,. \tag{2.50}$$

This relation determines the equilibrium value $\xi_{|_E} = \bar{\xi}(T, p, I_\alpha)$ of the degree of crystallinity.

The matrix of the second derivatives in equilibrium is, according to (2.13) and $(2.43)_3$,

$$\begin{aligned} \frac{\partial^2 \Pi_s}{\partial T_{,i} T_{,j}}|_E &= -\frac{1}{T^2}\frac{\partial q_{(i}}{\partial T_{,j)}}|_E = \frac{1}{T^2}\left[\kappa_1|_E \delta_{ij} + \kappa_2|_E \beta_{ij} + \kappa_3|_E (\boldsymbol{\beta}^2)_{ij}\right]\,, \\ \frac{\partial^2 \Pi_s}{\partial T_{,i} \partial A}|_E &= \frac{\partial \wedge^{\xi}}{\partial T_{,j}}|_E = 0\,, \\ \frac{\partial^2 \Pi_s}{\partial A^2}|_E &= \frac{\partial \wedge^{\xi}}{\partial A}|_E\,. \end{aligned}$$

From (2.48), there follows

$$\kappa_1|_E\delta_{ij} + \kappa_2|_E\beta_{ij} + \kappa_3|_E(\boldsymbol{\beta}^2)_{ij} \quad \sim \quad \text{non} - \text{negative} \;\; \text{difinite} \;\; , \tag{2.51}$$

$$\frac{\partial \wedge^{\xi}}{\partial A}|_{_E} \geq 0\,. \tag{2.52}$$

With these all general restrictions on the constitutive equations of rubber-like high polymers are obtained.

2.2 Uniaxial Extension

To obtain a first overview about the content of the thermodynamic constitutive theory, we will discuss the uniaxial extension at constant temperature T and constant external pressure P. The direction of extension shall be the 1-direction. Let the extensional force per unit cross section in the reference state be σ_1 (nominal stress). This is related to the 11-component of the 1^{st} Kirchhoff-Piola-stress

$$T_{i\alpha} = t_{ij}(\mathbf{F}^{-1})_{\alpha j}\; det\mathbf{F} \tag{2.53}$$

as follows:

$$\sigma_1 = T_{11} + P(\mathbf{F}^{-1})_{11}\; det\mathbf{F}\,. \tag{2.54}$$

The states of stress and deformation are uniform and along the Eigen-direction, where for the Cauchy-stress the following boundary conditions at the free surfaces perpendicular to the direction of extension apply:

$$t_{22} = t_{33} = -P\,, \tag{2.55}$$

Furthermore, the deformation gradient in the used Cartesian co-ordinate system has the representation

$$||F_{i\alpha}|| = \begin{pmatrix} \Lambda_1 & 0 & 0 \\ 0 & \Lambda_2 & 0 \\ 0 & 0 & \Lambda_3 \end{pmatrix}\,. \tag{2.56}$$

Λ_1 is the ratio of the length L at constant T and constant P of the extended material probe to the length L_R in the undeformed reference state at the reference temperature T_R, reference pressure P_R and crystallinity $\bar{\xi}_R$, namely

$$\Lambda_1 := \frac{L}{L_R} \qquad . \tag{2.57}$$

Using (2.6) the deformations $\Lambda_2 = \Lambda_3$ perpendicular to the extensional direction become

$$\Lambda_2 = \Lambda_3 = \sqrt{\frac{v}{v_R}\frac{1}{\Lambda_1}}\,. \tag{2.58}$$

The isochoric strain tensor is also in principal form

$$||G_{i\alpha}|| = \begin{pmatrix} \lambda_1 & 0 & 0 \\ 0 & \lambda_2 & 0 \\ 0 & 0 & \lambda_3 \end{pmatrix} . \tag{2.59}$$

The corresponding isochoric principal strains $\lambda_2 = \lambda_3$ perpendicular to the extensional direction follow from $(2.7)_2$ as

$$\lambda_2 = \lambda_3 = \sqrt{\frac{1}{\lambda_1}} . \tag{2.60}$$

The relationship between the deformation measures in (2.56) and (2.59) follows from $(2.7)_1$ as

$$\lambda_1 = (\frac{v}{v_R})^{-\frac{1}{3}} \Lambda_1 , \quad \lambda_2 = (\frac{v}{v_R})^{1/6} \frac{1}{\sqrt{\Lambda_1}} . \tag{2.61}$$

The left Cauchy-Green deformation tensor (2.12) has then the representation

$$||\beta_{ij}|| = \begin{pmatrix} \lambda_1^2 & 0 & 0 \\ 0 & \frac{1}{\lambda_1} & 0 \\ 0 & 0 & \frac{1}{\lambda_1} \end{pmatrix} . \tag{2.62}$$

The main invariants (2.14) are consequently

$$I_1 = \lambda_1^2 + \frac{2}{\lambda_1} , \quad I_2 = 2\lambda_1 + \frac{1}{\lambda_1^2} . \tag{2.63}$$

The components of the Cauchy-stress follow from (2.39):

$$\begin{aligned} t_{11} &= -p + \frac{4}{3}(\lambda_1^2 - \frac{1}{\lambda_1})(C_1 + C_2\frac{1}{\lambda_1}) , \\ t_{22} &= -p - \frac{2}{3}(\lambda_1^2 - \frac{1}{\lambda_1})(C_1 + C_2\frac{1}{\lambda_1}) = t_{33} . \end{aligned} \tag{2.64}$$

From the boundary condition (2.55) we obtain the internal pressure

$$p = P - \frac{2}{3}(\lambda_1^2 - \frac{1}{\lambda_1})(C_1 + C_2\frac{1}{\lambda_1}) . \tag{2.65}$$

The 11-component of the 1^{st} Kirchhoff-Piola-stress (2.53) is then given by

$$\begin{aligned} T_{11} &= t_{1j}(\mathbf{F}^{-1})_{1j}\, det\mathbf{F} = t_{11}\frac{1}{\Lambda_1}\Lambda_1\Lambda_2^2 = t_{11}\frac{v}{v_R}\frac{1}{\Lambda_1} \\ &= (\frac{v}{v_R})^{2/3} t_{11}\frac{1}{\lambda_1} = (\frac{v}{v_R})^{2/3}\frac{1}{\lambda_1}\left[-p + \frac{4}{3}(\lambda_1^2 - \frac{1}{\lambda_1})(C_1 + C_2\frac{1}{\lambda_1})\right] . \end{aligned} \tag{2.66}$$

Thus, from (2.54), with the help of (2.65), one deduces for the nominal extensional stress

$$\sigma_1 = (\frac{v}{v_R})^{2/3}(\lambda_1 - \frac{1}{\lambda_1^2})\ \ (2C_1 + 2C_2\frac{1}{\lambda_1})\,. \tag{2.67}$$

In the uniaxial extension experiment the independently given variables, and therefore measurable quantities, are the external pressure P, the temperature T and the length ratio Λ_1. It is therefore necessary for the experimental testing, to introduce P, T, Λ_1 (besides ξ) as independent variables. Any state function $\psi(p, T, \xi, I_\alpha)$ is thus representable as

$$\psi(p, T, \xi, I_\alpha) = \tilde{\psi}(P, T, \xi, \Lambda_1)\,, \tag{2.68}$$

where the dependence on the set of variables on the right-hand side is denoted by a ˜ above the function symbol. The specific volume is then given by

$$v = \tilde{v}(P, T, \xi, \Lambda_1)\,. \tag{2.69}$$

For the deformation invariants (2.63), (2.61) implies

$$\begin{aligned} I_1 = \tilde{I}_1(P, T, \xi, \Lambda_1) &= (\frac{\tilde{v}}{v_R})^{-2/3}(\Lambda_1^2 + \frac{2}{\Lambda_1}\frac{\tilde{v}}{v_R})\,, \\ I_2 = \tilde{I}_2(P, T, \xi, \Lambda_1) &= (\frac{\tilde{v}}{v_R})^{-1/3}(2\Lambda_1 + \frac{1}{\Lambda_1^2}\frac{\tilde{v}}{v_R})\,, \end{aligned} \tag{2.70}$$

and for the internal pressure (2.65) and the nominal extensional stress (2.66) we get the expressions

$$\begin{aligned} p &= \tilde{p}(P, T, \xi, \Lambda_1) \\ &= P - \frac{1}{3}\frac{1}{v_R}(\frac{\tilde{v}}{v_R})^{-2/3}\left(\Lambda_1 - \frac{1}{\Lambda_1^2}\frac{\tilde{v}}{v_R}\right)\left[2(\tilde{v}\tilde{C}_1) + 2(\tilde{v}\tilde{C}_2)\frac{1}{\Lambda_1}(\frac{\tilde{v}}{v_R})^{1/3}\right], \end{aligned} \tag{2.71}$$

$$\begin{aligned} \sigma_1 &= \tilde{\sigma}_1(P, T, \xi, \Lambda_1) \\ &= \frac{1}{v_R}(\frac{\tilde{v}}{v_R})^{-2/3}\left(\Lambda_1 - \frac{1}{\Lambda_1^2}\frac{\tilde{v}}{v_R}\right)\left[2(\tilde{v}\tilde{C}_1) + 2(\tilde{v}\tilde{C}_2)\frac{1}{\Lambda_1}(\frac{\tilde{v}}{v_R})^{1/3}\right]. \end{aligned} \tag{2.72}$$

The crystallinity ξ in non-equilibrium is, contrary to P, T, Λ_1, not directly measurable in uniaxial, isothermal and isochoric extension tests. The volume relaxation and the stress relaxation are measurable, because at fixed values of P, T, and Λ_1 the specific volume $\tilde{v}$ as well as the nominal stress $\tilde{\sigma}_1$ are measurable as functions of time. In the relations

$$\dot{\tilde{v}}|_{P,T,\Lambda_1} = \frac{\partial\tilde{v}}{\partial\xi}\dot{\xi}|_{P,T,\Lambda_1}\ \ ,\ \ \dot{\tilde{\sigma}}_1|_{P,T,\Lambda_1} = \frac{\partial\tilde{\sigma}_1}{\partial\xi}\dot{\xi}|_{P,T,\Lambda_1} \tag{2.73}$$

the left-hand sides are known and, consequently, also the ratio

$$\frac{\dot{\tilde{\sigma}}_1|_{P,T,\Lambda_1}}{\dot{\tilde{v}}|_{P,T,\Lambda_1}} = \frac{\partial\tilde{\sigma}_1/\partial\xi}{\partial\tilde{v}/\partial\xi} = \frac{\partial\tilde{\sigma}_1}{\partial\tilde{v}}|_{P,T,\Lambda_1} \,. \tag{2.74}$$

If one knows in addition the time rate of change of ξ, $\partial\tilde{v}/\partial\xi$ and $\partial\tilde{\sigma}_1/\partial\xi$ are indirectly determinable from (2.73). To calculate ξ approximately, we employ the following reasoning: For small departures of crystallinity ξ from its equilibrium value $\bar{\xi}(P,T,\Lambda_1)$, the chemical production rate density A is proportional to the "affinity" $\wedge^\xi$. Then one has

$$A = a|_{_E} \wedge^\xi \,. \tag{2.75}$$

According to (2.52) $a|_{_E} \geq 0$. If one develops $\wedge^\xi$ in a Taylor series for fixed values of T, P, Λ_1 with respect to ξ about the equilibrium value $\bar{\xi}$, one obtains, on using (2.41), (2.42) and (2.50),

$$\begin{aligned} \wedge^\xi &= \wedge^\xi|_{_E} + \left(\frac{\partial\wedge^\xi}{\partial\xi} + \frac{\partial\wedge^\xi}{\partial p}\frac{\partial\tilde{p}}{\partial\xi} + \sum_\alpha \frac{\partial\wedge^\xi}{\partial I_\alpha}\frac{\partial\tilde{I}_\alpha}{\partial\xi} \right)|_{_E} (\xi - \bar{\xi}) \qquad (2.76) \\ &= -\frac{1}{T}\left[\frac{\partial^2 g}{\partial\xi^2} + \frac{\partial v}{\partial\xi}\frac{\partial\tilde{p}}{\partial\xi} + \sum_\alpha \frac{\partial(vC_\alpha)}{\partial\xi}\frac{\partial\tilde{I}_\alpha}{\partial\xi} \right]|_{_E} (\xi - \bar{\xi}) \,. \end{aligned}$$

In equilibrium the free enthalpy assumes at fixed values of $T, p = p|_{_E}, I_\alpha = I_\alpha|_{_E}$ an extremum. If we assume that this extremum is a minimum, then $\partial^2 g/\partial\xi^2|_{_E} > 0$, and the crystallization equilibrium is stable. Then, the content of the square brackets can in (2.76) be positive.

We insert now (2.75) and (2.76) into the balance equation $(2.1)_5$ and obtain with $\psi_j = 0$

$$\dot{\xi} = -\frac{1}{\tau}(\xi - \bar{\xi}) \tag{2.77}$$

for the time rate of change of the crystallinity. $\tau = \tau(p,T,\bar{\xi},I_\alpha) = \tilde{\tau}(p,T,\Lambda_1)$ has the meaning of a relaxation time and is given by

$$\frac{1}{\tau} := \frac{a|_{_E}}{T}\left[\frac{\partial^2 g}{\partial\xi^2} + \frac{\partial v}{\partial\xi}\frac{\partial\tilde{p}}{\partial\xi} + \sum_\alpha \frac{\partial(vC_\alpha)}{\partial\xi}\frac{\partial\tilde{I}_\alpha}{\partial\xi} \right]_{|_E} \,. \tag{2.78}$$

For some uniaxial deformation history $\lambda_1(t)$ at constant temperature T and constant external pressure P, $\bar{\xi} = \bar{\xi}(t)$ and $\tau = \tau(t)$ are functions of time. Integration of (2.77) yields then for the non-equilibrium crystallinity ξ (the internal variable)

$$\xi(t) = \bar{\xi}(0)\; e^{-\int_0^t \frac{dt'}{\tau(t')}} + e^{-\int_0^t \frac{dx}{\tau(x)}} \int_0^t dt' \left[\frac{\bar{\xi}(t')}{\tau(t')}\; e^{\int_0^{t'} \frac{dt''}{\tau(t'')}} \right] , \tag{2.79}$$

where $\bar{\xi}(0)$ is the equilibrium crystallinity at the beginning of deformation. $\xi(t)$ is an after effect functional of stress history. This is the reason for volume and stress relaxation and stress-strain hysteresis. Conclusions from (2.79) will be drawn in the sequel.

In uniaxial extension experiments $\lambda_1(t)$ is prescribed at given values of the temperature T and the external pressure P. So, the independent variables are $T,\ P,\ \lambda_1$ and ξ. We need all equations in this set of variables. The derivatives of the function ψ with respect to T, P, ξ, λ_1 are, according to (2.68)-(2.72),

$$\begin{aligned}
\frac{\partial\tilde{\psi}}{\partial T} &= \frac{\partial\psi}{\partial T}+\frac{\partial\psi}{\partial p}\frac{\partial\tilde{p}}{\partial T}+\sum_\alpha\frac{\partial\psi}{\partial I_\alpha}\frac{\partial\tilde{I}_\alpha}{\partial T}\ ,\\
\frac{\partial\tilde{\psi}}{\partial P} &= +\frac{\partial\psi}{\partial p}\frac{\partial\tilde{p}}{\partial P}+\sum_\alpha\frac{\partial\psi}{\partial I_\alpha}\frac{\partial\tilde{I}_\alpha}{\partial P}\ ,\\
\frac{\partial\tilde{\psi}}{\partial \xi} &= \frac{\partial\psi}{\partial \xi}+\frac{\partial\psi}{\partial p}\frac{\partial\tilde{p}}{\partial \xi}+\sum_\alpha\frac{\partial\psi}{\partial I_\alpha}\frac{\partial\tilde{I}_\alpha}{\partial \xi}\ ,\\
\frac{\partial\tilde{\psi}}{\partial \lambda_1} &= +\frac{\partial\psi}{\partial p}\frac{\partial\tilde{p}}{\partial \lambda_1}+\sum_\alpha\frac{\partial\psi}{\partial I_\alpha}\frac{\partial\tilde{I}_\alpha}{\partial \lambda_1}\ .
\end{aligned}\tag{2.80}$$

Identifying ψ with the free enthalpy g we obtain, on using (2.41),

$$\begin{aligned}
\frac{\partial\tilde{g}}{\partial T} &= -\tilde{s}\ +\tilde{v}\frac{\partial\tilde{p}}{\partial T}+\sum_\alpha\tilde{v}\tilde{C}_\alpha\frac{\partial\tilde{I}_\alpha}{\partial T}\ ,\\
\frac{\partial\tilde{g}}{\partial P} &= +\tilde{v}\frac{\partial\tilde{p}}{\partial P}+\sum_\alpha\tilde{v}\tilde{C}_\alpha\frac{\partial\tilde{I}_\alpha}{\partial P}\ ,\\
\frac{\partial\tilde{g}}{\partial \xi} &= -T\tilde{\wedge}^\xi+\tilde{v}\frac{\partial\tilde{p}}{\partial \xi}+\sum_\alpha\tilde{v}\tilde{C}_\alpha\frac{\partial\tilde{I}_\alpha}{\partial \xi}\ ,\\
\frac{\partial\tilde{g}}{\partial \lambda_1} &= +\tilde{v}\frac{\partial\tilde{p}}{\partial \lambda_1}+\sum_\alpha\tilde{v}\tilde{C}_\alpha\frac{\partial\tilde{I}_\alpha}{\partial \lambda_1}\ .
\end{aligned}\tag{2.81}$$

With $\tilde{u}=\tilde{g}-\tilde{p}\tilde{v}+T\tilde{s}$ the derivatives of the internal energy are directly

obtained from (2.81),

$$\begin{aligned}
\frac{\partial \tilde{u}}{\partial T} &= T\frac{\partial \tilde{s}}{\partial T} - \tilde{p}\frac{\partial \tilde{v}}{\partial T} + \sum_\alpha \tilde{v}\tilde{C}_\alpha \frac{\partial \tilde{I}_\alpha}{\partial T} \ , \\
\frac{\partial \tilde{u}}{\partial P} &= T\frac{\partial \tilde{s}}{\partial P} - \tilde{p}\frac{\partial \tilde{v}}{\partial P} + \sum_\alpha \tilde{v}\tilde{C}_\alpha \frac{\partial \tilde{I}_\alpha}{\partial P} \ , \\
\frac{\partial \tilde{u}}{\partial \xi} &= T\frac{\partial \tilde{s}}{\partial \xi} - \tilde{p}\frac{\partial \tilde{v}}{\partial \xi} + \sum_\alpha \tilde{v}\tilde{C}_\alpha \frac{\partial \tilde{I}_\alpha}{\partial \xi} - T\tilde{\wedge}^\xi \ , \\
\frac{\partial \tilde{u}}{\partial \Lambda_1} &= T\frac{\partial \tilde{s}}{\partial \lambda_1} - \tilde{p}\frac{\partial \tilde{v}}{\partial \lambda_1} + \sum_\alpha \tilde{v}\tilde{C}_\alpha \frac{\partial \tilde{I}_\alpha}{\partial \lambda_1} \ .
\end{aligned} \tag{2.82}$$

Finally, the derivatives of the free energy $\tilde{f} := \tilde{g} + \tilde{p}\tilde{v} = \tilde{u} - T\tilde{s}$ are

$$\begin{aligned}
\frac{\partial \tilde{f}}{\partial T} &= -\tilde{s} \quad - \tilde{p}\frac{\partial \tilde{v}}{\partial T} + \sum_\alpha \tilde{v}\tilde{C}_\alpha \frac{\partial \tilde{I}_\alpha}{\partial T} \ , \\
\frac{\partial \tilde{f}}{\partial P} &= \qquad -\tilde{p}\frac{\partial \tilde{v}}{\partial P} + \sum_\alpha \tilde{v}\tilde{C}_\alpha \frac{\partial \tilde{I}_\alpha}{\partial P} \ , \\
\frac{\partial \tilde{f}}{\partial \xi} &= -T\tilde{\wedge}^\xi - \tilde{p}\frac{\partial \tilde{v}}{\partial \xi} + \sum_\alpha \tilde{v}\tilde{C}_\alpha \frac{\partial \tilde{I}_\alpha}{\partial \xi} \ , \\
\frac{\partial \tilde{f}}{\partial \lambda_1} &= \qquad -\tilde{p}\frac{\partial \tilde{v}}{\partial \lambda_1} + \sum_\alpha \tilde{v}\tilde{C}_\alpha \frac{\partial \tilde{I}_\alpha}{\partial \lambda_1} \ .
\end{aligned} \tag{2.83}$$

2.2.1 Approximations

All relations given so far are generally valid. They are correspondingly complicated. Especially, the choice of the pressure as an independent state variable, seems to make the formulas complicated. However, they are in this form especially well suited for approximations. This will be demonstrated now.

2.2.1.1 Incompressible, thermoelastic materials

In the older theories of rubber-elasticity, Kuhn [41] , Mooney [52], Rivlin [55], it is assumed, that rubber is an *incompressible* thermoelastic material, whose elasticity is solely traced back to the deformation dependence of the entropy. This theory is included as a special case of ours, if we assume that no state quantity depends on crystallinity, that the internal energy is independent of deformation and that the specific volume is independent of temperature, pressure and deformation, namely

$$s = s(T, p, I_\alpha) \,, \quad u = u(T, p) \,, \quad v = v_R = \text{const} \,. \tag{2.84}$$

From the consequence of equations (2.84) and $(2.42)_7$, the stress coefficients are independent of pressure, and they are linear homogeneous functions of the (absolute) temperature

$$C_\alpha(T, I_\beta) = T\ K_\alpha(I_\beta)\ \ ,\ \ \frac{\partial K_1}{\partial I_2} = \frac{\partial K_2}{\partial I_1}\ . \tag{2.85}$$

The specific heat capacity depends only on temperature,

$$c_p = c_p(T)\ ,\ \ \frac{\partial c_p}{\partial p} = 0\ ,\ \ \frac{\partial c_p}{\partial I_\alpha} = 0\ , \tag{2.86}$$

the entropy is independent of pressure

$$\frac{\partial S}{\partial T} = \frac{c_p}{T},\ \ \frac{\partial S}{\partial p} = 0,\ \ \frac{\partial S}{\partial I_\alpha} = -v_R \frac{\partial C_\alpha}{\partial T}$$

and given by

$$\begin{aligned} s(T, I_\alpha) = \quad & s_R + \int_{T_R}^{T} \frac{c_p(T')}{T'} dT' - v_R \frac{\partial}{\partial T}\left[T\left(\int_3^{I_1} K_1(I_1', 3) dI_1' \right.\right. \\ & \left.\left. + \int_3^{I_2} K_2(I_1, I_2') dI_2' \right)\right], \end{aligned} \tag{2.87}$$

and the internal energy is only a function of temperature

$$u(T) = u_R + \int_{T_R}^{T} c_p(T')\ dT'\,. \tag{2.88}$$

For uni-axial extension, from (2.61) $\lambda_1 = \Lambda_1$ and from (2.70), we obtain

$$I_1 = \tilde{I}_1(\Lambda_1) = \Lambda_1^2 + \frac{2}{\Lambda_1}\ \ ,\ \ I_2 = \tilde{I}_2(\Lambda_1) = 2\Lambda_1 + \frac{1}{\Lambda_1^2}\,. \tag{2.89}$$

With this the stress coefficients (2.85) take the form

$$\tilde{C}_\alpha(T, \Lambda_1) = T\tilde{K}_\alpha(\Lambda_1)\,, \tag{2.90}$$

and the entropy and internal energy are

$$\begin{aligned} \tilde{s}(T, \Lambda_1) = \quad & s_R + \int_{T_R}^{T} \frac{c_p(T')}{T'} dT' - v_R \frac{\partial}{\partial T}\left[2T \int_1^{\Lambda_1} \left\langle \tilde{K}_1(\Lambda_1') + \frac{1}{\Lambda_1'} \tilde{K}_2(\Lambda_1') \right\rangle \right. \\ & \left. \times \left(\Lambda_1' - \frac{1}{\Lambda_1'^2} \right) d\Lambda_1' \right] \\ \tilde{u}(T) = \quad & u_R + \int_{T_R}^{T} c_p(T')\ dT' \quad . \end{aligned} \tag{2.91}$$

Finally, according to (2.67), for nominal extension the stress $\tilde{\sigma}_1$ follows as

$$\tilde{\sigma}_1 = 2T\left(\Lambda_1 - \frac{1}{\Lambda_1^2}\right)\left(\tilde{K}_1 + \frac{1}{\Lambda_1}\tilde{K}_2\right) = -\frac{1}{v_R}T\frac{\partial \tilde{s}}{\partial \Lambda_1} \quad . \tag{2.92}$$

This relationship shows that the nominal tension stress is given by the deformation derivative of the entropy. This behaviour is called *Entropy Elasticity* of rubber. This implies two effects which are typical for rubber:

1. If one increases the temperature at constant stress $\tilde{\sigma}_1$ and constant external pressure P, the rubber sample shrinks (Gough-effect)[28].

2. If one extends a rubber sample under adiabatic isolation (e.g. at constant entropy $\tilde{s}$), and constant external pressure, the temperature is increased (Joule-Effect [34])[2].

From (2.92) follows additionally, that the stress at constant deformation and constant external pressure is a linear homogeneous function of temperature,

$$\tilde{\sigma}_1 - T\frac{\partial \tilde{\sigma}_1}{\partial T} = 0\,. \tag{2.93}$$

This means graphically, that the stress-temperature curves at constant extension are straight lines which for extrapolation to $T \to 0$ approach the origin $\tilde{\sigma}_1 = 0$, and whose inclination increases with increasing deformation as explained by equation (2.92) and shown in figure 2.1.

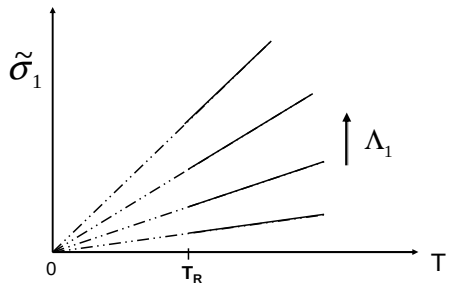

Figure 2.1: Stress-temperature curve of uniaxial extension.

In the statistical theories of rubber elasticity, first treated by Kuhn [42], it is assumed that the molecular chain between two crosslinking points can be divided

[2]For materials, which are essentially energy-elastic (e.g. metals) both effects are exactly reversed.

into (statistically equivalent) segments, which are connected to each other by free rotations. For this model the conformational entropy is calculated for small and medium deformations (strong coiling : $\frac{\text{distance crosslinking point}}{\text{Maximum length of stretched chain}} << 1$) in the so called Gaussian approximation, under the assumptions that crosslinking points move *affinely* to the macroscopic deformation and that the model substance is incompressible. From this model, there result constant stress coefficients,

$$v_R\tilde{K}_1 = \frac{k}{2Nm_o} \quad , \quad \tilde{K}_2 = 0\,. \tag{2.94}$$

Here, k is Boltzmann's constant, N is the number of segments between two crosslinking points, and m_o is the mass of *one* segment. The observed stress-strain curves can be described with this for small deformations. Especially, the effect is well described, that weakly cross-linked rubber can be deformed more easily than strongly cross-linked rubber.

For medium and large deformations the stress-strain behaviour is not correctly described by (2.94). The reason is, besides others, that the Gaussian approximation is employed for calculating the conformational entropy, even though for large deformations the strong coiling of the chain molecule is no longer valid. If one weakens this Gaussian assumption, then the conformational entropy can be calculated only approximately using a complicated Taylor series expansion in Λ_1, see Treloar [70]. With this one may derive by differentiation according to (2.92) a series expansion for the stress, which contains just one fitting parameter, $\frac{k}{Nm_o}\frac{1}{v_R}$.

In a continuum theory one has, in contrast to the statistical theory, two stress coefficients. Mooney [52] assumed that $\tilde{K}_1$ and $\tilde{K}_2$ are constants for uniaxial extension tests. With this, the measurements can be explained up to intermediate deformations. However, the steep upturn of the stress for large deformations cannot be described with constant values of stress coefficients.

Rivlin and Saunders [56] were able to describe also the steep upturn. They assume, that $\tilde{K}_1$ is constant and $\tilde{K}_2$ depends on the deformation. According to (2.85), $\tilde{K}_2$ can then depend only on the second deformation invariant,

$$K_1 = \text{const}\ , \quad K_2 = K_2(I_2)\,. \tag{2.95}$$

With this, Rivlin and Saunders can also explain quite well bi-axial stress-strain experiments, however they report, that K_2 seems to depend weekly on time in such a way that K_2, in the course of time, decreases at constant load. This time dependence cannot be understood with any theory of thermo-elasticity.

2.2.1.2 Incompressible, thermoelastic materials with thermal volume expansion

Mayer and Ferri [51] and Anthony, Casten and Guth [9] report, that the stress-temperature curve can be reproduced only, if as a deformation measure the thermal convective length ratio

$$\lambda_1 = \frac{L(T)}{L_o(T)} = \frac{\text{Length under load at temperature } T}{\text{Length without load at temperature } T}$$

is used as a curve parameter. If, however, the deformation measure $\Lambda_1 = \frac{L(T)}{L_R}$ is used, the measured curves for $T \to 0$ do not merge into the point $\tilde{\sigma}_1 = 0$. This observation is called *thermo-elastic inversion*. The relationship between the deformation measures λ_1 and Λ_1 is $\lambda_1 = \frac{L(T)}{L_R}\frac{L_R}{L_o(T)} = \Lambda_1 \left(\frac{v}{v_R}\right)^{-1/3}$ according to $(2.61)_1$. From this must be concluded, that for the description of the thermoelastic inversion the thermal convective deformation measure must be used.

The measurements show, that the nominal stress $\tilde{\sigma}_1$ in uni-axial extension at constant external pressure P and fixed thermal convective length ratio λ_1 is a homogeneous linear function of absolute temperature, i.e.,

$$\tilde{\sigma}_1 - T\left(\frac{\partial \tilde{\sigma}_1}{\partial T}\right)_{\lambda_1, P} = 0 \ , \tag{2.96}$$

For the stress coefficients, after insertion of (2.67), one obtains

$$\tilde{C}_\alpha(T, \lambda_1) = \left(\frac{v(T)}{v_R}\right)^{-2/3} T\tilde{K}_\alpha(\lambda_1) \qquad . \tag{2.97}$$

The stress coefficients are, consequently, not exactly linear in T (as in the approximation (2.85)), but they contain the volume factor $\left(\frac{v(T)}{v_R}\right)^{-2/3}$.

2.2.1.3 Continuum theory and Deformation-Induced Crystallization

For simplification of the theory, some approximations have been assumed about the specific volume $v = v(T, p, \xi, I_\alpha)$. We make now the following linear (Taylor) series expansion of the specific volume about the reference state:

$$v = v_R\left[1 + \alpha_o(T - T_R) + \beta_o(p - p_R) + \gamma_o(\xi - \xi_R) + \delta_o(I_1 - 3) + \varepsilon_o(I_2 - 3)\right] \tag{2.98}$$

For small departures of T, p, ξ, I_1, I_2 from the reference state values such an expansion should be valid.

The coefficients in this expansion are, in the reference state,

$$\begin{aligned}
\alpha_o &= \frac{1}{v_R}\left(\frac{\partial v}{\partial T}\right)_{p_R,\xi_R} &&= 6.6\times 10^{-4}\frac{1}{K}\,,\\
\beta_o &= \frac{1}{v_R}\left(\frac{\partial v}{\partial p}\right)_{T_R,\xi_R} &&= -5.1\times 10^{-5}\frac{1}{bar}\,,\\
\gamma_o &= \frac{1}{v_R}\left(\frac{\partial v}{\partial \xi}\right)_{T_R,p_R} &&,\\
\delta_o &= \tfrac{1}{v_R}\left(\tfrac{\partial v}{\partial I_1}\right)_{T_R,p_R,\xi_R} &&,\\
\varepsilon_o &= \tfrac{1}{v_R}\left(\tfrac{\partial v}{\partial I_2}\right)_{T_R,p_R,\xi_R} &&,
\end{aligned} \tag{2.99}$$

where α_o is the classical coefficient of thermal volume expansion, β_o the isothermal compressibility, γ_o the coefficient of volume expansion due to crystallization, δ_o and ε_o are volume expansion coefficients due to the deformation. The orders of magnitude of $\gamma_o, \delta_o, \varepsilon_o$ are unknown. Specialization to uniaxial extension at $T = T_R$ and $P = p_R$ yields, with (2.63) and (2.65),

$$\begin{aligned}
\bar{v} = \; v_R \;\Big[& 1 + \gamma_o(\xi - \xi_R) - \beta_o \frac{2}{3}(\lambda_1^2 - \frac{1}{\lambda_1})(C_1 + \frac{1}{\lambda_1}C_2) \\
+ \; & \delta_o(\lambda_1^2 + \frac{2}{\lambda_1} - 3) + \varepsilon_o(2\lambda_1 + \frac{1}{\lambda_1^2} - 3)\Big]\,.
\end{aligned} \tag{2.100}$$

For simplification, the change of volume with deformation is assumed to be linear, when $\bar{\xi} - \xi_R = \left(\frac{\partial \bar{\xi}}{\partial \lambda_1}\right)_{T_R,p_R,\lambda_1=1}(\lambda_1 - 1)$ holds. For the equilibrium volume thus follows

$$\begin{aligned}
v = \; v_R \;\Big[& 1 + \gamma_o\left(\frac{\partial \bar{\xi}}{\partial \lambda_1}\right)_{T_R,p_R}(\lambda_1 - 1) - \beta_o \frac{2}{3}(\lambda_1^2 - \frac{1}{\lambda_1})(\bar{C}_1 + \frac{1}{\lambda_1}\bar{C}_2) \\
+ \; & \delta_o(\lambda_1^2 + \frac{2}{\lambda_1} - 3) + \varepsilon_o(2\lambda_1 + \frac{1}{\lambda_1^2} - 3)\Big]\,.
\end{aligned} \tag{2.101}$$

$\bar{C}_\alpha = C_\alpha(T_R, p_R, \bar{\xi}, \lambda_1)$ $(\alpha = 1, 2)$ denote the values of the stress coefficients in crystallization equilibrium. For deformation up to 100% the Mooney approximation is valid. Then the stress-coefficients in equilibrium are independent of deformation and pressure, and functions of temperature alone, $\bar{C}_\alpha = C_\alpha(T_R)$. In this case, $\frac{\Delta\bar{v}}{v_R} = \frac{\bar{v} - v_R}{v_R}$ is a linear function of $\lambda_1 - 1$, only if $\beta_o = \delta_o = \varepsilon_o = 0$. This explains the experimental findings of Göritz [31].

The linear increase of volume up to deformations of about 100% can be explained only, if the compressibility and the dependence of the volume from the deformation invariants are neglected. Then,

$$v = v(T, \xi)\,. \tag{2.102}$$

This explains the linear increase of the specific equilibrium volume for small deformation ratios.

With the approximation (2.102) the formulas (2.42) to (2.45) simplify as follows:

$$\begin{aligned}
\frac{\partial C_\alpha}{\partial p} &= 0\,, \quad \frac{\partial C_1}{\partial I_2} = \frac{\partial C_2}{\partial I_1}\,, \\
\frac{\partial \wedge^\xi}{\partial p} &= -\frac{1}{T}\frac{\partial v}{\partial \xi}\,, \quad \frac{\partial \wedge^\xi}{\partial I_\alpha} = -\frac{1}{T}\frac{\partial (vC_\alpha)}{\partial \xi}\,, \\
\frac{\partial c_p}{\partial p} &= -\frac{1}{T}\frac{\partial^2 v}{\partial T^2}\ , \ \frac{\partial c_p}{\partial \xi} = -\frac{\partial}{\partial T}\left(T^2\frac{\partial \wedge^\xi}{\partial T}\right)\ , \ \frac{\partial c_p}{\partial I_\alpha} = -T\frac{\partial^2 (vC_\alpha)}{\partial T^2}\,, \\
\frac{\partial s}{\partial T} &= \frac{c_p}{T}\ , \ \frac{\partial s}{\partial p} = -\frac{\partial v}{\partial T}\ , \ \frac{\partial s}{\partial \xi} = \frac{\partial}{\partial T}(T\wedge^\xi), \ \frac{\partial s}{\partial I_\alpha} = -\frac{\partial (vC_\alpha)}{\partial T}\ , \\
\frac{\partial u}{\partial T} &= c_p - p\frac{\partial v}{\partial T}\ , \quad \frac{\partial u}{\partial p} = -T\frac{\partial v}{\partial T}, \quad \frac{\partial u}{\partial \xi} = T^2\frac{\partial \wedge^\xi}{\partial T} - p\frac{\partial v}{\partial \xi}\ , \\
\frac{\partial u}{\partial I_\alpha} &= vC_\alpha - T\frac{\partial (vC_\alpha)}{\partial T}\ .
\end{aligned} \tag{2.103}$$

The stress coefficients are consequently independent of the pressure.

These relations shall now be integrated, starting in the reference state $T = T_R,\ \ p = p_R,\ \ \xi = \xi_R,\ \ I_\alpha = 3$ $(\alpha = 1, 2)$. From $(2.103)_{3,4}$

$$\begin{aligned}
\wedge^\xi(T, p, \xi, I_\alpha) &= \bar{\wedge}^\xi(T, \xi) - \frac{1}{T}\frac{\partial v(T,\xi)}{\partial \xi}(p - p_R) \\
&\quad -\frac{1}{T}\frac{\partial}{\partial \xi}\left[v(T,\xi)\int_3^{I_1} C_1(T, \xi, I_1', 3)\, dI_1'\right] \\
&\quad -\frac{1}{T}\frac{\partial}{\partial \xi}\left[v(T,\xi)\int_3^{I_2} C_2(T, \xi, I_1, I_2')\, dI_2'\right]\ .
\end{aligned} \tag{2.104}$$

The integration function $\bar{\wedge}^\xi$ must be interpreted as $\wedge^\xi(T, p_R, \xi, 3, 3)$. The equilibrium values $\wedge^\xi|_{_E} = \wedge^\xi(T, p, \bar{\xi}, I_\alpha) = 0$ are zero according to (2.50). This implies, since the reference state has been chosen as an equilibrium state, that

$$\bar{\wedge}^\xi|_{_R} = \bar{\wedge}^\xi(T_R, p_R) = 0 \tag{2.105}$$

Moreover, with $\wedge^\xi|_{_E} = \wedge^\xi(T, p, \bar{\xi}, I_\alpha) = 0$, (2.104) is an equation for the determination of the equilibrium values $\xi|_{_E} = \bar{\xi}(T, p, I_\alpha)$ of the degree of crystallization outside the reference state.

Next we integrate formulas $(2.103)_{5-7}$ for the specific heat capacity. Use of

(2.104) yields

$$\begin{aligned} c_p(T,p,\xi,I_\alpha) &= \bar{c_p}(T) - T\frac{\partial^2 v(T,\xi)}{\partial T^2}(p-p_R) \\ &\quad + \frac{\partial}{\partial T}\left[T^2\frac{\partial}{\partial T}\int_{\xi_R}^{\xi}\bar{\wedge}^{\xi}(T,\xi')\,d\xi'\right] \\ &\quad - T\frac{\partial^2}{\partial T^2}\left[v(T,\xi)\int_3^{I_1} C_1(T,\xi,I_1',3)\,dI_1'\right] \\ &\quad - T\frac{\partial^2}{\partial T^2}\left[v(T,\xi)\int_3^{I_2} C_2(T,\xi,I_1,I_2')\,dI_2'\right] \quad . \end{aligned} \tag{2.106}$$

Here $\bar{c_p}(T)$ denotes the specific heat capacity at $p = p_R, \xi = \xi_R, I_1 = I_2 = 3$.

With this result, using (2.104), we now integrate formulas $(2.103)_{8-11}$ and $(2.103)_{12-15}$ for the specific entropy and the specific internal energy. After some calculation the following formulas are obtained:

$$\begin{aligned} s(T,p,\xi,I_\alpha) &= s_R + \int_{T_R}^{T}\frac{\bar{c}_p(T')}{T'}\,T' - \frac{\partial v(T,\xi)}{\partial T}(p-p_R) \\ &\quad + \frac{\partial}{\partial T}\left[T\int_{\xi_R}^{\xi}\bar{\wedge}^{\xi}(T,\xi')\,d\xi'\right] \\ &\quad - T\frac{\partial}{\partial T}\left[v(T,\xi)\int_3^{I_1} C_1(T,\xi,I_1',3)\,dI_1'\right] \\ &\quad - T\frac{\partial}{\partial T}\left[v(T,\xi)\int_3^{I_2} C_2(T,\xi,I_1,I_2')\,dI_2'\right] \quad , \end{aligned} \tag{2.107}$$

$$\begin{aligned} u(T,p,\xi,I_\alpha) &= u_R + \int_{T_R}^{T}\bar{c}_p\,dT' - p_R[v(T,\xi)-v_R] \\ &\quad - T\frac{\partial v(T,\xi)}{\partial T}(p-p_R) + T^2\frac{\partial}{\partial T}\int_{\xi_R}^{\xi}\bar{\wedge}^{\xi}(T,\xi')\,d\xi' \\ &\quad + \left[v(T,\xi)\int_3^{I_1} C_1(T,\xi,I_1',3)\,dI_I'\right] \\ &\quad + \left[v(T,\xi)\int_3^{I_2} C_2(T,\xi,I_1,I_2')\,dI_2'\right] \\ &\quad - T\frac{\partial}{\partial T}\left[v(T,\xi)\int_3^{I_1} C_1(T,\xi,I_1',3)\,dI_1'\right] \\ &\quad - T\frac{\partial}{\partial T}\left[v(T,\xi)\int_3^{I_2} C_2(T,\xi,I_1,I_2')\,dI_2'\right] \quad . \end{aligned} \tag{2.108}$$

s_R and u_R, respectively, denote the specific entropy and specific internal energy in the reference state.

The problem of deformation induced crystallization and the description of the related time effects (stress relaxation, hysteresis , reversible thermoplasticity, time delayed heat effects) would be solved, if $\bar{c}_p(T)$, $v(T,\xi)$, $\bar{\wedge}^{\xi}(T,\xi)$, $C_\alpha(T,\xi,I_1,I_2)$ would be known as functions of the given variables, and if the crystallization rate $A(T,p,\xi,I_\alpha)$ would be determined as a function of the given variables. The solution of the differential equation $(2.1)_5$ with $\psi_j = 0$ would determine $\xi(t)$ at fixed external pressure as a result of integration over the histories of deformation and temperature. Insertion of the result of integration (2.79) for $\xi(t)$ in (2.39), (2.107) and (2.108) will give the Cauchy stress $\mathbf{t}_{ij}$, the internal energy u and the entropy s as integrals over the histories of deformation and temperature.

However, the solution of this problem requires, first the determination of the explicit dependence of all involved functions upon their variables.

According to (2.63),(2.67), (2.102), (2.107) and (2.108) the formula for the nominal stress is

$$\sigma_1 = 2\left(\frac{v(T,\xi)}{v_R}\right)^{2/3}(\lambda_1 - \frac{1}{\lambda_1^2}) \quad \left[C_1(T,\xi,I_\alpha(\lambda_1)) + \frac{1}{\lambda_1}C_2(T,\xi,I_\alpha(\lambda_1))\right] \tag{2.109}$$

Based on (2.95) we assume in addition with Rivlin and Saunders [56] that the first stress coefficient is independent of I_α. Then, according to $(2.103)_2$, the second stress coefficient is independent of I_1:

$$C_1 = C_1(T,\xi) \quad , \quad C_2 = C_2(T,\xi,I_2) \ . \tag{2.110}$$

For qualitative understanding of stress-strain curves, one needs first the dependences of the stress coefficients C_α on the degree of crystallinity ξ. This will in sequel be derived within the framework of the statistical theory.

Chapter 3

Polymer Crystallization

Crystallization of polymers has been the focus of attention in the past four decades. It plays an important role in polymer applications, primarily in many manufacturing processes such as fiber spinning, extrusion drawing, film blowing, blow molding, and injection molding.

The mechanical behaviour of polymers is strongly depending on their morphology, which in turn is influenced by the thermo-mechanical history during processing. Molecular orientation affects the crystallization behaviour of polymers in two different aspects: thermodynamic and hydrodynamic. The thermodynamic effect involves the reduction of entropy in extended chains and this will increase the opportunity of crystal formation by increasing the melting point, while kinetically the extended chain is closer to a crystal state than a random chain. The hydrodynamic effect is a phase transformation, which is responsible for the resultant morphology such as shish, kebab or spherulite. Several on-going projects are designed to explore the underlying physics of this subject.

Mechanically, deformation induced crystallization in rubbery polymers produces internal inhomogeneity in their structure and leads to a significant redistribution of stresses, since the orientation of the crystals has a beneficial impact on the mechanical properties of the rubbery polymers. Crystallization of rubberlike polymer networks exhibits clear upturns in the stress-strain curve at high elongation. This is mainly due to the reinforcing effect of the crystallites that are generated.

3.1 Semi-Crystalline Polymers

Depending on the processing conditions, polymer-crystallization behaviour is attributed to the long chain length of the polymeric molecules, which makes

it difficult for these chains to disentangle from each other in disorganized and entangled melt and subsequently to achieve a regular conformation and align parallel to each other to form an ordered structure (i.e. crystal). Therefore, whether polymers are able to crystallize or not depends on their structure.

3.2 Models of Semi-Crystalline Polymers

The most obvious question that needs to be answered about polymer crystallites is '*How can long molecules give rise to small crystallites?*'. Two principal types of answer have been given: they lead to the *fringed-micelle* and the *chain-folded* model for polymer crystallites. A further type of crystallites is the *chain-extended* crystallite which will be discussed in detail.

3.2.1 Fringed-micelle model

The fringed-micelle model was an early attempt to inter-relate long molecules, small crystals and a 'sea' of amorphous material [22]. The crystalline regions are made up of different chains of short lengths aligned parallel to each other, while the amorphous regions are comprised of disordered conformations.

The model suggests the occurrence of *fibrillar crystallites*, which can grow both parallel and perpendicular to the chain axes. The long chain character of polymer allows a given chain to pass through several different crystallites [49, 48, 47] as shown in figure 3.1a. This model explains the mechanical properties of the sample based on the physical linkages (fringes) between two regions.

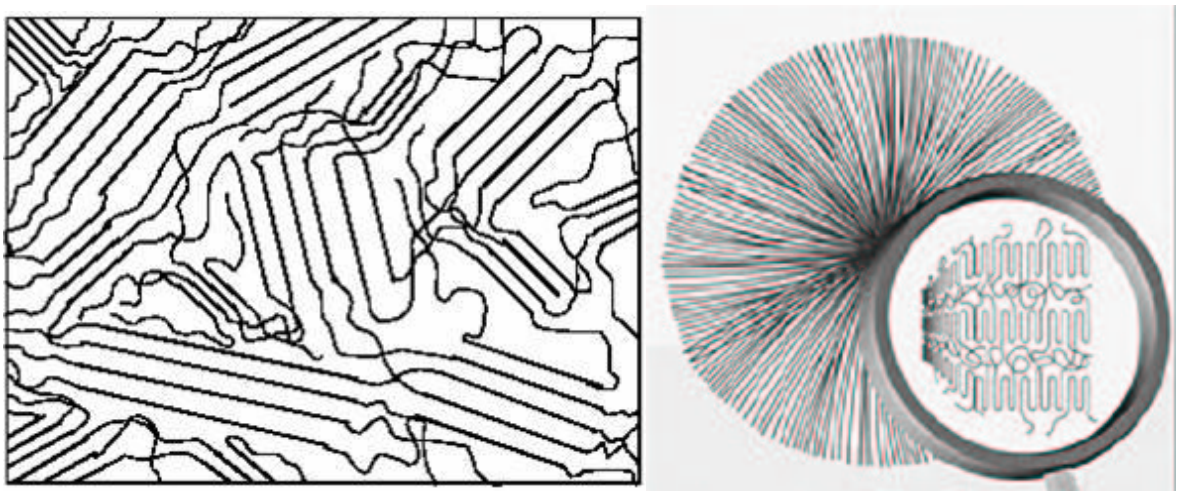

(a) (b)

Figure 3.1: Two different semi-crystalline structures: (a) Fringed-micelle structure (b) Spherulite structure.

3.2.2 Folded-chain model

It was reported by Keller [37, 38] that polyethylene single crystals, grown from a dilute solution, appear in the form of thin plates or *Lamellae* when viewed by electron diffraction to be composed of large crystallites with the chain axes normal to the plane of the lamellae. The only possibility to explain this was that chains folded back and forth upon themselves, so that adjacent segments were parallel and in crystal registers.

The adjacent re-entry model of Keller was challenged by Flory [24]. In an early theoretical treatment, Flory [24] examined some of the factors related to the generation of a crystalline phase from long chain molecules in random conformations. He established that "no more than half of the chains emanating from the lamellar crystal surface can be accommodated by the neighbouring disordered amorphous phase". As a result, more than half of those sequences must return to the crystal face from which they departed. This re-entry is proposed to occur via loops of varying lengths that are present in the spaces between the crystal and the amorphous regions. There also exist a number of chains that do not re-enter a given crystallite, but leave the basal plane of the crystal to become part of a disordered amorphous region. These chains could eventually enter another neighbouring crystallite. Such a possibility of chain folding is often referred to as the "switchboard model".

When crystallized from the melt, the lamellae often aggregate together in the form of a superstructure called a *spherulite*. Spherulites may be viewed as spherical aggregates of lamellae that originate from a common center and radiate outwards as shown in figure 3.1b. The spherical shape is formed as a result of branching and splaying of lamellae at dislocation points. Typical dimensions of spherulites are of the order of microns and sometimes, even millimeters. Therefore, they can be easily viewed under an optical microscope. The spherulites continue to grow radially until they impinge upon one another. A measure of their growth rate until the time of impingement provides a wealth of information regarding the mechanism of crystallization in the polymer, and has been the focus of several investigations.

3.2.3 Extended-chain crystallite

Extended, or fully extended, chain crystallites contain long oriented chains that can be formed mechanically. Crystallization induced by orientation can be described as stretching of long chains to form fibrous crystals. During stretching, distortion of chains from their most probable conformations results and hence a decrease in the conformational entropy takes place. If this deformation is maintained in this lower conformational entropy state then less conformational entropy needs to be sacrificed by transforming to a crystalline state. This decrease in to-

tal entropy of fusion allows the crystallization to occur at higher temperatures than will take place under quiescent conditions.

Natural and synthetic rubbers are excellent examples of such an effect as they show great tendency to crystallize under stretched conditions, whereas they crystallize slowly under quiescent conditions. Also, crystallization in an already oriented polymer results in a reduction of retractive force (with respect to the oriented state). This can be explained on the basis of rubber-elasticity theory according to which the force exerted by fixed chain ends is inversely proportional to the number of statistical segments and the magnitude of end to end distance. The reduction in force results because of a lesser number of statistical segments sitting in the amorphous domain and also because the end to end distance of the amorphous segments is smaller than that in the crystal. Melting of such extended crystals leads to contraction, and crystallization leads to elongation. That is why the deformation is considered to be of affine type, since macroscopic dimensional changes and changes in retractive force can be related to the crystal phase transformation.

The formation of the so-called 'Shish-Kebab' kind of morphology consists of the outside 'kebab-like' regions which are essentially folded chain regions comprised of chains which do not crystallize during the orientation process, while the inner 'shish' regions form first. The formation of folded chain discs occurs due to nucleation events taking place on the extended chain surface. This has been used as a strong argument in favor of kinetic theories that discuss the chain folded model of crystallization. Keller and Machin [39] showed essentially a perpendicularly oriented shish-kebab type lamellar morphology, they proposed a two step nucleation and growth for crystallization under orientation. The nucleation process is thought to be associated with the formation of extended chain shish from oriented molecules and the growth process is associated with the formation of lamellar crystals from an isotropic melt by chain folding onto the line nuclei. Alternatively, Yeh [45] revealed the presence of a nodular structure ($\sim 100\mathring{A}$) within perpendicularly oriented "lamellae". Indeed, Gent [26, 27] had concluded that the form and the magnitude of the stress changes during the crystallization of stretched networks are generally the same for different types of rubber. Thus, based on axial stress-relaxation evidence, Gent ruled out the possibility of chain folding during oriented crystallization.

Thermodynamically, if the coiled chains in a polymer melt are stretched, their entropy approaches that of the crystalline state. The difference between the entropies of the oriented and crystalline states decreases and thus, as indicated by equation (3.1), the melting point is raised. If the melting point is raised above the environment, stress crystallization takes place [72].

$$T_m^\circ = \Delta\mathbb{H}_\circ/\Delta\mathbb{S}_\circ \,, \tag{3.1}$$

where $\Delta\mathbb{H}_\circ$ and $\Delta\mathbb{S}_\circ$ are the enthalpy and the entropy of melting, respectively, defined as the changes in state for the conversion of 1 Mole from the crystal to the melt phase.

The following relationship was derived by Flory [21] for the dependence of the melting point on strain for a crosslinked elastomer:

$$1/T_m - 1/T_m^\circ = -(R/\Delta\mathbb{H}_\circ)\, g(\lambda)\ , \tag{3.2}$$

where the function $g(\lambda)$ - not the free enthalpy - depends on the type of applied chain statistics. According to Flory [21, 72]:

$$g(\lambda) = (6/\pi N)^{1/2}\lambda - (\lambda^2/2 + 1/\lambda)/N \tag{3.3}$$

where N is the number of statistical chain segments per network chain, and λ is the deformation ratio.

The foregoing brief survey of semi-crystalline polymers, with its emphasis on the importance of the types of crystalline chains would not be complete without a brief mention of amorphous polymer chains. The amorphous polymer chains are those with a randomly coiled and entangled state. They possess a large specific volume v_a compared with the crystalline volume v_c domain at room temperature. Thus, the total volume of a piece of rubber is given by

$$V = m_a v_a + m_c v_c\ , \tag{3.4}$$

where m_a is the amorphous mass and m_c is the crystalline mass. The total mass is consequently

$$m = m_a + m_c\ , \tag{3.5}$$

Accordingly, the specific volume of the rubber is given by the equation

$$v = (1-\xi)v_a + \xi v_c\ , \tag{3.6}$$

where ξ denotes the degree of crystallinity,

$$\xi = \frac{m_c}{m} = \frac{\text{Number of chain segment in crystallites}}{\text{Total number of chains segments}}\ . \tag{3.7}$$

Göritz [30] performed some experiments for cis-1,4-Polybutadiene rubber and reported a relationship between volume change and strain up to large extension; on the basis of an affine deformation this dependence is proportional to $\lambda - 1$, where λ is the extension ratio. Furthermore, he studied the elongation-induced

crystallization and found that the final degree of crystallization depends on temperature and elongation. The dependence on elongation does not follow Flory's theory of crystallization induced by stretching polymeric networks [21, 31].

Toki [68, 69] extensively studied the strain-induced crystallization phenomenon in sulfur vulcanized natural rubber by X-ray diffraction techniques. The detected structures were not only in a stretched but also in a relaxed state to accommodate the relatively weak X-ray intensity.

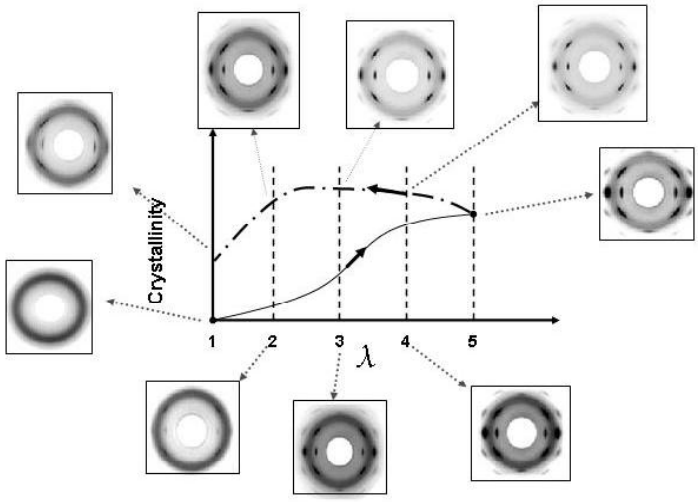

Figure 3.2: Structure change and selected Wide Angle X-ray Diffraction (WAXD) patterns during stretching and retraction process of rubber. Where λ is the deformation ratio.

The crystallization curve and selected Wide Angle X-ray Diffraction (WAXD) patterns during stretching and retraction are shown in figure 3.2 [1]. It is seen that highly oriented crystalline reflection peaks begin to appear at strains around $\lambda = 2.0$ at which orientation of the chain segments occurs. The intensity of these reflections increases with strain during stretching, and darker spots are noticed to form at the maximum stretching deformation ratio ($\lambda = 5.0$), while an amorphous halo is found to persist in WAXD during both processes of stretching and retraction (even at the highest applied strain). When the mechanical drawing ceases and the retraction process occurs, secondary crystallites develop, and stress relaxation is a direct consequence of folded lamella formation at the surface

[1]The WAXD patterns appearing in this figure have been taken from the work of S.Toki [68,69].

of extended-chain crystals. However, we believe that some of the strain-induced crystallites might transform their morphology to secondary crystallites that do not contribute to the stress. This is obvious since the reflection intensities will decrease if they are compared at the same deformation ratio for retraction and stretching processes. While the retraction unloading process is proceeding the crystallinity and the orientation are larger than during stretching at a certain deformation ratio. This can be noticed at all deformation ratios (e.g. $\lambda = 2.0$), see figure 3.2. This also is shown by WAXD pattern in figure 3.2 during retraction. For example, at the strain of 1.0, no crystalline pattern is observed during stretching but clear crystalline reflections are seen during retraction. This is a great evidence for shish-kebab formation during retraction due to stress relaxation which is responsible for having a hysteresis in the stress-strain curve. When that the strain-induced crystallites are totally molten at elevated temperature and no further folded crystallite types exist, then the crystallization curve coincides during the stretching and retraction processes.

Based on this, crystallites formed by deformation may be composed of two types:

Type 1. The important portion of the crystallites are the extended-chain crystallites that develop by the strain directly during stretching (loading process). These serve as nuclei for further crystallization.

Type 2. The secondary crystallite types are the folded-chain crystallites (lamellae, Shish-kebab structure). These develop during retraction on nuclei of extended type and may decrease or increase with retraction depending on the process conditions. Without a further increase in strain, this type of crystallite is able to form at low temperature.

3.3 Crystallization Kinetics

Our present concern is to simulate crystallization kinetics induced by deformation and taking place at different strain rates and temperatures. The simplest applicable differential equation for this process, according to irreversible thermodynamics, is the following first order equation

$$\dot{\xi} = \frac{-1}{\tau}(\xi - \bar{\xi}) \,, \tag{3.8}$$

where $\tau = \tau(T, \lambda, \xi)$ is the relaxation time and $\bar{\xi} = \bar{\xi}(T, \lambda)$ is the equilibrium crystallinity. For this we assume saturation behaviour:

$$\bar{\xi} = \bar{\xi_\circ} + (\bar{\xi_s} - \bar{\xi_\circ}) \tanh(\lambda - 1) \quad , \tag{3.9}$$

where $\bar{\xi_\circ}$ is the equilibrium crystallinity at the reference state, $\bar{\xi_s}$ is the equilibrium maximum (saturation) degree of crystallinity, and λ is the extension ratio defined as the ratio of the final to the initial length for uniaxial extension.

$\bar{\xi_\circ}$ and $\bar{\xi_s}$ are temperature dependent and given by the relations

$$\bar{\xi_\circ} = \frac{T_{mo} - T_o}{T_{mo} - T} \xi_\circ \quad , \tag{3.10}$$

$$\bar{\xi_s} = \frac{T_{mo} - T_o}{T_{mo} - T} \xi_s \quad , \tag{3.11}$$

where $T_{mo}\,,\ T_o\,,\ T$ are the melting (absolute) temperature, the reference temperature, and the temperature, respectively, $\xi_\circ$ is the degree of crystallinity at the reference state, while ξ_s is the maximum (saturation) degree of crystallinity at reference temperature.

After carrying out the integration and appropriate rearrangement of equation (3.8), we obtain

$$\xi(t) = \bar{\xi}(0)\, e^{-\int_0^t \frac{dt'}{\tau(t')}} + e^{-\int_0^t \frac{dx}{\tau(x)}} \int_0^t \left[\frac{\bar{\xi}(t')}{\tau(t')} \quad e^{\int_0^{t'} \frac{1}{\tau(t'')}\, dt''} \right] dt' \tag{3.12}$$

This equation implies two limiting cases that explain the content of the complicated relaxation behaviour and its effect on crystallization kinetics:

(A) In the limit of low temperatures, the relaxation time $\tau \longrightarrow \infty$ which is independent of strain rate. Then the crystallinity does not change with deformation: $\xi(t) = \bar{\xi}(0)$.

(B) In the limit of high temperatures, the relaxation time $\tau \longrightarrow 0$ which is independent of strain rate. Then, the crystallinity will be momentarily at an equilibrium state.

Between these two extreme cases there exists a time delay for the equilibrium approach which also is the reason for stress- and volume relaxations.

We consider now a loading process with constant loading speed $\dot{\varepsilon}$

$$\lambda_1(t) - 1 = \dot{\varepsilon} t \quad , \quad 0 \le t \le t_f\,, \tag{3.13}$$

where t is the loading time, and t_f is the loading time required to reach the maximum deformation ratio. Furthermore, we assume that the relaxation time τ is merely a function of temperature T namely

$$\tau(T) = a_L \ \exp[b_L/(\mathbb{R}T)] := \tau_L\,, \tag{3.14}$$

where a_L, b_L are constants and $\mathbb{R}$ is the universal gas constant. From the dimensions of the parameters a_L, b_L, it can be concluded that b_L is a jump energy per mole for crystallization, and a_L is an inverse jump frequency, and it is proportional to the jump probability of the chain segment for the transformation from amorphous to crystalline state.

For an isothermal *loading* process one may then deduce from (3.12), together with (3.9), (3.13) and (3.14),

$$\xi(t) = \bar{\xi}(0) + (\bar{\xi}_s - \bar{\xi}_\circ)\left[\tanh(\dot{\varepsilon}t) - e^{\frac{-t}{\tau_L}}\dot{\varepsilon}\tau_L \int_0^{\frac{t}{\tau_L}} \frac{e^x}{\cosh^2(\dot{\varepsilon}\tau_L x)}\, dx\right], \qquad (3.15)$$

$$\text{in } 0 \le t \le t_f \ .$$

The non-equilibrium crystallization at the end of the loading process is

$$\xi(t_f) = \bar{\xi}(0) + (\bar{\xi}_s - \bar{\xi}_\circ)\left[\tanh(\dot{\varepsilon}t_f) - e^{\frac{-t_f}{\tau_L}}\dot{\varepsilon}\tau_L \int_0^{\frac{t_f}{\tau_L}} \frac{e^x}{\cosh^2(\dot{\varepsilon}\tau_L x)}\, dx\right], \qquad (3.16)$$

where $\xi(t_f)$ is the degree of crystallinity at the maximum deformation ratio for the loading process and can be calculated directly from equation (3.15) for $t = t_f$.

Next, we consider the corresponding isothermal *unloading* process with reversed speed of deformation,

$$\lambda(t) = \lambda_f - \dot{\varepsilon}(t - t_f) \quad , \quad t_f \le t \le 2t_f \ , \qquad (3.17)$$

where λ_f is the maximum deformation ratio at the end of loading. Using (3.12) we obtain for the non-equilibrium crystallization in unloading

$$\xi(t) = e^{-\int_{t_f}^{t} \frac{dx}{\tau(x)}} \left\{ \xi(t_f) + \int_{t_f}^{t} \left[\frac{\bar{\xi}(t')}{\tau(t')} \quad e^{\int_{t_f}^{t'} \frac{dt''}{\tau(t'')}} \right] dt' \right\}, \qquad (3.18)$$

$$\text{for } t_f \le t \le 2t_f \ .$$

As mentioned before, in unloading, crystallite structures of *shish-kebab-types* are formed besides the extended crystallites of loading. This means, that the relaxation time in unloading is different from that in loading.

We assume again a constant relaxation time τ for isothermal unloading but assume otherwise a temperature dependence as follows:

$$\tau(T) = a_u \ \exp\left[b_u/(\mathbb{R}T)\right] := \tau_u \ . \qquad (3.19)$$

Insertion into (3.18) yields then for the crystallinity during an unloading process[2]

$$\begin{aligned}\xi(t) &= \xi(t_f)e^{-\frac{t-t_f}{\tau_u}} + \bar{\xi}_o\left(1 - e^{-\frac{t-t_f}{\tau_u}}\right) + (\bar{\xi}_s - \bar{\xi}_o)\Big\{ \tanh[(\lambda_f - 1) \\ &\quad -\dot{\varepsilon}(t - t_f)] - e^{-\frac{t-t_f}{\tau_u}} \tanh(\lambda_f - 1) \\ &\quad + e^{-\frac{t-t_f}{\tau_u}} . \dot{\varepsilon}\tau_u \int_0^{\frac{t-t_f}{\tau_u}} \frac{e^x}{\cosh^2[(\lambda_f - 1) - \dot{\varepsilon}\tau_u x]}\, dx \Big\} ,\end{aligned} \tag{3.20}$$

$$\text{for} \quad t_f \leq t \leq 2t_f \quad .$$

[2]The mathematical calculations of equations (3.15) and (3.20) are available upon request.

Chapter 4

Deformation-Induced Crystallization: Statistical Approach

4.1 Introduction

The rubber elasticity approach includes a great variety of descriptions, models and concepts. The research has started last century in the late thirties by Kuhn, Guth and H.F. Mark. It became a very active field in the forties and fifties with important contributions by Flory, James, Guth, Treloar, Wall and many other researchers, based mostly on the analysis of Gaussian chain models. The sixties and seventies were the times of the establishment of the basis for the statistical mechanical treatment of polymers and elastomeric materials, with fundamental works by Flory and many other scientists. In the seventies the computer technology of polymers became very important and the role of these simulations rapidly increased in the eighties and the nineties.

The simple, elementary statistical theory which paved the way to the current understanding of rubber elasticity was proposed in the pioneering work of Kuhn [41, 42]. Other important early contributions to the early rubber elasticity theory were given by Flory [21]. Flory was the first to develop a thermodynamic theory of strain induced crystallization which is considered to be the simplest and the most convenient among the multitude of the statistical theories. Starting from the simple model of Kuhn, Flory's theory is based on many simplifying assumptions. According to it, a rubber network consists of freely-joint Gaussian chains, of which the positions of crosslinking points deform affinely upon deformation. Each chain contains a certain number of statistically equivalent rigid and simply connected segments with complete freedom of orientation. Flory, imposing

the assumption of constant volume, calculated the changes of the crystalline and amorphous entropies with deformation. So far, the following crucial points of worthiness may be mentioned: (i) Flory's theory is based on the assumption that, the change of entropy is unequal to zero in the undeformed state, in contradiction to his assumption since he performed his calculations starting from the totally crystalline network; (ii) the change of entropy in the deformed state approaches for complete crystallization a negative infinitely large value.

Flory's theory is inadequate to describe real rubber, because of his assumptions, that *there is no crystallization in the undeformed state, and that complete crystallization is possible*. Both assumptions are not consistent with reality.

In the present context, we correct the shortcomings of Flory's theory. We return to the picture of freely-joint chains crosslinked at junction points, of which the motions are affine to the macroscopic deformation. A modified Gaussian distribution is employed for chains of finite lengths to describe the end-to-end vector distribution function and the contribution of that chain to crystallinity.

4.2 Overview of the Model

In our model, we start treating the amorphous chain. According to Kuhn [41, 42], we shall be concerned primarily with those statistical properties which may conveniently be dealt with in terms of an idealized chain of N numbers of freely rotating equivalent segments of length ℓ. (A "chain" is defined as that portion of the network extending from one crosslinking point to the next [21], as shown in figure 4.1).

Figure 4.1: Example of a long chain of freely rotating segments.

The statistical form of the long-chain molecule is illustrated by figure 4.2, in which the angle between successive segments (i.e. the valence angle) is fixed but complete freedom of rotation of any given segment with respect to adjacent segments in the chain is allowed. The actual chain conformation will be subject to continual fluctuation due to thermal agitation which enhances these segments to shift at a rapid rate from one position to another, consistent with their attachments to neighbouring segments of the same chain and the availability of free space in their immediate environment [21, 70].

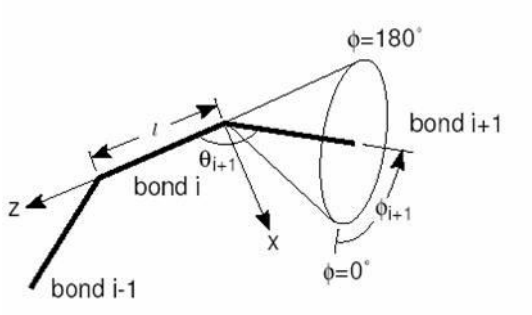

Figure 4.2: Statistical schematic of a freely rotating segments around bonds.

Polymers can exist in various *conformations* and various *configurations*. Two polymers which differ only by rotations about single bonds are said to be two conformations of that polymer. A schematic view of two polymer conformations is shown in figure 4.3. Two polymers which have the same chemical composition but can only be made identical (e.g. superposable) by breaking and reforming bonds are said to be two configurations of that polymer. No manner of rotations about single bonds can turn polymers in different configurational states into superposable polymers.

The above definitions of *conformations* and *configurations* are standard, but they have not always been rigorously followed in the literature. For example, Flory used configuration in his writings when he meant conformation. Fortunately a writer's meaning is usually obvious from the context.

There are different ways to characterize the size of a polymer chain. The *contour length* L is the total length of a stretched chain,

$$L = N\ell \tag{4.1}$$

The contour length has a fixed value, no matter what the value of the chain conformation.

The so called *freely joint chain* (figure 4.1), or *random walk* model is employed to get the averages over all the possible chain conformations. In this model

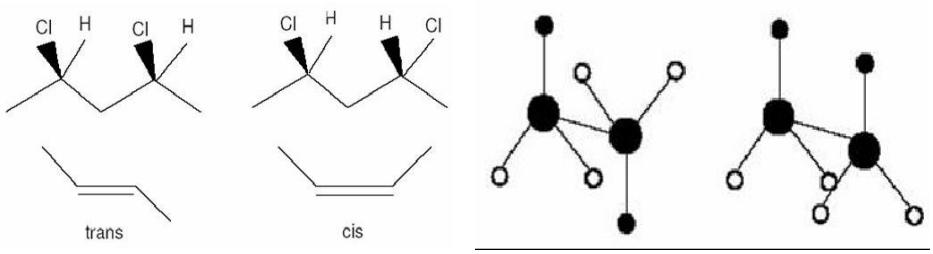

(a) (b)

Figure 4.3: A schematic view of (a) polymer configuration and (b) polymer conformation.

the angle of each segment is independent of every other, including the nearest neighbouring segments. To describe it, another measure of polymer chain size is needed, the *end-to-end* vector. It is used when a chain is in a given conformation as shown in figure 4.4. The end-to-end length varies from one chain conformation to the next. The end-to-end vector $\mathbf{r}$ is the vector sum over the bonds $\boldsymbol{\ell}_i$ for bonds i=1,2,3,...,N

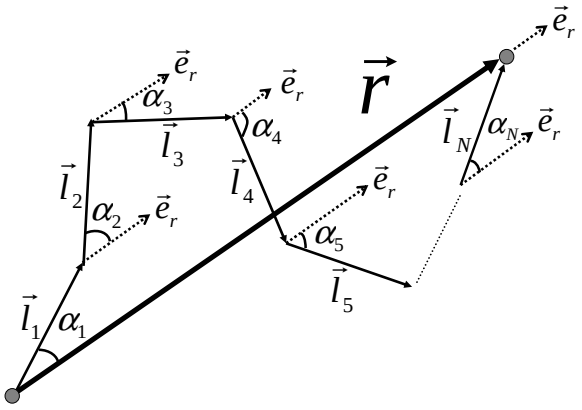

Figure 4.4: End-to-end chain length, with N segments: five segments are shown somewhere in the chain, the remaining ones of which are represented by the dotted line till the N^{th} segment. The angle α_i is the angle between the i^{th} segment and the $\mathbf{r}$ axis.

$$\mathbf{r} = \sum_{i=1}^{N} \boldsymbol{\ell}_i \,. \tag{4.2}$$

The end-to-end length can not be greater than the contour length. The end-to-end length changes when a polymer is subjected to applied forces.

The z-component of the end-to-end vector is

$$r_z = \sum_{i=1}^{N} z_i, \tag{4.3}$$

where $z_i = \ell \cos\alpha_i$ is the projection on the $z_i - axis$ of the ith vector and α_i is the angle of segment i relative to the $z_i - axis$. If all the segment vectors have the same length ℓ, then

$$r_z = \ell \sum_{i=1}^{N} \cos\alpha_i. \tag{4.4}$$

The mean value of the end-to-end vector does not contain useful information, since it equals zero ($\langle r \rangle = 0$). This is so because the average over randomly oriented vectors is $\langle \cos\alpha_i \rangle = 0$ assuming that all conformations have equal probabilities. Thus, the *mean square root* (rms) is a more expressive quantity for the conformation of the polymer chain [70]. So,

$$\langle r_z^2 \rangle = N\ell^2. \tag{4.5}$$

Fully stretched, the size of the chain is determined by its contour length, $L = N\ell$. In its undeformed state, its average size is $\langle r_z^2 \rangle^{1/2} = N^{1/2}\ell$, so a polymer chain can be stretched by nearly a factor of $\sqrt{N}$. However, this model suffers from severe simplifications. The chains do not interact with any environment. Even as a single chain model this is a dramatic simplification, since the chain can interact with itself.

It is important to realize, since we start treating the amorphous chain in our model, that all conformations of the chain described within this theory are purely entropic. The shape of the chain is driven purely by entropy. This means that

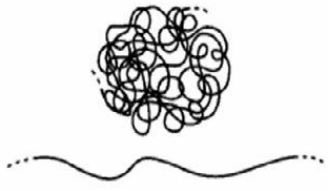

Figure 4.5: Conformational change in polymer.

the mean square root of the chain fluctuates around its value given by equation (4.5).

The shape, or "conformation" of a polymer molecule can range from the fully extended chain to the randomly coiled sphere as shown in figure 4.5. The extended chain picture is the way we might choose to draw a polymer structure. The random coil picture, however, is a more realistic view of the shape of real polymer molecules. Statistically, the coiled shape is much more likely than the extended one, simply because there are so many ways the chain can be coiled and only one way it can be fully extended.

4.2.1 Thermodynamic approach of an amorphous network

To understand why rubbers are elastic, the full distribution function of the end-to-end lengths is needed to count all the stretched and all the coiled conformations of a polymer chain. More precisely, we would like to know how many different conformations of the chain have the same end-to-end vector. Thus, Gaussian distribution is used in this context for the probability of a conformation of the end-to-end vector of a randomly wriggling segment.

In the context of our recent model, we start treating the amorphous chain. According to Kuhn [41, 42], the number of conformations of the simply connected chain from N statistically equivalent segments of length ℓ for a given end-to-end distance $\mathbf{R}$ and under the prerequisite of large coiling $\frac{R}{L} = \frac{R}{N\ell} << 1$ is given by

$$W(\mathbf{R}) = K(\frac{\beta}{\sqrt{\pi}})^3 \exp\left[-\beta^2 \mathbf{R}^2\right], \tag{4.6}$$

where β is a measure for the average end-to-end distance in the standard models of random walk,

$$\beta^2 = \frac{3}{2\ell}\frac{1}{L}, \tag{4.7}$$

K is a proportionality constant, and L is the length of the totally stretched molecular chain.

Carved on the tombstone of Ludwig Boltzmann in the Zentralfriedhof (central cemetery) in Vienna as shown in figure 4.6, is the inscription

$$S \;=\; k \log W. \tag{4.8}$$

This equation is the historical foundation of statistical mechanics. It connects the microscopic and macroscopic properties. It defines the *entropy* S, a macroscopic quantity, in terms of the multiplicity W of the microscopic degrees of freedom of a system. For thermodynamics, $k = 1.380662 \times 10^{-23} JK^{-1}$ is a quantity

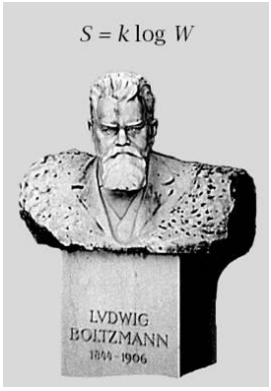

Figure 4.6: Boltzmann grave stone in Vienna.

called Boltzmann's constant, and Boltzmann's inscription refers to the natural logarithm, $\log_e = \ln$.

Employing this fundamental equation (4.8) of Boltzmann's formula to calculate the entropy of <u>one</u> chain molecule, will yield immediately the expression

$$H(\theta_i) \quad = \quad k[3\,\ln(\frac{\beta}{\sqrt{\pi}})] - \beta^2(\theta_1^2+\theta_2^2+\theta_3^2)] + k\,\ln K\ . \tag{4.9}$$

The number of chains with one end at the origin and the other end within the interval $(\theta_i, \theta_i + d\theta_i)$ is proportional to equation (4.6) and given by

$$Z(\theta_i)\,d\theta_1\,d\theta_2\,d\theta_3 \quad = \quad C\left(\frac{\beta}{\sqrt{\pi}}\right)^3 \exp\left[-\beta^2(\theta_1^2+\theta_2^2+\theta_3^2)\right]\ \ d\theta_1\,d\theta_2\,d\theta_3\ , \tag{4.10}$$

where C is a constant that is determined by the requirement that the total number of the chains in the material is σ . Then,

$$\int_{-\infty}^{\infty}\int_{-\infty}^{\infty}\int_{-\infty}^{\infty} Z(\theta_i)\,d\theta_1\,d\theta_2\,d\theta_3 \quad = \quad \sigma = C \tag{4.11}$$

must hold. Rubbers and polymeric elastomers are chemically or physically crosslinked networks of polymer chains. The end points of the molecular chain are the crosslinking points. One of the simplest and earliest assumptions regarding microscopic deformation in networks is that the crosslinking points in the network move *affinely* with the macroscopic deformation, which means that every part of the specimen deforms as does the whole (this is the elastic assumption). If one lays the co-ordinate axes of the chosen Cartesian co-ordinate system in the Eigen directions of the stretch tensor, the crosslinking points are shifted as shown in figure 4.7 according to

$$\vartheta_1 = \Lambda_1\theta_1 \quad , \quad \vartheta_2 = \Lambda_2\theta_2 \quad , \quad \vartheta_3 = \Lambda_3\theta_3\ . \tag{4.12}$$

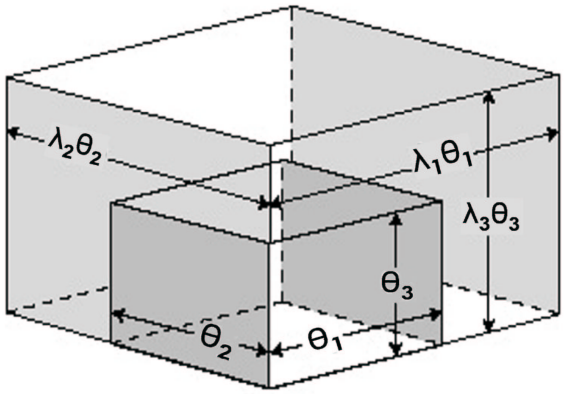

Figure 4.7: An *affine* deformation of a material.

Hence, the entropy of *one* chain molecule with affinely deformed endpoints is

$$H(\vartheta_i) \;=\; k[3\,\ln(\frac{\beta}{\sqrt{\pi}}) - \beta^2(\vartheta_1^2+\vartheta_2^2+\vartheta_3^2)] + k\,\ln K\;. \tag{4.13}$$

Since an affine deformation of endpoints does not change the number of chains of the network, one has

$$z(\vartheta_i)\;\; d\vartheta_1\, d\vartheta_2\, d\vartheta_3 \;=\; Z(\theta_i)\;\; d\theta_1\, d\theta_2\, d\theta_3\;. \tag{4.14}$$

According to equations (4.10) (4.12), the number of chains for the affinely deformed network is

$$z(\vartheta_i) \;=\; \frac{\sigma}{\Lambda_1\Lambda_2\Lambda_3}\left(\frac{\beta}{\sqrt{\pi}}\right)^3 \exp\left[-\beta^2(\frac{\vartheta_1^2}{\Lambda_1^2}+\frac{\vartheta_2^2}{\Lambda_2^2}+\frac{\vartheta_3^2}{\Lambda_3^2})\right] \tag{4.15}$$

The entropies of the amorphous rubber in the undeformed and deformed states are then

$$\begin{aligned} S_o \;&=\; \int_{-\infty}^{\infty}\int_{-\infty}^{\infty}\int_{-\infty}^{\infty} H(\theta_i)\;\; Z(\theta_i)\;\; d\theta_1\, d\theta_2\, d\theta_3 \\ &=\; \sigma k\left[3\,\ln\left(\frac{\beta}{\sqrt{\pi}}\right) - \frac{3}{2} + \ln K\right]\;, \end{aligned} \tag{4.16}$$

and

$$\begin{aligned} S_a \;&=\; \int_{-\infty}^{\infty}\int_{-\infty}^{\infty}\int_{-\infty}^{\infty} H(\vartheta_i)\;\; z(\vartheta_i)\;\; d\vartheta_1\, d\vartheta_2\, d\vartheta_3 \\ &=\; \int_{-\infty}^{\infty}\int_{-\infty}^{\infty}\int_{-\infty}^{\infty} H(\vartheta_i)\;\; Z(\theta_i)\;\; d\theta_1\, d\theta_2\, d\theta_3 \\ &=\; \sigma k\left[3\ln\left(\frac{\beta}{\sqrt{\pi}}\right) - \frac{1}{2}(\Lambda_1^2+\Lambda_2^2+\Lambda_3^2) + \ln K\right]\;. \end{aligned} \tag{4.17}$$

The specific entropy of amorphous rubber can be expressed if one refers to a mass unit, by division through the mass of network chains

$$m = \sigma N m_o \,, \tag{4.18}$$

where m_o is the mass of a segment. Thus, the specific entropy of the amorphous rubber networks is

$$s_a = s_o - \frac{1}{2}\frac{k}{N m_o}(\Lambda_1^2 + \Lambda_2^2 + \Lambda_3^2 - 3) \,, \tag{4.19}$$

and this delivers just the stress coefficients (2.95) of the statistical theory for pure entropy elasticity.

4.2.2 Thermodynamic approach of a partially crystalline network

The main purpose now is to propose a model that describes the deformation induced crystallization of a network with partially crystallized chains. The undeformed amorphous state has been chosen as a reference state for the entropy.

For partial crystallization some changes on the conformational entropy of the molecular chain must be made, since the molecular chain passes through different domains, mainly, amorphous and crystalline domains. However, when the chain folds back to form a crystalline phase (lamellae), part of the amorphous chain forms closed loops which are free of force at the beginning of the deformation, until breakage of the crystalline folded-chains occurs, and then these closed loop chains become exposed to force. According to figure 4.8, the total number of chain segments N is the summation of segments which are sitting in the crystalline domains and those in the amorphous domains. The amorphous domain segments include segments which are exposed to deformation forces and those segments sitting in the closed loops. Let ζ be the number of segments sitting within a crystalline domain (folded chain) in the chain. Then the total number of segments is given by

$$N = \underbrace{\zeta}_{\substack{\text{crystalline}\\ \text{chain}\\ \text{segments}}} + \underbrace{N_{force} + N_{loops}}_{\substack{\text{amorphous}\\ \text{chain}\\ \text{segments}}} \,, \tag{4.20}$$

where N is the total number of chain segments, N_{force} is the number of segments exposed to deformation stress, and N_{loops} is the number of segments sitting in the force-free closed loops.

Both N_{force} and N_{loops} have full conformational freedom. However with deformation, the number of segments exposed to force, N_{force} increases as the folded

lamellae break. This breakage occurs at the early stages of deformation. Consequently, many loops will be opened and hence become part of the main chain which is exposed to force. This process continues until all loops are opened and all folded-parallel crystallites become extended. As a result, the number of segments exposed to uniaxial stress N_{force}, will become equal to the total number of chain segments N.

The total length of the extended chain of N segments of length ℓ is shortened as shown by the following equation and illustrated in figure 4.8.

$$L_\xi = L - \zeta\ell + d = N\ell(1 - \frac{\zeta}{N} + \frac{d}{N\ell}) \, . \tag{4.21}$$

The degree of crystallinity ξ is introduced by

$$\xi \;\; = \;\; \frac{\zeta}{N} = \frac{m_c}{m} \, , \tag{4.22}$$

where m_c is the mass of the crystalline segments, m is the total mass of the chain, and $d = |\mathbf{d}|$ is the distance between the inlet and the exit of the chains to the crystalline domain. This distance vector is proportional to the degree of crystallinity and is expressible as

$$\mathbf{d} \;\; = \;\; \mathbf{a} N\ell \, \xi \, , \tag{4.23}$$

where $a = |\mathbf{a}|$ is a parameter of the theory depending on the type of crystallites. For parallel unfolded crystallites $a = 1$, and for folded or mixture type crystallites $a < 1$.

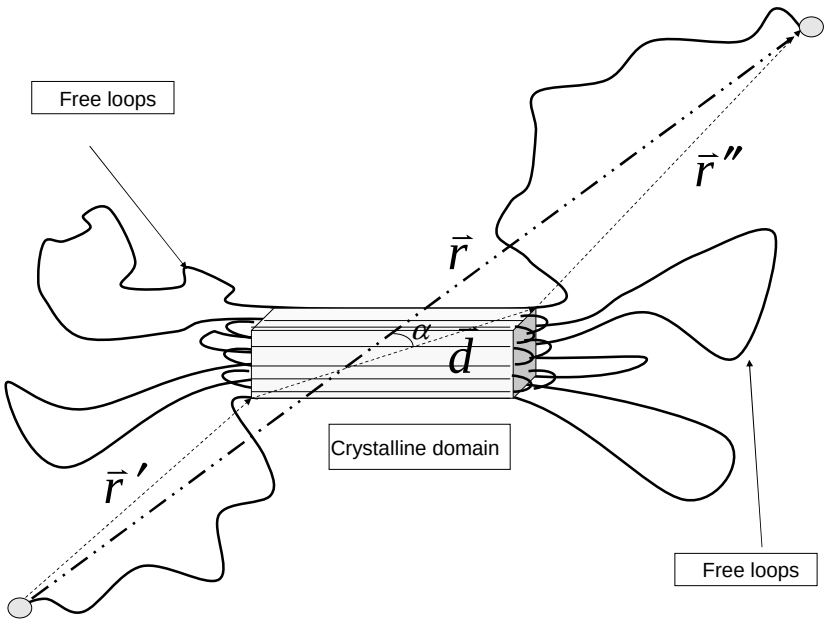

Figure 4.8: A schematic of the proposed model of partially crystalline chain .

Consequently, the total length of the stretched and partially crystallized chain is

$$L_\xi \;=\; L(1-\xi+a\xi)\,. \tag{4.24}$$

The length of the crystallite is equal to the length of the extended chain whenever complete crystallization exists (which, theoretically, is never realized in crosslinked network) and parallel crystallites with $a = 1$ are formed. This will be consistent with equation (4.1) that $L_{\xi=1} = a\,L$.

When the length of the amorphous chain L in equation (4.7) is replaced by the length of the partially crystalline chain L_ξ, the parameter β becomes

$$\beta_\xi^2 = \frac{3}{2\ell}\frac{1}{L_\xi} = \beta^2\frac{1}{(1-\xi+a\xi)}\,. \tag{4.25}$$

Since the parameter β is related to the mean square distance of the free chain ends by $\frac{3}{2\beta^2} = \langle r^2\rangle$, an increase from β to β_ξ means a reduction of the square root mean of the chain by crystallization. Consequently, a piece of rubber with free surfaces shrinks when it is crystallized.

The crystalline domains are relatively immobile compared to the chain segments within the amorphous chain. This means that $\zeta = N\xi$ segments within the crystallites are frozen. Hence, the number of conformations of the $N-\zeta$ segments of the amorphous remainder of the chain is then

$$W_\xi(\mathbf{r}'+\mathbf{r}'') \;=\; K_\xi\left(\frac{\beta_\xi}{\sqrt{\pi}}\right)^3\exp\left[-\beta_\xi^2(\mathbf{r}'+\mathbf{r}'')^2\right], \tag{4.26}$$

where

$$\mathbf{r}'+\mathbf{r}'' = \mathbf{r}-\mathbf{d}\,. \tag{4.27}$$

As shown in figure 4.8, equation (4.27) is the sum of possible statistical shifts of the $N-\zeta$ segments in the amorphous rest chain for a given distance vector $\mathbf{r}$ and given distance vector $\mathbf{d}$ between the inlet point and the exit point of the chain in the crystallite.

The partially crystallized chain still contains a very large number of degrees of freedom. Therefore, Boltzmann's formula (4.8) is applicable to calculate the conformational entropy of *the* chain. With equations (4.26) and (4.27) there follows

$$\begin{aligned} H_\xi(\mathbf{r},\mathbf{d}) &= k\,\ln W_\xi \\ &= k[3\,\ln\left(\frac{\beta_\xi}{\sqrt{\pi}}\right) - {\beta_\xi}^2(\mathbf{r}-\mathbf{d})^2 + \ln K_\xi] \\ &= k\left[3\,\ln(\frac{\beta_\xi}{\sqrt{\pi}}) - {\beta_\xi}^2(r^2 - 2\,r\,d\,\cos\alpha + d^2) + \ln K_\xi\right], \end{aligned} \tag{4.28}$$

where α is the angle between the distance vector $\mathbf{d}$ and the distance vector $\mathbf{r}$. Evidently, the value of α depends on the distance $r = |\mathbf{r}|$ of the chain end points and the "diameter" $d = |\mathbf{d}|$ of the crystallite. With increasing r and d the angle α decreases in the mean, i.e., the crystallites in the mean are directed into the direction of the chain endpoints as well as by deformation and by crystallization, respectively.

For the calculation of the mean value $\langle \cos\alpha \rangle$ of $\cos\alpha$ in equation (4.28) one needs the probability density for the angle α as shown in figure 4.8 at fixed values of r and d. From (4.26) and (4.27) this is

$$w_\xi(\alpha; r; d) = C \exp(A \cos\alpha)\,, \qquad A := \beta_\xi^2\, 2\, r\, d\,, \tag{4.29}$$

where C is a constant that can be determined by the requirement that $w_\xi(\alpha; r; d)$ is normalized to the complete solid angle, so that

$$\int_0^\pi \int_0^{2\pi} w_\xi(\alpha; r; d)\, \sin\alpha\, d\alpha\, d\varphi = C\, 4\pi \frac{\sinh(A)}{A} = 1\,, \tag{4.30}$$

For the mean value of $\cos\alpha$ there follows then

$$\langle \cos\alpha \rangle \;=\; \mathscr{L}(A) = \coth A - \frac{1}{A}\,, \tag{4.31}$$

where $\mathscr{L}(A)$ denotes the Langevin Function.

The mean value of the entropy (4.28) over all angles α at fixed values of r and d is then

$$\begin{aligned} \langle H_\xi(\mathbf{r}, \mathbf{d}) \rangle \;=\; & k\big[3 \ln\left(\frac{\beta_\xi}{\sqrt{\pi}}\right) - {\beta_\xi}^2 (r^2 + d^2) \\ & + {\beta_\xi}^2\, 2\, r\, d\, \mathscr{L}({\beta_\xi}^2\, 2\, r\, d) + \ln K_\xi\big]\,. \end{aligned} \tag{4.32}$$

If one end point of the chain is in the origin of a Cartesian co-ordinate system and the other end point is at (x_1, x_2, x_3), then r in equation (4.32) is to be replaced by

$$r \;=\; \sqrt{x_1^2 + x_2^2 + x_3^2}\,. \tag{4.33}$$

As a special case of equation (4.32) the mean entropy of a chain with degree of crystallinity ξ_R, with one end point of the chain in the origin and the other end at (X_1, X_2, X_3), is as follows

$$\begin{aligned} \langle H_{\xi_R}(\mathbf{R}, \mathbf{d}_R) \rangle \;=\; & k\big[3 \ln\left(\frac{\beta_R}{\sqrt{\pi}}\right) - {\beta_R}^2 (R^2 + d_R^2) \\ & + {\beta_R}^2\, 2\; R\, d_R\, \mathscr{L}({\beta_R}^2\, 2\, R\, d_R) + \ln K_R\big]\,, \end{aligned} \tag{4.34}$$

where $R = \sqrt{X_1^2 + X_2^2 + X_3^2}$ is the end-to-end distance between the chain ends, $d_R = aN\ell\xi_R$ is the distance between the chain input and output to the crystallite, and $\beta_R^2 = \beta^2 \frac{1}{1-\xi_R+a\xi_R}$ is the radius of inertia of the partially crystallized chain of ξ_R.

For preparation of the subsequent calculations we need some formulae. These are the approximations [1]

$$\begin{aligned} z\,\mathscr{L}(z) &= \frac{1}{3}z^2 - \frac{1}{45}z^4\,, \qquad in \quad 0 \le z \le 2\,, \\ z\,\mathscr{L}(z) &= z - 1\,, \qquad\qquad in \quad 2 \le z \end{aligned} \tag{4.35}$$

for the Langevin Function, the error integral

$$\mathrm{erf}(z) := \frac{2}{\sqrt{\pi}} \int_0^z \exp\left(-x^2\right) dx\,, \tag{4.36}$$

and the integrals

$$\begin{aligned} \int_0^{z^2} x^{\frac{1}{2}} e^{-x} dx &= \frac{\sqrt{\pi}}{2} f_1(z)\ , \\ \int_0^{z^2} x^{\frac{3}{2}} e^{-x} dx &= \frac{3\sqrt{\pi}}{4} f_2(z)\ , \\ \int_0^{z^2} x^{\frac{5}{2}} e^{-x} dx &= \frac{15\sqrt{\pi}}{8} f_3(z)\ , \\ \int_0^{z^2} x e^{-x} dx &= 1 - (1+z^2)e^{-z^2} := 1 + \frac{\sqrt{\pi}}{2}\ f_4(z)\ , \end{aligned} \tag{4.37}$$

where the functions $f_i(z)$ are given by the following expressions

$$\begin{aligned} f_1(z) &:= \mathrm{erf}(z) - \frac{2}{\sqrt{\pi}}\, z\, e^{-z^2}\,, \\ f_2(z) &:= \mathrm{erf}(z) - \frac{2}{\sqrt{\pi}}\, z\, (1 + \frac{2}{3}z^2) e^{-z^2}\,, \\ f_3(z) &:= \mathrm{erf}(z) - \frac{2}{\sqrt{\pi}}\, z\, (1 + \frac{2}{3}z^2 + \frac{4}{15}z^4) e^{-z^2}\,. \end{aligned} \tag{4.38}$$

Numerical calculation yields for large arguments z :

$$f_i(z) = 1 \qquad \text{for } z \ge 4\,, \qquad i = 1, 2, 3\,. \tag{4.39}$$

The entropy of the partially crystallized rubber can be calculated, if the distribution function for the number of chains is known. The number of chains is given for the purely amorphous material with *finite chain length* $L = N\ell$

$$Z_o(\theta_i)\; d\theta_1\, d\theta_2\, d\theta_3 = \sigma \left(\frac{\beta}{\sqrt{\pi}}\right)^3 \frac{1}{f_1(\beta L)} \exp[-\beta^2(\theta_1^2 + \theta_2^2 + \theta_3^2)]\; d\theta_1\, d\theta_2\, d\theta_3\ . \tag{4.40}$$

Here $f_1(\beta L)$ comes from the finite chain length concept. However, this equation is the same as equation (4.10) for *infinite chain length*, once $L \to \infty$ then $f_1(\beta L) = 1$.

Since with crystallization no chains disappear, the number of chains in the partially crystalline state is the same as in the amorphous undeformed reference state $|_o$. Then, one necessarily has

$$Z_R(X_i)\, dX_1\, dX_2\, dX_3 \;=\; Z_o(\theta_i)\, d\theta_1\, d\theta_2\, d\theta_3\,, \tag{4.41}$$

for the partially crystallized chain, of which the endpoints in the undeformed state $|_R$ have the distance R. However, for the partially crystallized chains with distance r in the deformed state the following expression is valid

$$z_r(x_i)\, dx_1\, dx_2\, dx_3 \;=\; Z_o(\theta_i)\, d\theta_1\, d\theta_2\, d\theta_3\,. \tag{4.42}$$

To get the distribution function $Z_R(X_i)$ with respect to $z_r(x_i)$, one must know how the cross linking points $(\theta_1^2+\theta_2^2+\theta_3^2)$ of the undeformed amorphous reference state $|_o$ are transformed to the cross linking points (X_1, X_2, X_3) in the reference state $|_R$ of the partially crystalline undeformed material. Furthermore the crosslinking points (x_1, x_2, x_3) of the partially crystalline and deformed state must be related to either one, $|_o$ or $|_R$, of the undeformed states.

The transformation from the amorphous reference state $|_o$ with specific volume v_o to the partially crystalline reference state $|_R$ with specific volume v_R is connected with volume shrinkage. If crystallization takes place at constant hydrostatic external pressure p_R, the corresponding (affine) shift of all crosslinking points is isotropic so that

$$X_i \;=\; \Lambda_c \theta_i \qquad (i = 1, 2, 3)\,, \quad \text{where} \quad \Lambda_c = \left(\frac{v_R}{v_o}\right)^{\frac{1}{3}}\,. \tag{4.43}$$

Equations (4.41) and (4.40) imply

$$Z_R(X_i) = \frac{\sigma}{f_1(\beta L)} \left(\frac{\gamma}{\sqrt{\pi}}\right)^3 \exp\left[-\gamma^2 (X_1^2 + X_2^2 + X_3^2)\right]\,, \tag{4.44}$$

with

$$\gamma := \beta \left(\frac{v_o}{v_R}\right)^{\frac{1}{3}}\,. \tag{4.45}$$

The transformation from the amorphous reference state $|_o$ to the deformed partially crystalline state goes via the partially crystalline (undeformed) reference state $|_R$. The total shift of the crosslinking points is then

$$x_1 = \Lambda_1 \Lambda_c \theta_1 \;\;, \quad x_2 = \Lambda_2 \Lambda_c \theta_2 \;\;, \quad x_3 = \Lambda_3 \Lambda_c \theta_3\,. \tag{4.46}$$

Inserting equation (4.46) into equation (4.42) with the help of equation (4.40), the following equation can be obtained

$$z_r(x_i) \;=\; \frac{1}{\Lambda_1\Lambda_2\Lambda_3}\;\frac{\sigma}{f_1(\beta L)}\left(\frac{\gamma}{\sqrt{\pi}}\right)^3 exp\Big[-\gamma^2(\frac{x_1^2}{\Lambda_1^2}+\frac{x_2^2}{\Lambda_2^2}+\frac{x_3^2}{\Lambda_3^2})\Big]\;. \quad (4.47)$$

Now, the conformational entropy can be calculated for a partially crystallized network at the undeformed reference state $|_R$,

$$S_{KR} = \int\int\int \langle H_{\xi R}(\mathbf{R},\mathbf{d}_R)\rangle\, Z_R(X_i)\; dX_1\, dX_2\, dX_3\;. \quad (4.48)$$

Inserting equations (4.35) and (4.44) yields, after transformation to spherical coordinates and performance of the angular integrations,

$$\begin{aligned} S_{KR} \;=\; & \frac{\sigma k}{f_1(\beta L)}\left(\frac{\gamma}{\sqrt{\pi}}\right)^3 4\pi\big[3\,\ln(\frac{\beta_R}{\sqrt{\pi}}) - {\beta_R}^2\, d_R^2 \\ & + \ln K_R\big]\int_{d_R}^{L_R} R^2\, e^{\left(-\gamma^2R^2\right)}\, dR - \frac{\sigma k}{f_1(\beta L)}(\frac{\gamma}{\sqrt{\pi}})^3\, 4\pi\, \beta_R^2 \\ & \times \int_{d_R}^{L_R}[R^4 - 2\,R^3\, d_R\, \mathscr{L}(\beta_R^2\, 2\,R\, d_R)]e^{(-\gamma^2R^2)}\; dR\;. \end{aligned} \quad (4.49)$$

The R-integration must be performed from the smallest possible distance d_R of the crosslinking points to the largest possible distance $L_R = N\ell(1-\xi_R) + d_R$ of the partially crystalline chain. For the theoretical limit of complete crystallization $\xi_R = 1$ one has $L_R = d_R = aN\ell$, and the integrals in (4.49) vanish. This means, that the conformational entropy vanishes in the completely crystallized state, as it must do so.

The conformational entropy of the purely amorphous reference state $|_o$ is the other limiting case. This is obtained, if $\xi_R = 0$ and $v_R = v_o$ is chosen. With equations (4.40) or (4.44) and equation (4.23) we then obtain ($d = 0$, $\gamma = \beta$)

$$\begin{aligned} S_o \;=\; & \frac{\sigma k}{f_1(\beta L)}\left(\frac{\beta}{\sqrt{\pi}}\right)^3 4\pi\left[3\,\ln(\frac{\beta_R}{\sqrt{\pi}}) + \ln K_o\right]\int_0^L R^2 e^{-\beta^2R^2}\; dR \\ & -\frac{\sigma k}{f_1(\beta L)}\left(\frac{\beta}{\sqrt{\pi}}\right)^3 4\pi\beta^2\int_0^L R^4 e^{-\beta^2R^2}\; dR\;. \end{aligned} \quad (4.50)$$

In the statistical theory of amorphous rubber one normally replaces the upper integration limit $L = N\ell$ by ∞. We will not do that, in order to have a smooth connection to the partially crystallized reference state.

The integrations for the conformational entropy in the undeformed amorphous state $|_o$ can also be performed with the result

$$S_o = \sigma k\left[3\,\ln\left(\frac{\beta}{\sqrt{\pi}}\right) + \ln K_o\right] - \sigma\, k\,\frac{3}{2}\;\frac{f_2(\beta L)}{f_1(\beta L)}\;. \quad (4.51)$$

In the following we insert the approximations (4.35) for the Langevin Function into equation (4.49). Separating the integration interval in domains $d_R \leq R \leq \frac{1}{\beta_R^2 d_R}$ and $\frac{1}{\beta_R^2 d_R} \leq R \leq L_R$ and performing the integrations yields for the configurational entropy of the undeformed and partially crystalline reference state[1] $|_R$

$$\begin{aligned} S_{KR} &= \frac{\sigma k}{f_1(\beta L)} \left[3 \ln \left(\frac{\beta_R}{\sqrt{\pi}} \right) - {\beta_R}^2 d_R^2 + \ln K_R \right] [f_1(\gamma L_R) - f_1(\gamma d_R)] \\ &\quad - \frac{\sigma k}{f_1(\beta L)} \frac{3}{2} \frac{\beta_R^2}{\gamma^2} [f_2(\gamma L_R) - f_2(\gamma d_R)] \\ &\quad + \frac{\sigma k}{f_1(\beta L)} He(d_R \leq D_R) \frac{3}{2} \frac{\beta_R^2}{\gamma^2} \left\{ \frac{4}{3} {\beta_R}^2 d_R^2 [f_2(\gamma D_R) - f_2(\gamma d_R)] \right. \\ &\quad \left. - \frac{8}{9} \frac{\beta_R^6 d_R^4}{\gamma^2} [f_3(\gamma D_R) - f_3(\gamma d_R)] \right\} \\ &\quad - \frac{\sigma k}{f_1(\beta L)} He(D_R \leq L_R) \left\{ [f_1(\gamma L_R) - f_1(\gamma D_R)] \right. \\ &\quad \left. - \frac{2 \beta_R^2 d_R}{\gamma} [f_4(\gamma L_R) - f_4(\gamma D_R)] \right\}, \end{aligned} \tag{4.52}$$

with

$$\begin{aligned} He(x \leq y) &:= \left\{ \begin{array}{lll} 1 & \text{for} & x \leq y \\ 0 & \text{for} & x > y \end{array} \right\}, \\ D_R &= D(\xi_R) := \inf_{0 \leq \xi_R \leq 1} \left\{ \frac{1}{\beta_R^2 d_R}, L_R \right\}, \end{aligned}$$

where $He(x \leq y)$ is the Heaviside unit jump that is used to distinguish both integration intervals of the Langevin function for its approximation shown by equation (4.35).

It is pointed out, that the parameter $\ln K_R$, besides the parameters N and ℓ, depends in addition on the macroscopic variables ξ_R, T_R, p_R. The form of this dependence is not given by the statistical theory. We have to determine this by reasonable macroscopic requirements. This will be done later on.

The purely amorphous limit of equation (4.51) results as a special case for $\xi_R = 0$ and $v_R = v_o$, if $\ln K_{R_{|\xi_R=0}} = \ln K_o$. The theoretical limit of complete

[1] The computations of equation (4.52) have been done analytically and they are available upon request.

crystallization[2] is $d_{R_{|\xi_R=1}} = L_{R_{|\xi_R=1}} = D_{R_{|\xi_R=1}}$. The conformational entropy of equation (4.52) is then zero, as it must be.

In the sequel, the conformational entropy in the deformed and partially crystallized state of crystallinity ξ is calculated starting from the following expressions

$$S_K = \int\int\int \langle H_\xi(\mathbf{r},\mathbf{d})\rangle z_r(x_i)\; dx_1 dx_2 dx_3 \quad . \tag{4.53}$$

If one inserts the expressions in (4.32) for the mean conformational entropy of *one* chain and (4.47) for the distribution of the chain end points and if one introduces the isochoric deformations along the eigen-axes of deformation,

$$\lambda_i = (\frac{v}{v_R})^{-\frac{1}{3}}\Lambda_i \qquad (i=1,2,3)\;, \qquad \lambda_1\lambda_2\lambda_3 = 1\,, \tag{4.54}$$

then the following can be obtained

$$\begin{aligned} S_K &= \frac{\sigma k}{f_1(\beta L)}\left(\frac{\delta}{\sqrt{\pi}}\right)^3 \int\int\int \left[3\,\ln\left(\frac{\beta_\xi}{\sqrt{\pi}}\right) - \beta_\xi^2\,(r^2+d^2) + \ln K_\xi \right. \\ &\left. +\beta_\xi^2\, 2r\, d\,\mathscr{L}(\beta_\xi^2\, 2\, r\, d)\right] \exp\left[-\delta^2(\frac{x_1^2}{\lambda_1^2}+\frac{x_2^2}{\lambda_2^2}+\frac{x_3^2}{\lambda_3^2})\right] dx_1\, dx_2\, dx_3, \end{aligned} \tag{4.55}$$

where δ is the abbreviation

$$\delta := \beta(\frac{v_o}{v})^{\frac{1}{3}} \quad . \tag{4.56}$$

To incorporate the integration limits spherical coordinates $x_1 = r\cos\vartheta\,, \quad x_2 = r\,\sin\vartheta\,\cos\varphi\,, \quad x_3 = r\,\sin\vartheta\,\sin\varphi$ are introduced. The integration limits are the $d \le r \le L_\xi = N\ell(1-\xi)+d,\; 0\le\vartheta\le\pi, \quad 0\le\varphi\le 2\pi$. For the entropy thence follows

$$\begin{aligned} S_K &= \frac{\sigma k}{f_1(\beta L)}(\frac{\delta}{\sqrt{\pi}})^3 \int_0^\pi d\vartheta \int_0^{2\pi} d\varphi \int_d^{L_\xi} dr\; r^2\,\sin\vartheta \times \exp(-\delta^2\mu r^2) \\ &\times\left[3\ln(\frac{\beta_\xi}{\sqrt{\pi}}) - \beta_\xi^2\,(r^2+d^2) + \beta_\xi^2\, 2\, r\, d\,\mathscr{L}(\beta_\xi^2\, 2\, r\, d) + \ln K_\xi\right], \end{aligned} \tag{4.57}$$

where μ is the abbreviation

$$\mu(\vartheta,\varphi,\lambda_i) := \frac{\cos^2\vartheta}{\lambda_1^2} + \frac{\sin^2\vartheta\;\cos^2\varphi}{\lambda_2^2} + \frac{\sin^2\vartheta\;\sin^2\varphi}{\lambda_3^2} \tag{4.58}$$

and

$$\delta = \beta(\frac{v_o}{v})^{\frac{1}{3}} = \beta_\xi = \beta\frac{1}{\sqrt{1-\xi+a\xi}} \quad . \tag{4.59}$$

[2]In crosslinked high polymers; complete crystallization is not possible due to steric hindrances of the chemical bonds around the cross links (excluded volume). The degree of crystallinity varies consequently between $0 \le \xi \le \xi_{\max} < 1$.

The $r-$integration can be performed at once using the approximation (4.35) for the Langevin function and using the relations (4.37). After some calculation one obtains[3]

$$\begin{aligned} S_K &= \frac{\sigma k}{f_1(\beta L)}\left[3\ln\left(\frac{\beta_\xi}{\sqrt{\pi}}\right)-\beta_\xi^2\,d^2+\ln K_\xi\right]\left[F_1(\delta L_\xi,\lambda_i)-F_1(\delta d,\lambda_i)\right] \\ &-\frac{\sigma k}{f_1(\beta L)}\,\frac{3}{2}\,\frac{\beta_\xi^2}{\delta^2}\left[F_2(\delta L_\xi,\lambda_i)-F_2(\delta d,\lambda_i)\right] \\ &+\frac{\sigma k}{f_1(\beta L)}\,He(d\le D_\xi)\,\frac{3}{2}\,\frac{\beta_\xi^2}{\delta^2}\left\{\frac{4}{3}{\beta_\xi}^2 d^2\left[F_2(\delta D_\xi,\lambda_i)-F_2(\delta d,\lambda_i)\right]\right. \\ &\left.-\frac{8}{9}\,\frac{\beta_\xi^6 d^4}{\delta^2}\left[F_3(\delta D_\xi,\lambda_i)-F_3(\delta d,\lambda_i)\right]\right\} \\ &-\frac{\sigma k}{f_1(\beta L)}\,He(D_\xi\le L_\xi)\left\{\left[F_1(\delta L_\xi,\lambda_i)-F_1(\delta D_\xi,\lambda_i)\right]\right. \\ &\left.-\frac{2\beta_\xi^2 d}{\delta}\left[F_4(\delta L_\xi,\lambda_i)-F_4(\delta D_\xi,\lambda_i)\right]\right\}, \end{aligned} \tag{4.60}$$

with

$$\begin{aligned} He(x\le y) &:= \left\{\begin{array}{lll} 1 & \text{for} & x\le y \\ 0 & \text{for} & x>y \end{array}\right\}, \\ D_\xi &= D(\xi) := \inf_{0\le\xi_R\le 1}\left\{\frac{1}{\beta_\xi^2 d}, L_\xi\right\}. \end{aligned}$$

The functions F_1, F_2, F_3, F_4 are given by the integrals

$$\begin{aligned} F_1(\alpha;\lambda_i) &= \frac{1}{4\pi}\int_0^\pi\int_0^{2\pi}\frac{1}{\mu^{3/2}}\,f_1(\alpha\mu^{1/2})\,\sin\vartheta\,d\vartheta\,d\varphi\,, \\ F_2(\alpha;\lambda_i) &= \frac{1}{4\pi}\int_0^\pi\int_0^{2\pi}\frac{1}{\mu^{5/2}}\,f_2(\alpha\mu^{1/2})\,\sin\vartheta\,d\vartheta\,d\varphi\,, \\ F_3(\alpha;\lambda_i) &= \frac{1}{4\pi}\int_0^\pi\int_0^{2\pi}\frac{1}{\mu^{7/2}}\,f_3(\alpha\mu^{1/2})\,\sin\vartheta\,d\vartheta\,d\varphi\,, \\ F_4(\alpha;\lambda_i) &= \frac{1}{4\pi}\int_0^\pi\int_0^{2\pi}\frac{1}{\mu^{2}}\,f_4(\alpha\mu^{1/2})\,\sin\vartheta\,d\vartheta\,d\varphi\,, \end{aligned} \tag{4.61}$$

for $\alpha=\delta L_\xi$ or $\alpha=\delta d$ or $\alpha=\delta D_\xi$.
For the undeformed, partially crystallized reference state $|_R$ with $\xi=\xi_R$ and

[3]The computations of equation (4.60) have been done analytically and they are available upon request.

$\lambda_i = 1$ $(i = 1, 2, 3)$ are $\mu = 1$, $\delta = \gamma$, $d = d_R$, $\beta_\xi = \beta_R$, and $D_\xi = D_R$. Then, $F_a(\alpha_R; 1) = f_a(\alpha_R)$ $(a = 1, 2, 3, 4)$ for $\alpha_R = \gamma L_R$, $\alpha_R = \gamma d_R$, $\alpha_R = \gamma D_R$, respectively.

The major problem is now the performance of the integrations (4.61). For simplification we consider uniaxial extension. If $\lambda_1 \geq 1$ is the isochoric length ratio in the direction of extension, then

$$\lambda_2 = \lambda_3 = \frac{1}{\sqrt{\lambda_1}} \, . \tag{4.62}$$

According to equation (4.58), μ is then independent of the angle φ and given by

$$\mu = \lambda_1 \left[1 - (1 - \frac{1}{\lambda_1^3}) \cos^2 \vartheta \right] \, . \tag{4.63}$$

The φ-integration in equation (4.61) can be performed directly. After substitution of

$$\omega = \sqrt{(1 - \frac{1}{\lambda_1^3}) \cos^2 \vartheta} \tag{4.64}$$

and integration by parts in ω, using the relations

$$\begin{aligned}
\frac{1}{(1-\omega^2)^{3/2}} &= \frac{d}{d\omega} \left[\frac{\omega}{(1-\omega^2)^{1/2}} \right] , \\
\frac{1}{(1-\omega^2)^{5/2}} &= \frac{d}{d\omega} \left[\frac{\omega}{(1-\omega^2)^{3/2}} + 2 \frac{\omega}{(1-\omega^2)^{1/2}} \right] , \\
\frac{1}{(1-\omega^2)^{7/2}} &= \frac{d}{d\omega} \left[\frac{\omega}{(1-\omega^2)^{5/2}} + \frac{4}{3} \frac{\omega}{(1-\omega^2)^{3/2}} + \frac{8}{3} \frac{\omega}{(1-\omega^2)^{1/2}} \right] , \\
\frac{1}{(1-\omega^2)^2} &= \frac{1}{2} \frac{d}{d\omega} \left[\frac{\omega}{(1-\omega^2)} + \operatorname{artanh}(\omega) \right] , \\
\frac{1}{(1-\omega^2)} &= \frac{d}{d\omega} \left[\operatorname{artanh}(\omega) \right] ; \\
e^{-\alpha^2 \lambda_1 (1-\omega^2)} &= 1 - (1-\omega^2) \int_0^{\alpha^2 \lambda_1} e^{-\beta(1-\omega^2)} \, d\beta \, ,
\end{aligned} \tag{4.65}$$

the further substitution of $y = \alpha^2 \lambda_1 \omega^2$ and integration by parts once more using

equations (4.38) and $(4.37)_4$,then yields[4]

$$
\begin{aligned}
F_1(\alpha;\lambda_1) &= f_1(\frac{\alpha}{\lambda_1}) + \frac{2}{\sqrt{\pi}}\frac{\alpha}{\lambda_1}\, e^{-\frac{\alpha^2}{\lambda_1^2}} - \frac{2}{\sqrt{\pi}}\frac{1}{\lambda_1^{3/2}\sqrt{D}}\, e^{-\alpha^2\lambda_1}\int_0^{\alpha\sqrt{\lambda_1 D}} e^{x^2}\,dx \\
&= \operatorname{erf}(\frac{\alpha}{\lambda_1}) - \frac{2}{\sqrt{\pi}}\frac{1}{\lambda_1^{3/2}\sqrt{D}} e^{\frac{-\alpha^2}{\lambda_1^2}}\mathbb{D}(\alpha\sqrt{\lambda_1 D}) \quad , \\
F_2(\alpha;\lambda_1) &= \frac{1}{3}(\lambda_1^2 + \frac{2}{\lambda_1})\, f_2(\frac{\alpha}{\lambda_1}) + \frac{2}{\sqrt{\pi}}\frac{2}{3}\frac{\alpha}{\lambda_1}\, e^{\frac{-\alpha^2}{\lambda_1^2}}\left[\alpha^2\frac{1}{3}(1+\frac{2}{\lambda_1^3}) + \frac{1}{\lambda_1}\right] \\
&\quad -\frac{2}{\sqrt{\pi}}\frac{2}{3}\left[\alpha^2 + \frac{1}{\lambda_1}\right]\frac{1}{\lambda_1^{3/2}\sqrt{D}}\, e^{-\alpha^2\lambda_1}\int_0^{\alpha\sqrt{\lambda_1 D}} e^{x^2}\,dx \\
&= \frac{1}{3}\left(\lambda_1^2 + \frac{2}{\lambda_1}\right)\operatorname{erf}(\frac{\alpha}{\lambda_1}) - \frac{2}{\sqrt{\pi}}\frac{1}{3}\alpha\lambda_1\, e^{-\frac{\alpha^2}{\lambda_1^2}} \\
&\quad -\frac{2}{\sqrt{\pi}}\frac{2}{3}(\alpha^2 + \frac{1}{\lambda_1})\frac{1}{\lambda_1^{3/2}\sqrt{D}} e^{\frac{-\alpha^2}{\lambda_1^2}}\mathbb{D}(\alpha\sqrt{\lambda_1 D}) \quad , \\
F_3(\alpha;\lambda_1) &= \frac{1}{5}(\lambda_1^4 + \frac{4}{3}\lambda_1 + \frac{8}{3}\frac{1}{\lambda_1^2})\, f_3(\frac{\alpha}{\lambda_1}) \qquad (4.66) \\
&\quad +\frac{2}{\sqrt{\pi}}\frac{4}{15}\frac{\alpha}{\lambda_1}\, e^{\frac{-\alpha^2}{\lambda_1^2}}\left[\frac{\alpha^4}{5}\left(1+\frac{4}{3}\frac{1}{\lambda_1^3}+\frac{8}{3}\frac{1}{\lambda_1^6}\right) - \frac{4}{3}\frac{\alpha^2}{\lambda_1}\left(1-\frac{1}{\lambda_1^3}\right)\right. \\
&\quad \left.+\frac{2}{\lambda_1}\left(\alpha^2+\frac{1}{\lambda_1}\right)\right] \\
&\quad -\frac{2}{\sqrt{\pi}}\frac{4}{15}\left[\alpha^4 + \frac{2}{\lambda_1}\left(\alpha^2+\frac{1}{\lambda_1}\right)\right]\frac{1}{\lambda_1^{3/2}\sqrt{D}} e^{-\alpha^2\lambda_1}\int_0^{\alpha\sqrt{\lambda_1 D}} e^{x^2}\,dx \\
&= \frac{1}{5}(\lambda_1^4 + \frac{4}{3}\lambda_1 + \frac{8}{3}\frac{1}{\lambda_1^2})\operatorname{erf}(\frac{\alpha}{\lambda_1}) \\
&\quad -\frac{2}{\sqrt{\pi}}\frac{2}{15}\alpha\lambda_1\left[\alpha^2 + \frac{2}{\lambda_1}(1+\frac{4}{3}\lambda_1^3)\right] e^{-\frac{\alpha^2}{\lambda_1^2}} \\
&\quad -\frac{2}{\sqrt{\pi}}\frac{4}{15}\left[\alpha^4 + \frac{2}{\lambda_1}(\alpha^2+\frac{1}{\lambda_1})\right]\frac{1}{\lambda_1^{3/2}\sqrt{D}}\, e^{-\frac{\alpha^2}{\lambda_1^2}}\mathbb{D}(\alpha\sqrt{\lambda_1 D}) \quad , \\
F_4(\alpha;\lambda_1) &= \frac{2}{\sqrt{\pi}}\frac{1}{\lambda_1^2\sqrt{D}}\left[\int_0^{\alpha\sqrt{\lambda_1}} e^{-y^2}\int_0^{y\sqrt{D}}\left(e^{x^2}\,dx\right)dy - \frac{1}{2}\operatorname{artanh}(\sqrt{D})\right] \\
&\quad -\frac{2}{\sqrt{\pi}}\frac{\lambda_1}{2}\, e^{\frac{-\alpha^2}{\lambda_1^2}} - \frac{2}{\sqrt{\pi}}\frac{\alpha}{\lambda_1}\frac{e^{-\alpha^2\lambda_1}}{\sqrt{\lambda_1 D}}\int_0^{\alpha\sqrt{\lambda_1 D}} e^{x^2}\,dx \\
&= \frac{1}{\sqrt{\lambda_1 D}}\mathbb{D}\operatorname{erf}(\lambda_1\sqrt{\lambda_1 D};\frac{\alpha}{\lambda_1}) - \frac{2}{\sqrt{\pi}}\frac{1}{2\lambda_1^2\sqrt{D}}\operatorname{artanh}(\sqrt{D}) \\
&\quad -\frac{2}{\sqrt{\pi}}\frac{\lambda_1}{2}\, e^{\frac{-\alpha^2}{\lambda_1^2}} - \frac{2}{\sqrt{\pi}}\frac{\alpha}{\lambda_1\sqrt{\lambda_1 D}}\, e^{\frac{-\alpha^2}{\lambda_1^2}}\mathbb{D}(\alpha\sqrt{\lambda_1 D}) \quad .
\end{aligned}
$$

[4]The cumbersome computations of equations (4.66) have been done analytically and are available upon request.

where the abbreviation

$$D := 1 - \frac{1}{\lambda_1^3} \tag{4.67}$$

has been used, and $\mathbb{D}(z)$ denotes the Dawson-Integral [1]

$$\mathbb{D}(z) := e^{-z^2} \int_0^z e^{x^2}\, dx \quad . \tag{4.68}$$

Moreover, $\mathbb{D}\mathrm{erf}(b; z)$ is a modified error function [57, 44], which is modified with the Dawson-Integral,

$$\mathbb{D}\mathrm{erf}(b; z) := \frac{2}{\sqrt{\pi}} \int_0^z \mathbb{D}(bx) e^{-x^2}\, dx \quad . \tag{4.69}$$

If $\lambda_1 = 1$, then

$$F_j(\alpha; 1) = f_j(\alpha) \qquad (j = 1, 2, 3, 4) \quad . \tag{4.70}$$

Therefore the conformational entropy at the undeformed partially crystallized reference state $|_R$, calculated by equation (4.60), is reduced to equation (4.52) in the limiting case of $\xi = \xi_R$.

On the other hand, the conformational entropy of the totally amorphous material in the deformed state is also included in equation (4.60). It is obtained if one sets $\xi = 0$, $v = v_o$, $\delta = \beta$, $L_\xi = L$, and $d = 0$. For $\alpha = \delta L_\xi = \beta L$ and $\alpha = \delta d = 0$, respectively, one obtains from equation (4.66)

$$\begin{aligned}
F_1(\beta L; \lambda_1) &= \mathrm{erf}(\frac{\beta L}{\lambda_1}) - \frac{2}{\sqrt{\pi}} \frac{1}{\lambda_1^{3/2}\sqrt{D}} e^{-\beta^2 L^2 \lambda_1} \int_0^{\beta L\sqrt{\lambda_1 D}} e^{x^2}\, dx \quad , \\
F_2(\beta L; \lambda_1) &= \frac{1}{3}(\lambda_1^2 + \frac{2}{\lambda_1}) \,\mathrm{erf}(\frac{\beta L}{\lambda_1}) - \frac{2}{\sqrt{\pi}} \frac{1}{3} \beta L \lambda_1 e^{-\frac{\beta^2 L^2}{\lambda_1^2}} \\
&\quad - \frac{2}{\sqrt{\pi}} \frac{2}{3} (\beta^2 L^2 + \frac{1}{\lambda_1}) \frac{1}{\lambda_1^{3/2}\sqrt{D}} e^{-\beta^2 L^2 \lambda_1} \int_0^{\beta L\sqrt{\lambda_1 D}} e^{x^2}\, dx \quad , \\
F_1(0; \lambda_1) &= 0 \quad , \\
F_2(0; \lambda_1) &= 0 \quad ,
\end{aligned} \tag{4.71}$$

and with this, (4.60) and (4.70) imply

$$S_a = \sigma k \left[3 \ln(\frac{\beta}{\sqrt{\pi}}) + \ln K_a \right] \times \frac{F_1(\beta L; \lambda_1)}{F_1(\beta L; 1)} - \sigma k \frac{3}{2} \frac{F_2(\beta L; \lambda_1)}{F_1(\beta L; 1)} \; . \tag{4.72}$$

For the undeformed amorphous material $\lim_{\lambda_1 \to 1} S_a = S_o$. As a consequence, due to (4.70),

$$K_a = K_o \; . \tag{4.73}$$

Hence from (4.51) and (4.70) follows the entropy of the totally amorphous material

$$\begin{aligned} S_a - S_o &= -\sigma k \frac{3}{2} \frac{F_2(\beta L;\lambda_1) - F_2(\beta L;1)}{F_1(\beta L;1)} + \sigma k \left[3 \ \ln(\frac{\beta}{\sqrt{\pi}}) + \ln \ K_o\right] \\ &\quad \times \frac{F_1(\beta L;\lambda_1) - F_1(\beta L;1)}{F_1(\beta L;1)} \quad . \end{aligned} \tag{4.74}$$

For control we consider the infinitely long chain. According to (4.1) and (4.7) we have $\beta L = \sqrt{\frac{3}{2}N}$. Furthermore, since

$$\lim_{\beta L \to \infty} F_1(\beta L) = 1 \,, \qquad \lim_{\beta L \to \infty} F_2(\beta L) = \frac{1}{3}(\lambda_1^2 + \frac{2}{\lambda_1}) \,, \tag{4.75}$$

the entropy difference (4.74) is

$$\lim_{\lambda_1 \to \infty} (S_a - S_o) = -\sigma k \frac{1}{2} \left[(\lambda_1^2 + \frac{2}{\lambda_1}) - 3 \right] \,, \tag{4.76}$$

the classical result, as given in (4.16) and (4.17).

So far, we considered only the conformational entropy of the chains. The crystalline regions themselves, however, also have entropy. That is due to the fact that, when the transformation occurs from the partially crystallized state to the amorphous state, the entropy increases by the melting entropy ΔS. The entropy of the partially crystallized rubber is then reduced as compared to the amorphous state (reference state), by the melting entropy

$$S - S_o = S_k - S_o - \Delta S \,. \tag{4.77}$$

Let $s_o = S_a(\xi = 0, \ T)$ be the specific entropy of the undeformed, totally amorphous material, $s_c(T)$ the specific entropy of the crystalline domain, and m_o the mass of a statistical segment. Then the melting entropy per segment is

$$S_\sigma(T) = m_o[s_o(T) - s_c(T)] \,. \tag{4.78}$$

The melting entropy of the rubber is obtained by multiplication with the number of total segments in the network $\sigma\zeta = \sigma N\xi$, which is bounded in the crystalline domains

$$\Delta S = \sigma N \xi \ S_\sigma(T) \,. \tag{4.79}$$

The entropy of the partially crystallized rubber[5] follows from equations (4.77) to

[5]The computations of equation (4.80) have been done analytically and are available upon request.

(4.79) and equations (4.60) and (4.59):

$$\begin{aligned} S - S_o \;\; = \;\; & -\sigma N \xi S_\sigma + \sigma k \frac{3}{2} \frac{F_2(\beta;1)}{F_1(\beta;1)} - \sigma k \left[3 \; \ln(\frac{\beta}{\sqrt{\pi}}) + \ln K_o \right] \\ & + \sigma k [3 \; \ln(\frac{\beta_\xi}{\sqrt{\pi}}) - \beta_\xi^2 d^2 + \ln K_\xi] \frac{F_1(\beta_\xi L_\xi;\lambda_1) - F_1(\beta_\xi d;\lambda_1)}{F_1(\beta L;1)} \\ & - \sigma k \frac{3}{2} \frac{F_2(\beta_\xi L_\xi;\lambda_1) - F_2(\beta_\xi d;\lambda_1)}{F_1(\beta L;1)} \\ & + \sigma k \; He(d \le D_\xi) \, 2\beta_\xi^2 d^2 \left\{ \frac{F_2(\beta_\xi D_\xi;\lambda_1) - F_2(\beta_\xi d;\lambda_1)}{F_1(\beta L;1)} \right. \\ & \left. - \frac{2}{3} \beta_\xi^2 d^2 \; \frac{F_3(\beta_\xi D_\xi;\lambda_1) - F_3(\beta_\xi d;\lambda_1)}{F_1(\beta L;1)} \right\} \\ & - \sigma k \; He(D_\xi \le L_\xi) \left\{ \frac{F_1(\beta_\xi L_\xi;\lambda_1) - F_1(\beta_\xi D_\xi;\lambda_1)}{F_1(\beta L;1)} \right. \\ & \left. - 2\beta_\xi d \; \frac{F_4(\beta_\xi L_\xi;\lambda_1) - F_4(\beta_\xi D_\xi;\lambda_1)}{F_1(\beta L;1)} \right\} \end{aligned} \tag{4.80}$$

The entropy difference $S_R - S_o$ of the partially crystallized reference state $|_R$ for $\xi = \xi_R$, $\beta_\xi = \beta_R$, $L_\xi = L_R$, $d = d_R$, $T = T_R$, and $\lambda_1 = 1$ is included as a special case. Both entropy differences are smaller or equal to zero $S - S_o \le 0$ and $S_R - S_o \le 0$. The entropy of the rubber decreases with crystallization as well as with deformation by increasing the state of ordering and orientation, as it must do so.

For the calculation of the stress one needs the free energy and for this the internal energy. We assume now that within the molecular chain, apart from the kinetic and binding energies within the crystalline domains, no internal energy of deformation can be stored. This corresponds to the model of Kuhn (simply and freely joint chains). We refer again to the undeformed totally amorphous state as a reference state for the energy. Thus the binding energy is just melting energy. Consequently, the change of the internal energy with crystallization and deformation is

$$U - U_o = -\Delta U = -\sigma N \xi \; U_\sigma(T) \,, \tag{4.81}$$

where $U_\sigma(T)$ is the melting energy per segment. This is given by

$$U_\sigma(T) = m_o[u_o(T) - u_c(T)] \quad , \tag{4.82}$$

where $u_o(T)$ is the specific (thermal) internal energy of the amorphous undeformed material and $u_c(T)$ is the specific internal energy of the crystalline domains, both at temperature T.

The free energy related to the undeformed totally amorphous state at temperature T is given by

$$F - F_o = U - U_o - T(S - S_o)\,, \qquad F_o(T) = U_o(T) - T\,S_o(T)\,. \tag{4.83}$$

For the calculation of the nominal stress for uniaxial extension we need the derivative of the free energy with respect to λ_1 for fixed values of ξ and T. According to equations (4.81) and (4.82),

$$\frac{\partial F}{\partial \lambda_1} = -T\frac{\partial S}{\partial \lambda_1}\,, \tag{4.84}$$

since U, U_o, S_o and F_o are independent of λ_1. The nominal stress is

$$\sigma_1 = \frac{1}{v_R}(\frac{v_R}{v_o})^{1/3}\ \ \frac{\partial F}{\partial \lambda_1}\,. \tag{4.85}$$

Dividing by the total mass of the rubber $\sigma N m_o$ and using the relations $\frac{\beta_\xi}{\beta} = (\frac{v_o}{v})^{1/3}$ and $\frac{\beta_R}{\beta} = (\frac{v_o}{v_R})^{1/3}$, following from equation (4.59), for the volume ratios, (4.85) takes the form

$$\sigma_1 = \rho_R\frac{\beta_\xi}{\beta_R}\ \frac{1}{\sigma N m_o}\ \frac{\partial F}{\partial \lambda_1} = -\rho_R\frac{\beta_\xi}{\beta_R}\ \frac{T}{\sigma N m_o}\ \frac{\partial S}{\partial \lambda_1}\ \ . \tag{4.86}$$

Let $\mathbb{N}_L$ be the Loschmidt-Avogadro number; then $\mathbb{R} = k\mathbb{N}_L$ is the universal gas constant and $\mathbb{M}_o = \mathbb{N}_L m_o$ is the molecular weight of the statistical segment.

Using (4.80) the nominal stress in uniaxial extension thus becomes

$$\begin{aligned}
\sigma_1 \;=\;& \rho_R\frac{\beta_\xi}{\beta_R}\frac{\mathbb{R}T}{N\mathbb{M}_o}\frac{1}{F_1(\beta L;1)} \\
&\times\Bigg\{\left[3\ \ln(\frac{\beta_\xi}{\sqrt{\pi}}) - \beta_\xi^2 d^2 + \ln K_\xi\right]\frac{\partial}{\partial\lambda_1}\left[F_1(\beta_\xi L_\xi;\lambda_1) - F_1(\beta_\xi d;\lambda_1)\right] \\
&+\frac{3}{2}\frac{\partial}{\partial\lambda_1}\left[F_2(\beta_\xi L_\xi;\lambda_1) - F_2(\beta_\xi d;\lambda_1)\right] \\
&-He(d\le D_\xi)\ 2\ \beta_\xi^2 d^2\ \ \frac{\partial}{\partial\lambda_1}\left[F_2(\beta_\xi D_\xi;\lambda_1) - F_2(\beta_\xi d;\lambda_1)\right] \\
&+He(d\le D_\xi)\ \frac{4}{3}\beta_\xi^4 d^4\ \frac{\partial}{\partial\lambda_1}\left[F_3(\beta_\xi D_\xi;\lambda_1) - F_3(\beta_\xi d;\lambda_1)\right] \\
&+He(D_\xi\le L_\xi)\ \frac{\partial}{\partial\lambda_1}\left[F_1(\beta_\xi L_\xi;\lambda_1) - F_1(\beta_\xi D_\xi;\lambda_1)\right] \\
&-He(D_\xi\le L_\xi)\ 2\beta_\xi d\ \ \frac{\partial}{\partial\lambda_1}\left[F_4(\beta_\xi L_\xi;\lambda_1) - F_4(\beta_\xi D_\xi;\lambda_1)\right]\Bigg\}\,.
\end{aligned} \tag{4.87}$$

The derivatives of the functions $F_j(\alpha,\lambda_1),(j=1,2,3,4)$ are obtained from (4.66). After some lengthy calculations and appropriate rearrangement one obtains

$$\begin{aligned}
\frac{\partial F_1(\alpha;\lambda_1)}{\partial\lambda_1} &= \frac{2}{3}\left(\lambda_1-\frac{1}{\lambda_1^2}\right)\left[-\frac{9}{4}\frac{\alpha}{\lambda_1}\ R_1(\alpha;\lambda_1)\right],\\
\frac{\partial F_2(\alpha;\lambda_1)}{\partial\lambda_1} &= \frac{2}{3}\left(\lambda_1-\frac{1}{\lambda_1^2}\right)\left[\mathrm{erf}\left(\frac{\alpha}{\lambda_1}\right)-\frac{2}{3}\frac{\alpha}{\lambda_1}\ R_2(\alpha;\lambda_1)\right], \qquad (4.88)\\
\frac{\partial F_3(\alpha;\lambda_1)}{\partial\lambda_1} &= \frac{2}{3}\left(\lambda_1-\frac{1}{\lambda_1^2}\right)\left[\frac{6}{5}\left(\lambda_1^2+\frac{4}{3}\frac{1}{\lambda_1}\right)\mathrm{erf}\left(\frac{\alpha}{\lambda_1}\right)\right.\\
&\quad \left.-\frac{3}{5}\frac{\alpha}{\lambda_1}\ R_3(\alpha;\lambda_1)\right],\\
\frac{\partial F_4(\alpha;\lambda_1)}{\partial\lambda_1} &= -\frac{1}{2}(\lambda_1-\frac{1}{\lambda_1^2})\left[\frac{3+D}{(\lambda_1 D)^{5/2}}\ \mathbb{D}\mathrm{erf}(\lambda_1\sqrt{\lambda_1 D};\frac{\alpha}{\lambda_1})\right.\\
&\quad \left.+\frac{1}{\lambda_1}\ R_4(\alpha;\lambda_1)-\frac{2}{\sqrt{\pi}}\frac{3+D}{2(\lambda_1 D)^2}\frac{1}{\sqrt{D}}\ \mathrm{artanh}(\sqrt{D})\right],
\end{aligned}$$

with the abbreviations

$$\begin{aligned}
R_1(\alpha;\lambda_1) &= \frac{2}{\sqrt{\pi}}\frac{e^{\frac{-\alpha^2}{\lambda_1^2}}}{(\lambda_1 D)^2}\left\{1-(1+\frac{2}{3}\alpha^2\lambda_1 D)\ \frac{\mathbb{D}(\alpha\sqrt{\lambda_1 D})}{\alpha\sqrt{\lambda_1 D}}\right\},\\
R_2(\alpha;\lambda_1) &= \frac{2}{\sqrt{\pi}}\frac{e^{\frac{-\alpha^2}{\lambda_1^2}}}{(\lambda_1 D)^2}\left\{[\alpha^2+\frac{1}{3}(2\lambda_1^2+\frac{1}{\lambda_1})]\right.\\
&\quad \left.-\left[(\alpha^2+\frac{1}{\lambda_1})(1+\frac{2}{3}\alpha^2\lambda_1 D)+\frac{2}{3}\frac{D}{\lambda_1}\right]\frac{\mathbb{D}(\alpha\sqrt{\lambda_1 D})}{\alpha\sqrt{\lambda_1 D}}\right\}, \qquad (4.89)\\
R_3(\alpha;\lambda_1) &= \frac{2}{\sqrt{\pi}}\frac{e^{\frac{-\alpha^2}{\lambda_1^2}}}{(\lambda_1 D)^2}\left\{\left[\alpha^4+\alpha^2\frac{2}{\lambda_1}(1+\frac{2}{3}\lambda_1^3 D)+2\lambda_1^4\right]\right.\\
&\quad -\left[(\alpha^2+\frac{1}{\lambda_1})^2(1+\frac{2}{3}\alpha^2\lambda_1 D)+(\alpha^2+\frac{1}{\lambda_1})\frac{2D}{\lambda_1}\right.\\
&\quad \left.\left.+\frac{1}{\lambda_1^2}(1+\frac{2}{3}D)\right]\frac{\mathbb{D}(\alpha\sqrt{\lambda_1 D})}{\alpha\sqrt{\lambda_1 D}}\right\},\\
R_4(\alpha;\lambda_1) &= \frac{2}{\sqrt{\pi}}\frac{e^{\frac{-\alpha^2}{\lambda_1^2}}}{(\lambda_1 D)^2}\left\{\left[3(\alpha^2+\frac{1}{2\lambda_1})+\lambda_1^2 D\right]\right.\\
&\quad \left.-\alpha^2\left[2(\alpha^2+\frac{1}{2\lambda_1})\lambda_1 D+3\right]\ \frac{\mathbb{D}(\alpha\sqrt{\lambda_1 D})}{\alpha\sqrt{\lambda_1 D}}\right\}.
\end{aligned}$$

We insert now the expressions of equation (4.88) into equation (4.87), by identification of α with $\beta_\xi L_\xi$, $\beta_\xi d$, and $\beta_\xi D_\xi$, respectively. For the nominal stress

we obtain the expression

$$
\begin{aligned}
\sigma_1 \;=\; & \rho_R \frac{\beta_\xi}{\beta_R} \frac{\mathbb{R}T}{N\mathbb{M}_o} \left(\lambda_1 - \frac{1}{\lambda_1^2}\right) \frac{1}{F_1(\beta L;1)} \\
& \times \Bigg\{ - \left[3\ \ln\left(\frac{\beta_\xi}{\sqrt{\pi}}\right) - \beta_\xi^2 d^2 + \ln K_\xi \right] \\
& \times \frac{3}{2}\frac{1}{\lambda_1} \left\langle \beta_\xi L_\xi\ R_1(\beta_\xi L_\xi;\lambda_1) - \beta_\xi d\ R_1(\beta_\xi d;\lambda_1) \right\rangle \\
& + \Bigg[\mathrm{erf}(\frac{\beta_\xi L_\xi}{\lambda_1}) - \mathrm{erf}(\frac{\beta_\xi d}{\lambda_1}) \\
& - \frac{3}{2}\frac{1}{\lambda_1} \left\langle \beta_\xi L_\xi\ R_2(\beta_\xi L_\xi;\lambda_1) - \beta_\xi d\ R_2(\beta_\xi d;\lambda_1) \right\rangle \Bigg] \\
& - He(d \le D_\xi)\ \frac{4}{3}\ \beta_\xi^2 d^2 \Bigg[\mathrm{erf}(\frac{\beta_\xi D_\xi}{\lambda_1}) - \mathrm{erf}(\frac{\beta_\xi d}{\lambda_1}) \\
& - \frac{3}{2}\frac{1}{\lambda_1} \left\langle \beta_\xi D_\xi\ R_2(\beta_\xi D_\xi;\lambda_1) - \beta_\xi d\ R_2(\beta_\xi d;\lambda_1) \right\rangle \Bigg] \\
& + He(d \le D_\xi)\ \frac{8}{15}\beta_\xi^4 d^4 \ \Bigg[2(\lambda_1^2 + \frac{4}{3}\frac{1}{\lambda_1}) \left\langle \mathrm{erf}(\frac{\beta_\xi D_\xi}{\lambda_1}) - \mathrm{erf}(\frac{\beta_\xi d}{\lambda_1}) \right\rangle \\
& - \frac{1}{\lambda_1} \left\langle \beta_\xi D_\xi\ R_3(\beta_\xi D_\xi;\lambda_1) - \beta_\xi d\ R_3(\beta_\xi d;\lambda_1) \right\rangle \Bigg] \\
& - He(D_\xi \le L_\xi)\ \frac{3}{2}\frac{1}{\lambda_1}\ \left\langle \beta_\xi L_\xi\ R_1(\beta_\xi L_\xi;\lambda_1) - \beta_\xi D_\xi\ R_1(\beta_\xi D_\xi;\lambda_1) \right\rangle \\
& + He(D_\xi \le L_\xi)\ \beta_\xi d \ \Bigg[\frac{3+D}{(\lambda_1 D)^{5/2}}\ \Bigg\langle \mathbb{D}\mathrm{erf}(\lambda_1\sqrt{\lambda_1 D};\frac{\beta_\xi L_\xi}{\lambda_1}) \\
& - \mathbb{D}\mathrm{erf}(\lambda_1\sqrt{\lambda_1 D};\frac{\beta_\xi D_\xi}{\lambda_1}) \Bigg\rangle \\
& + \frac{1}{\lambda_1} \left\langle R_4(\beta_\xi L_\xi;\lambda_1) - R_4(\beta_\xi D_\xi;\lambda_1) \right\rangle \Bigg] \Bigg\} \,.
\end{aligned}
\tag{4.90}
$$

4.2.3 Mooney representations

The phenomenological theory of Mooney [52] has played a dominant part in the field of large elastic deformation.

Mooney's theoretical assumptions, as has been noted earlier in connection with the statistical theory, is that the rubber is incompressible, and that it is isotropic in the unstrained state. Mooney formula is presented as follows:

$$
\sigma_1 = (\lambda_1 - \frac{1}{\lambda_1^2})(2C_1 + \frac{2C_2}{\lambda_1})\,, \tag{4.91}
$$

where σ_1 is the nominal (engineering) stress (force per unit undeformed area), and C_1, C_2 are empirical constants. We now write equation (4.91) in the form

$$\frac{\sigma_1}{(\lambda_1 - \frac{1}{\lambda_1^2})} = 2C_1 + \frac{2C_2}{\lambda_1} \ . \tag{4.92}$$

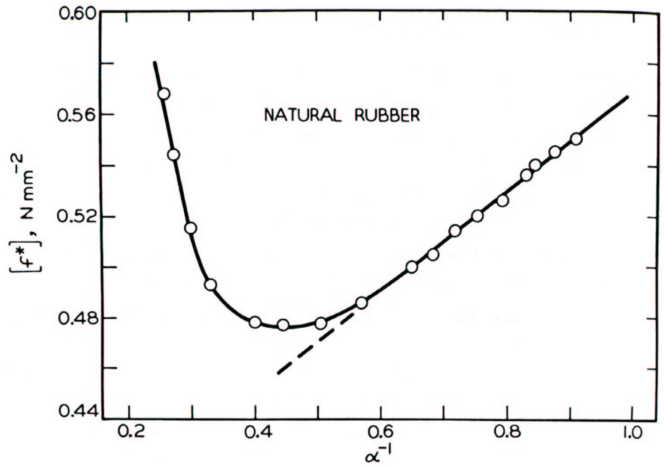

Figure 4.9: Mooney-Rivlin representation for cross-linked natural rubber, where f^* equals to $\frac{\sigma_1}{(\lambda_1 - \frac{1}{\lambda_1^2})}$ and α^{-1} equals $\frac{1}{\lambda_1}$.

It is clear that plotting $\frac{\sigma_1}{(\lambda_1 - \frac{1}{\lambda_1^2})}$ against $\frac{1}{\lambda_1}$ should yield a line of slope $2C_2$, with intercept $2(C_1 + C_2)$ on the vertical axis of $\frac{1}{\lambda} = 1$. Thus more details about the stress coefficients can be obtained using this formula. A large increase in modulus at high elongation is illustrated by figure 4.9 for natural rubber [50, 20] in the Mooney-Rivlin representation. This increase in the modulus is generally observed in crystallizable networks with chemical cross-linking that undergo strain-induced crystallization.

This is included in the present statistical model, in which these stress coefficients C_1 and C_2 are functions of (λ_1, ξ). Identification of (4.90) with (4.91)

yields for the Mooney coefficients:

$$
\begin{aligned}
2\,C_1 \;=\;& \rho_R \frac{\beta_\xi}{\beta_R} \frac{\mathbb{R}T}{N\mathbb{M}_o}\; \frac{1}{F_1(\beta L;1)} \\
& \times \Bigg\{ \left[\mathrm{erf}\left(\frac{\beta_\xi L_\xi}{\lambda_1}\right) - \mathrm{erf}\left(\frac{\beta_\xi d}{\lambda_1}\right)\right] \\
& - He(d \le D_\xi)\; \frac{4}{3}\; \beta_\xi^2 d^2 \left[\mathrm{erf}\left(\frac{\beta_\xi D_\xi}{\lambda_1}\right) - \mathrm{erf}\left(\frac{\beta_\xi d}{\lambda_1}\right)\right] \\
& + He(d \le D_\xi)\; \frac{8}{15} \beta_\xi^4 d^4 \left[2(\lambda_1^2 + \frac{4}{3}\frac{1}{\lambda_1}) \left\langle \mathrm{erf}(\frac{\beta_\xi D_\xi}{\lambda_1}) - \mathrm{erf}(\frac{\beta_\xi d}{\lambda_1}) \right\rangle \right] \\
& - He(D_\xi \le L_\xi)\; \beta_\xi d \left[\frac{3+D}{(\lambda_1 D)^{5/2}}\; \left\langle \mathbb{D}\mathrm{erf}(\lambda_1\sqrt{\lambda_1 D}; \frac{\beta_\xi L_\xi}{\lambda_1}) \right.\right. \\
& \left.\left. - \mathbb{D}\mathrm{erf}(\lambda_1\sqrt{\lambda_1 D}; \frac{\beta_\xi D_\xi}{\lambda_1}) \right\rangle \right] \Bigg\}\,,
\end{aligned}
\tag{4.93}
$$

$$
\begin{aligned}
2\,C_2 \;=\;& \rho_R \frac{\beta_\xi}{\beta_R} \frac{\mathbb{R}T}{N\mathbb{M}_o}\; \frac{1}{F_1(\beta L;1)} \\
& \times \Bigg\{ - [3\;\ln(\frac{\beta_\xi}{\sqrt{\pi}}) - \beta_\xi^2 d^2 + \ln K_\xi] \\
& \times \frac{3}{2} \left\langle \beta_\xi L_\xi\; R_1(\beta_\xi L_\xi;\lambda_1) - \beta_\xi d\; R_1(\beta_\xi d;\lambda_1) \right\rangle \\
& - \frac{3}{2} \left\langle \beta_\xi L_\xi\; R_2(\beta_\xi L_\xi;\lambda_1) - \beta_\xi d\; R_2(\beta_\xi d;\lambda_1) \right\rangle \\
& + He(d \le D_\xi)\; \frac{4}{3}\; \beta_\xi^2 d^2 \frac{3}{2} \left\langle \beta_\xi D_\xi\; R_2(\beta_\xi D_\xi;\lambda_1) - \beta_\xi d\; R_2(\beta_\xi d;\lambda_1) \right\rangle \\
& + He(d \le D_\xi)\; \frac{8}{15} \beta_\xi^4 d^4\; \left\langle \beta_\xi D_\xi\; R_3(\beta_\xi D_\xi;\lambda_1) - \beta_\xi d\; R_3(\beta_\xi d;\lambda_1) \right\rangle \\
& - He(D_\xi \le L_\xi) \frac{3}{2} \left\langle \beta_\xi L_\xi\; R_1(\beta_\xi L_\xi;\lambda_1) - \beta_\xi D_\xi\; R_1(\beta_\xi D_\xi;\lambda_1) \right\rangle \\
& + He(D_\xi \le L_\xi)\; \beta_\xi d \left\langle R_4(\beta_\xi L_\xi;\lambda_1) - R_4(\beta_\xi D_\xi;\lambda_1) \right\rangle \Bigg\}\,.
\end{aligned}
$$

Chapter 5

Model Application

5.1 Model Parameters

Three crucial parameters are included in our proposed statistical theory of deformation induced crystallization: the degree of crystallinity ξ, the number of segments which are exposed to the deformation stress N_{force}, the parameter a, and the entropy constant K_ξ of partially crystallized rubber. Besides, we need the total number of N of chain segments and their length ℓ.

5.1.1 Degree of crystallinity ξ

The degree of crystallinity is a vital parameter to our statistical model. In Chapter 3, a mathematical model has been developed to simulate the deformation-induced crystallization at different parameters (e.g. temperature and strain rate).

The relaxation time τ, for loading and unloading deformation, is greatly affected by temperature as it is evident by equations (3.14) and (3.19), and the strain rates. The effect of strain rates is summarized by the following tables 5.1, 5.2 for both polyisoprene rubber and polyethylene-butene copolymer as well[1].

Table 5.1: Effect of strain rate on the constants of the relaxation time for loading-unloading polyisoprene rubber at all temperatures

Strain rate [min^{-1}]	a_L [s]	$b_L[J/\text{mole}]$	a_U [s]	$b_U[J/\text{mole}]$
0.039	0.050	15000	0.005	15000
2.340	0.004	15000	0.002	15000

[1]These constants were fitted using Mathematica fitting technique.

Table 5.2: Effect of strain rate on the constants of the relaxation time for loading-unloading of the thermoplastic elastomer (both types) at all temperatures

Strain rate [min^{-1}]	a_L[s]	$b_L[J/mole]$	$a_U[s]$	$b_U[J/mole]$
0.09	0.050	15000	0.0250	15000
5.40	0.001	15000	0.0002	15000

From the above tables, it is clear that a_L and a_U are dependent on both strain rates. Unfortunately, few experiments have been performed with respect to strain rates, however, this is not sufficient to perform fitting for this dependence.

The degree of crystallinity is calculated for both loading and unloading, from equations (3.15) and (3.20), respectively. Then they are inserted into the stress-strain equation (4.90) as an input parameter. To meet agreement with the measurement data, the parameter a must be properly chosen. This is discussed in the following section.

5.1.2 Parameter a

The parameter a as introduced by equation (4.23) and figure 4.8, is a measure for the type of crystallite attributed to our molecular chain. Its value changes depending on the type of crystallites, whether extended or folded or mixed. Within the context of the statistical theory, the value of a is unknown. It must be determined by fitting of statistical stress-strain relation (4.90) to the measured stress-strain curves for isothermal (and isobaric) uniaxial extension.

It turns out, that the parameter a depends on temperature, on deformation speed and, of course, on the rubber-elastic and crystallizable materials considered. Moreover, chain parameter a may depend on deformation λ_1 for uniaxial extension.

The best fit to the stress-strain loading curves is obtained with the constant chain parameter a, independent of deformation λ_1.

This reflects the physical expectation that during loading the extensional type of crystallinity is favoured. Best fit values for the polyisoprene are given in table 5.3 for different temperature and two loading speeds. Corresponding values for the two thermoplastic elastomers ENX-7086 and ENX-7256 are given in tables 5.4 and 5.5, respectively[2].

[2]The constants shown in Tables 5.3, 5.4, and 5.5 were fitted using Mathematica fitting technique.

For unloading the crystallization behaviour is more complex. Besides the extended type of crystallization the folded type develops in unloading using the extended type as a nuclei for growing perpendicular to this to a shish-kebab structure.The formation of these crystallites requires relaxation of chain ordering, for which λ_1 is a measure. Consequently, the chain parameter a depends on λ_1 for unloading. With the following expression[3]:

$$a(T) = a_o + a_1\lambda_1 + a_2\lambda_1^2 + a_3\lambda_1^3 + a_4 \cosh\sqrt{\lambda_1^{-1}} + a_5\, e^{\lambda_1^2}\,, \tag{5.1}$$

and perfect fitting of the unloading curves can be obtained. The temperature dependent fitting parameters a_o, a_1, a_2, a_3, a_4, and a_5 obtained by Mathematica curves-fitting technique are tabulated in Appendix A for two given strain rates, and the three considered rubber-like materials.

Table 5.3: Parameter a values for loading process of polyisoprene

Temperature [°C]	strain rate [min^{-1}]	a
21	0.039 and 2.34	0.261
50	0.039 and 2.34	0.375
80	0.039	0.490

Table 5.4: Parameter a values for loading process of ENX-7086

Temperature [°C]	strain rate [min^{-1}]	a
23	0.09	0.280
23	5.40	0.150
50	0.09	0.370
50	5.40	0.380

Table 5.5: Parameter a values for loading process of ENX-7256

Temperature [°C]	strain rate [min^{-1}]	a
23	0.09	0.240
23	5.40	0.250
50	0.09	0.300
50	5.40	0.150

[3]This formula has been fitted using Mathematica curves-fitting technique.

5.1.3 Number of segments exposed to deformation, N_{force}

As has been discussed in equation (4.20), N_{force} increases with deformation during loading extension until it reaches the total number of chain segments N. This is expressed as[4]

$$N_{force}(\lambda_1) = b_o + b_1\lambda_1 + b_2\lambda_1^2 + b_3\lambda_1^3 + b_4\lambda_1^4 + b_5 e^{\left[1.25(\lambda_1^2 + \frac{2}{\lambda_1})\right]} , \tag{5.2}$$

where b_o, b_1, b_2, b_3, b_4, and b_5 are adjustable fitting parameters of the model depending on temperature. The values of these fitting parameters obtained by Mathematica curve-fitting technique are tabulated in Appendix B.

However for unloading, since all lamellae of the folded chain crystallites are split and become extended, N_{force} will equal to the total number of chain segments as follows

$$N_{force} = N . \tag{5.3}$$

(The total number of segments per chain N can be obtained, if a reasonable assumption is made about the molecular weight $\mathbb{M}_o$ of the segment. For this it is observed, that the identity unit of the molecule contains five carbon single bonds, around which almost iso-energetic rotations can take place. At a 1.5-fold length, e.g. 7.5 carbon single bonds, the end point of the 1.5-fold identity unit can reach almost all positions in space if one end is held fixed. Thus the poly-cis-isoprene molecule has the molecular weight of $183\, g/mole$ and a total number of segments per one chain $N = 55$. However, the Ethylene-butene molecule has the molecular weight of $120\, g/mole$ and a total number of segments per one chain $N = 63$.

It should be remarked, that the identity unit of the poly-cis-isoprene molecule and ethylene-butene molecule without attacking the valence angles of the carbon-carbon distances in the extended state of the chain has a length of $8.8\mathring{A}$. The length of the extended segment without attacking the valence angle is then $\ell = 1.5 \times 8.8\,\mathring{A} = 13.2\,\mathring{A}$)[5].

5.1.4 Entropy constant K_ξ of partially crystallized chains

Now the entropy constant K_ξ of the conformational entropy of the partially crystallized state is proposed as the expression

$$K_\xi = e^{\nu_o N_s} , \tag{5.4}$$

[4]This formula has been fitted using Mathematica curves-fitting technique.

[5]These informations have been obtained by personal communication with Prof. Dr. Rolf Hosemann, Bundesanstalt für Materialprüfung BAM-Berlin.

where ν_o is an adjustable parameter. N_s is the number of free conformational uncrystallized segments determined by

$$N_s = N(1-\xi) = N - \zeta \ . \tag{5.5}$$

ν_o is found to be temperature dependent for each material. The values of this parameter, depending on the material, are shown in Table 5.6[6].

Table 5.6: Values of ν_o for three different polymeric materials.

T(°C)	polyisoprene rubber	$\nu_o(ENX-7086)$	$\nu_o(ENX-7256)$
21	0.75	–	–
23	–	2.75	1.50
50	0.60	1.65	0.53
80	0.50	–	–

5.2 Application of the Model

With the above proposed model we are now in the position with this statistical theory of deformation induced crystallization to describe in an analytical way the pseudo-plastic effect and hysteresis in cross-linked rubber, elastomers and high polymers.

5.2.1 Polyisoprene crosslinked rubber

The old term *Cauotchouc*[7] was taken from the word *Cauo-Chu* meaning the "weeping tree". Many useful objects are made from the milk of the weeping tree. Batonists gave it the name *Hevea Brasiliensis*. The milk produced is an aqueous emulsion or dispersion of oils, fats, waxes, resins, starch, proteins. The main component is polyisoprene that is described by the chemical formula $(C_5H_8)_n$. C_5H_8 is called an isoprene and natural rubber is built up of regular sequences of isoprene, which are arranged in cis-configuration, forming long chains of high elasticity, see figure 5.1. The chains are linked and lie in the material like agitated snakes, they are perfectly regular in the backbone and have freely rotating links at given distance.

[6]These constants were fitted using Mathematica software.

[7]This complicated French word is said to stem from the Indian word Ca-hu-chu which means "weeping tree". Others maintain that it comes from the Kechuan language where cauchu means "he who casts the evil eye"; they find that notion appropriate because of the atrocious conditions under which the Indians were forced to collect rubber. So we may safely assume that the origin of the word is unknown. As caucho, caucciu and Kautschuk it provides the scientific name for rubber in Spanish, Italian and German.

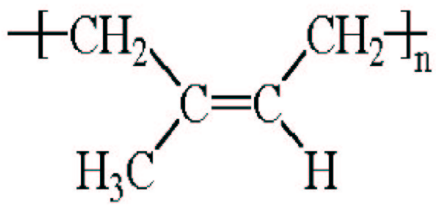

Figure 5.1: Structural formula of one isoprene molecule.

Rubber at that time was called India rubber because it came from India discovered by Columbus. There were problems though with India rubber: The "Macintouchs" were stiff in cold weather and sticky when it was warm since the raw rubber is non-crosslinked. Something had to be done and Charles Goodyear in 1839 found out what; he invented the process of vulcanization of rubber. Rubber was mixed with sulphur and heated. Through a change in its chemical structure (i.e. crosslinking), it is converted to a condition in which the elastic properties are conferred or re-established or improved. In this manner rubber became a dry flexible material largely unaffected by temperature changes in the normal range [70, 62, 63]

5.2.1.1 Crystallization results for the statistical model

It is well known that natural and synthetic rubbers crystallize upon the application of stress at room temperature, and this has been studied in both the stretched and the unstretched condition at various temperatures. At low temperatures, the effect of strain on crystallization has been studied by Gent [26], Kim and Mandelkern [40], and Stevenson [65, 66]. In general, an applied strain increases the rate of crystallization.

In this work, it is apparent that the equations obtained permit prediction of crystallinity at any strain rate or temperature within the studied range. However, it would also be interesting to use these equations to predict effects of changing the values of strain rate and temperature beyond the range examined so far, even though the validity of the results would be uncertain.

The crystallization during stretching is less than that during an unloading retraction process. Investigation of the influence of the draw temperature on the crystallinity development has been performed at two different strain rates, and it is observed that increasing temperature always decreases the crystallinity values in both loading stretching and unloading retraction processes. At low strain rate ($= 0.039 \quad \text{min}^{-1}$) this behaviour is confirmed as shown for example in figure 5.2. This is so, since the maximum saturated value of crystallinity is inversely temperature dependent.

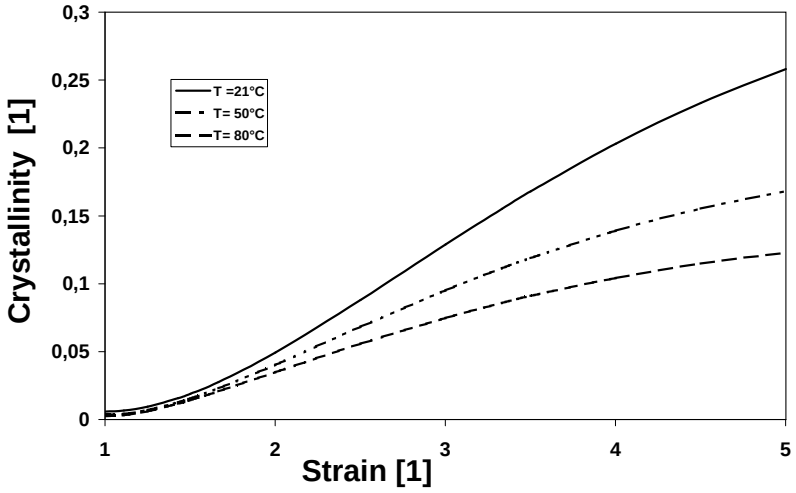

Figure 5.2: Theoretical results which show the effect of temperature on crystallization of polyisoprene rubber at low strain rate of 0.039 min^{-1} during the loading process.

Also, the crystallization during retraction is different from the crystallization during stretching; this is apparent at relatively low temperature (T= 21°C) in figure 5.3. At moderate temperature (e.g. 50°C), deviation will be noticed as shown in figure 5.4. However, crystallization deviation in stretching-retraction processes is diminished with increasing temperature and at low strain rates. For example at T= 80°C, it is clear that crystallizations are compatible in loading and unloading processes with some deviation at a strain ratio $\lambda_1 = 4.75$ as shown in figure 5.5. In a retraction process the curve goes back to the origin which indicates that melting of crystallites will occur at high temperature. This, the only type of crystallite which will survive the high temperature is only the mechanically-induced-type (the extended one).

At low strain rate (= 0.039 min^{-1}), the process is almost close to the equilibrium state, and the deviation of crystallization during stretching and retraction disappears at high temperatures. According to equation (3.8), the relaxation time τ plays a vital role on the deviation of crystallization from the equilibrium values, while at high temperature, the relaxation time has a rather small value, which enables the process to be close to the equilibrium state, see figures 5.3, 5.4 and 5.5.

The effect of strain rate has also been investigated and it was found, that at low strain rate the crystallinity values are close to the equilibrium state and no large hysteresis loops are observed in a loading-unloading process. On the other

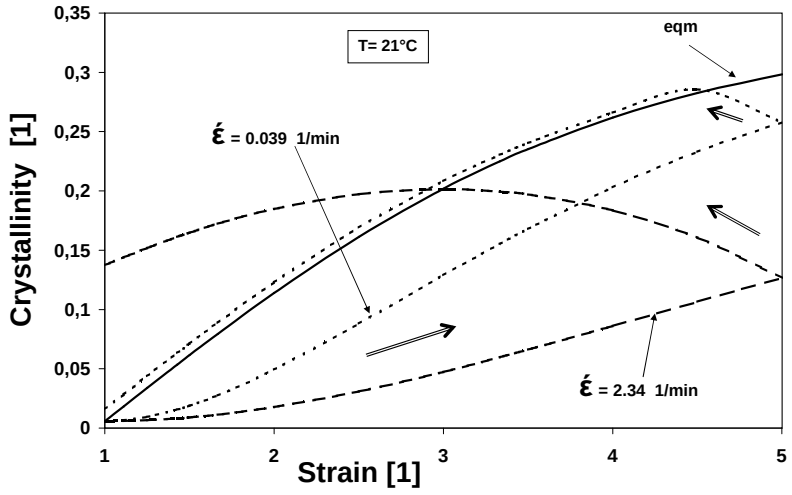

Figure 5.3: Theoretical results which show the crystallization of polyisoprene rubber at 21°C and different strain rates during the loading-unloading processes (arrows indicate load path direction).

hand, at high strain rate the values of crystallinity keep increasing during retraction while the change in crystallinity during stretching is low. It is approved that

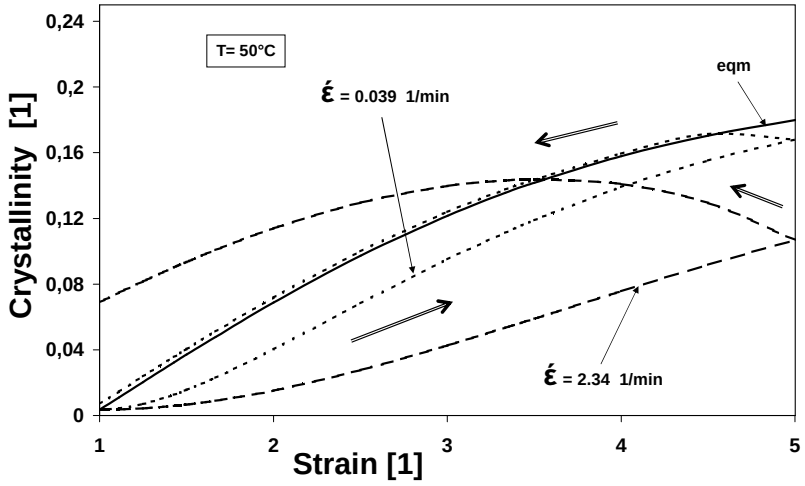

Figure 5.4: Theoretical results which show the crystallization of polyisoprene rubber at 50°C and different strain rates during the loading-unloading processes (arrows indicate load path direction).

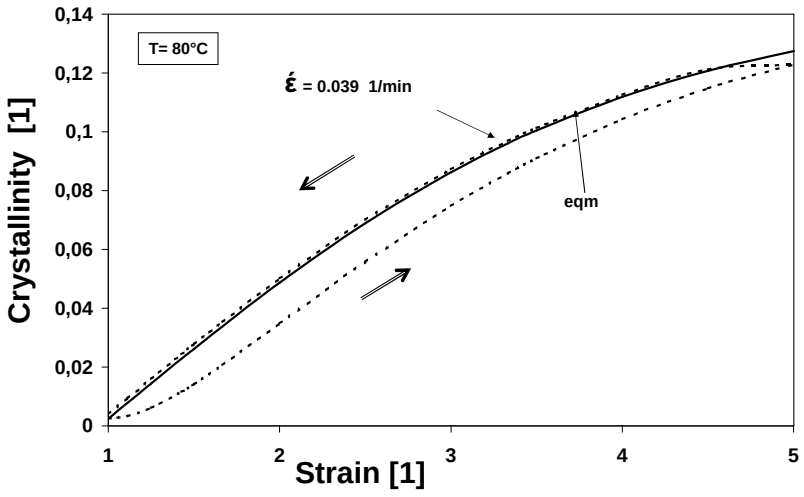

Figure 5.5: Theoretical results which show crystallization of polyisoprene rubber at 80°C and low strain rates during the loading-unloading processes (arrows indicate load path direction).

the type of crystallites during retraction is different from those in the stretching process. Consequently, a residual crystallinity will exist at the end of the unloading retraction process, and this residual amount of crystallinity will cause the thermodynamical irreversibility.

5.2.1.2 Experimental part

Polyisoprene rubber probes ($\rho = 0.9392 g/cm^3$) have been made by Dr. Eisele at *Bayer AG, Leverkusen*, however, the tensile experiments have been performed at the *Bundesanstalt für Materialprüfung BAM-Berlin* by Prof. Dr. Rolf Hosemann. In these experiments, rectangular-shaped polyisoperene rubber samples were cut from the sheet. The tensile test device was employed to stretch and retract the samples at a certain chosen speed and temperature. Wide Angle X-ray Diffraction (WAXD) patterns were measured in the undeformed state and at the end of the loading state.

5.2.1.3 Uniaxial stress-strain results

For the stress-strain measurements, the sample was stretched and allowed to retract by the same strain rate. Generally, both sequential and simultaneous measurements of stress-strain and birefringence were made in order to understand and investigate what occurred during stretching loading and retraction unloading processes and at different temperatures [68, 69, 53, 67]. These authors showed that the birefringence during retraction is more than that developed dur-

ing stretching, but the stress during retraction is less than that developed during stretching. This indicates that a substantial portion of the total orientation of the amorphous and crystalline regions is delayed until the retraction stage. The induced crystalline order itself can be analyzed directly by Wide Angle X-Ray techniques.

In what follows, we compare our predicted results with the experimental uniaxial extension tests of crosslinked isoprene rubbers. Both the stress-strain curves and the evolution of the degree of crystallinity are presented at different model parameters such as temperature and strain rate.

The increase of stress with temperature is due to rubber elasticity. This elastic force is entirely due to entropic effects, specifically, the tendency of the network chains to increase their entropy by retracting to more random conformations. This ideal situation would occur when intermolecular interactions do not depend on deformation (one of the major assumptions of molecular theories: absence of energy effects). As can be seen in the final statistical formula of stress, see equation (4.90), the force or stress at constant length is then proportional to the absolute temperature. This effect is clearly shown in figure 5.6a, while stress strain curves are shown at three different temperatures. As the temperature is raised, the Brownian-type wriggling of the polymer is intensified, so that the material seeks more vigorously to assume its random high-entropy state. From another view point, once the temperature is raised the crystalline portion of the chain starts to melt, thus the end-to-end distances for the remaining amorphous portions of the chain are increased and, due to that, the entropic effect is increased as well. Figure 5.6b shows the effect of the temperature on crystallization.

The stress-strain curve shows high upturn with a significant hysteresis. Hysteresis of rubber is defined as the amount of mechanical free energy dissipated or part of it converted into heat and other forms of energy during cyclic deformation. So, the rate of heat generation (dissipated deformation energy) is expected to increase with an increase of the hysteresis loops [35, 36].

Figures 5.7, 5.8, 5.9 show the expected behaviour of the dependence of the hysteresis loops on strain rate and temperature (i.e., the hysteresis decreases with an increase in temperature and with a decrease in strain rate). It is clear, that the stress during retraction is much smaller than the stress during the stretching loading process. In the unloading retraction process, the sample is allowed to retract after being stretched to a maximum strain, then the stress decreases drastically but the degree of the strain-induced crystallinity is still increasing during the unloading process. Therefore, the degree of crystallinity during an unloading retraction process is higher than that during loading stretching. Birefringence measurements [68, 53, 67, 69] have shown that the birefringence during

retraction is higher than that during stretching. This difference may be due to the fact that the birefringence represents a measure of total orientation of amorphous and crystalline chains. Thus, the secondary crystallites with folded-chain

(a)

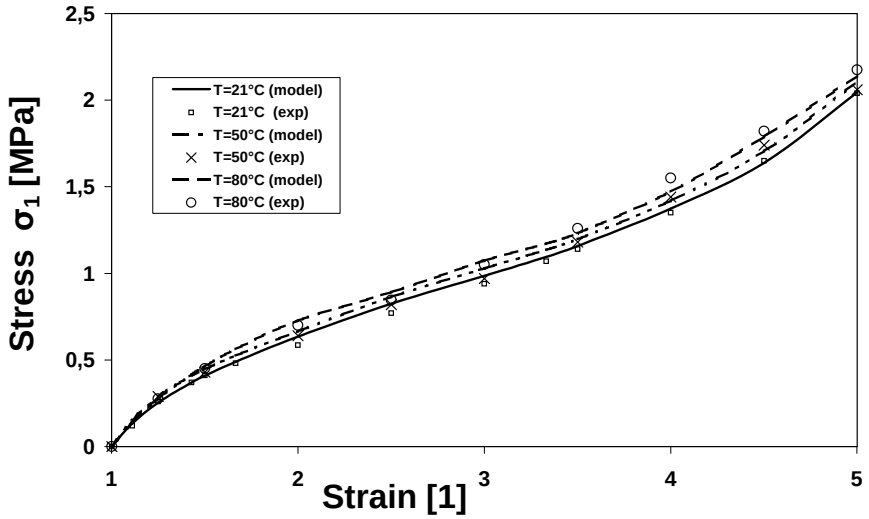

(b)

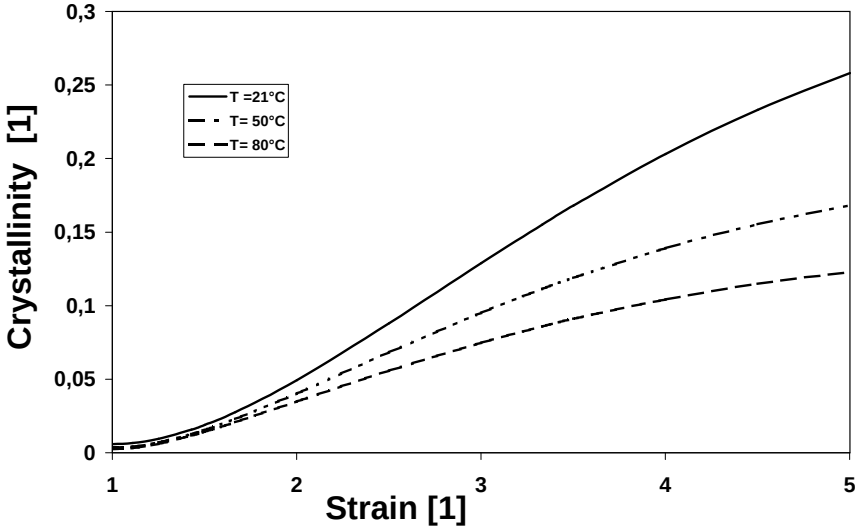

Figure 5.6: Temperature effect at $0.039\,\mathrm{min}^{-1}$ strain rate on, (a) stress-strain curves for uniaxial loading of polyisoprene rubber (theoretical results are represented by the solid line, while the experimental results by points) and, (b) crystallinity for uniaxial loading of polyisoprene rubber (theoretical results).

lamellae develop during retraction and cause the stress relaxation. Consequently, the hysteresis of the stress-strain curve is attributed to the formation of the stress induced crystallites and their transformation.

(a)

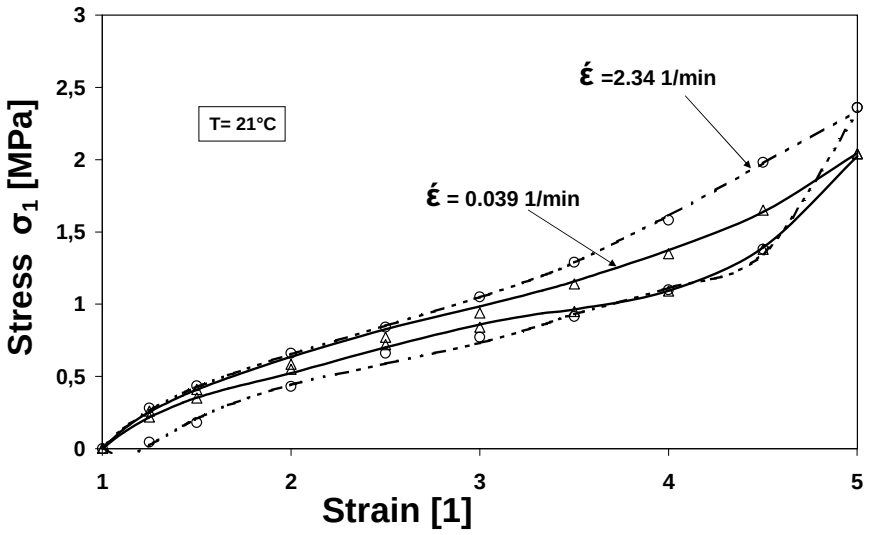

(b)

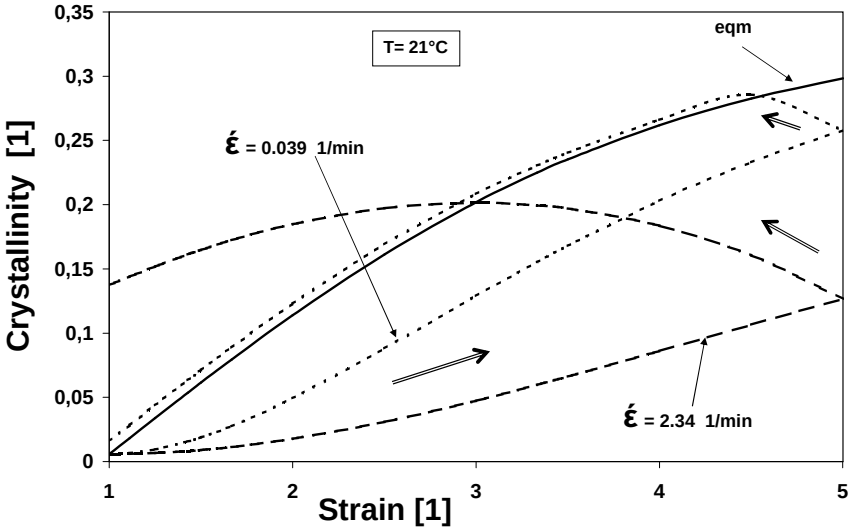

Figure 5.7: Effect of strain rates on uniaxial loading-unloading of polyisoprene rubber for, (a) stress-hysteresis at 21°C (theoretical results are represented by solid and dashed lines, while the experimental results by points) and, (b)crystallization at 21°C (arrows indicate load path direction).

Crystallization kinetics in stretching and retraction processes determine the amount of hysteresis of the stress-strain curves. Comparing the total cycles in figures 5.7, 5.8, 5.9 for the low strain rate, we recognise that the hysteresis loops

(a)

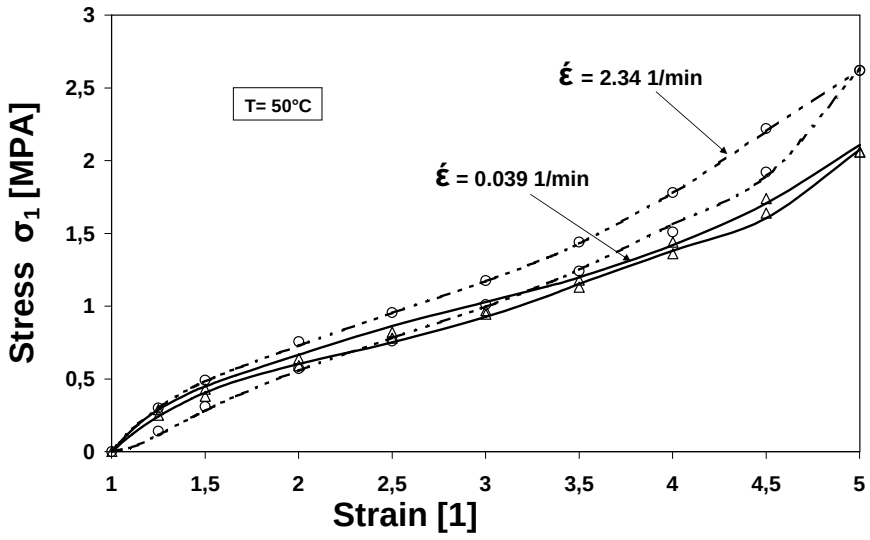

(b)

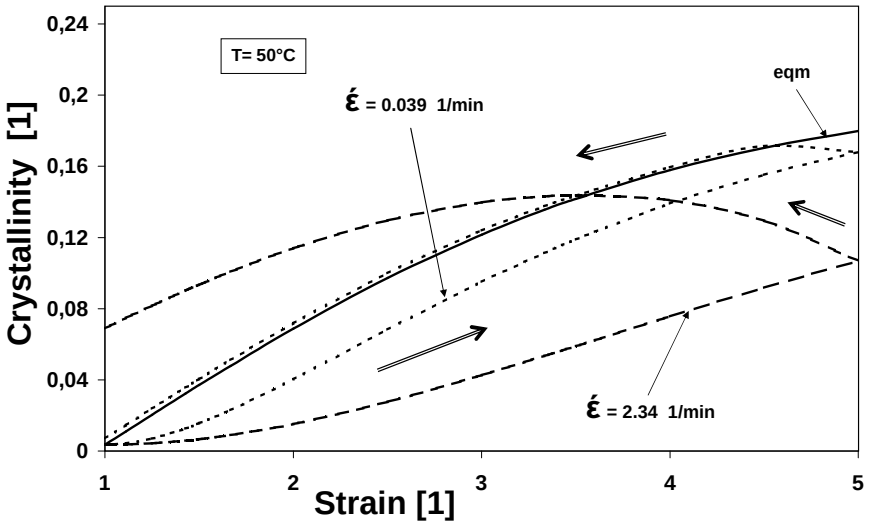

Figure 5.8: Effect of strain rates on uniaxial loading-unloading of polyisoprene rubber for, (a) stress-hysteresis at 50°C (theoretical results are represented by solid and dashed lines, while the experimental results by points) and, (b) crystallization at 50°C (arrows indicate load path direction).

(a)

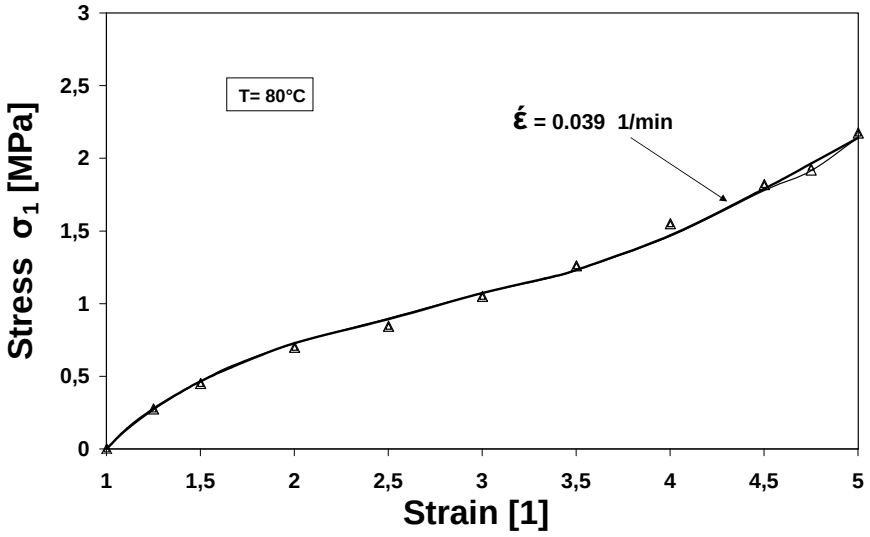

(b)

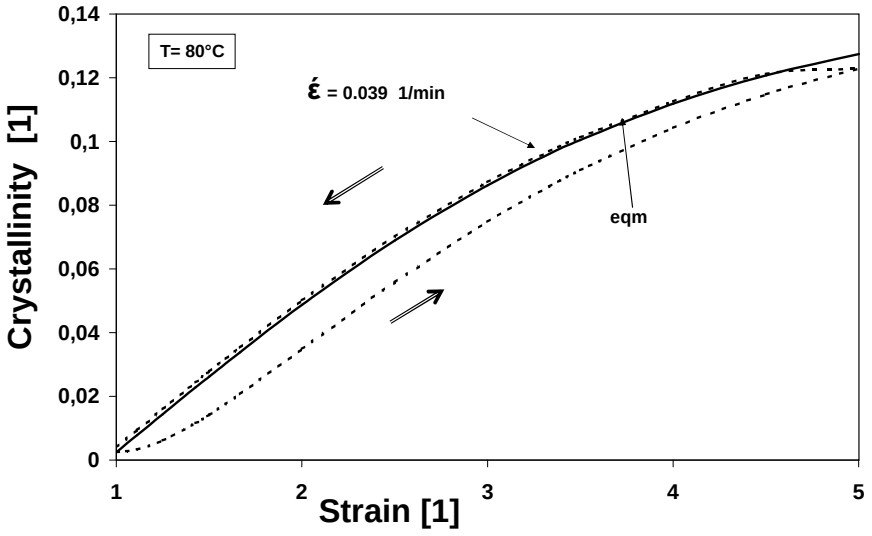

Figure 5.9: Effect of strain rate on uniaxial loading-unloading of polyisoprene rubber for, (a) stress-hysteresis at 80°C (theoretical results are represented by solid and dashed lines, while the experimental results by points) and, (b) crystallization at 80°C (arrows indicate load path direction).

are getting narrower with increasing temperature, and dissappear at 80°C. This is due to the fact that crystallinity formation decreases with increasing temperature. This is also related to the relaxation time which has smaller value when the temperature is lower. This explains qualitatively the different widths of the hysteresis loops. The disappearance of the hysteresis loop at 80°C is due to the fact, that at 80°C the crystallinity is assumed to be "momentarily" at its equilibrium value $\bar{\xi}(P, T = 80°C, \Lambda_1(t))$, so no further crystallization formation occurs during the retraction unloading process.

For high strain rate, it is apparent that the hysteresis loops are always much broader than for low strain rate. This phenomenon is interpreted as follows: For high strain rate, the degree of crystallinity is always (for both loading and unloading) far away from its equilibrium value $\bar{\xi}(P, T, \Lambda_1(t))$. However, during loading the degree of crystallinity formation is too small while its formation is relatively large during the retraction unloading process. Therefore, stress has high values during stretching, and in the unloading process it has low values in comparison with the equilibrium values. According to this, two limiting cases are mentioned for which no hysteresis loops are formed:

(i) Infinitely quick loading and unloading processes (infinitely large strain rate); in this case the crystallinity cannot follow the changes of the loading and so it will be kept frozen to the starting reference value ξ_R. As a result, the loading and unloading stress curves will be the same.

(ii) Infinitely sluggish loading and unloading processes (infinitely small strain rates): in this case the crystallinity will change through a sequence of equilibrium states $\xi = \bar{\xi}(P, T, \lambda_1(t))$.

Pseudo-plastic residual deformation is observed in the unloading retraction process as a result of the transformation of crystallites and the formation of *Shish Kebab* [45] structure, as shown in figure 5.10, due to stress relaxation during unloading retraction process. This is clear in figures 5.7 and 5.8. At a temperature of 80°C, the stress during stretching and that during retraction coincide towards the origin, the strain induced crystallites are totally molten or equal to the state crystallinity of the reference. This can be noticed in figure 5.9.

Two X-ray pictures have been obtained for polyisoprene rubber sample, one in the undeformed state ($\lambda_1 = 1$) and the other at the maximum elongation ratio of the loading process ($\lambda_1 = 5$). As shown in figure 5.11 the undeformed state picture, there appear no oriented crystalline reflection peaks. However, at $\lambda_1 = 5$, the sample is observed to be well oriented with sharp reflections on the equator and on the first layer.

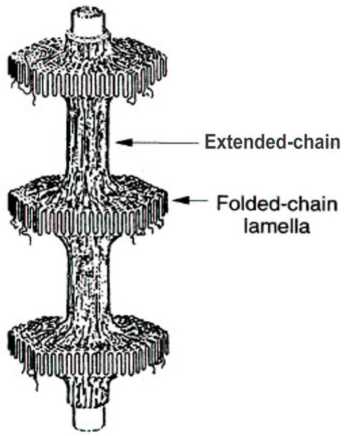

Figure 5.10: Shish-Kebab structure of a polyisoprene rubber sample.

(a) (b)

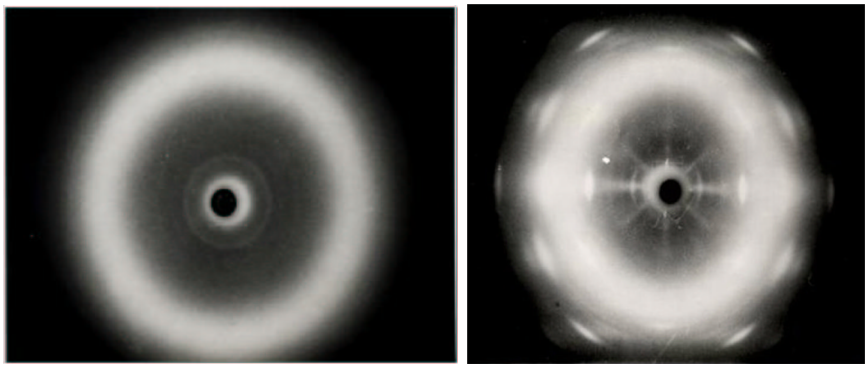

Figure 5.11: WAXD of polyisoprene rubber at 21°C and high strain rate 2.34 min^{-1}, provided by Prof. T. Alts, for, (a) an undeformed state ($\lambda_1 = 1$) and, (b) maximum deformation ratio ($\lambda_1 = 5$).

5.2.1.4 Mooney representation results

The Mooney representations of our stress-strain measured data, will be discussed as follows:

It is clear that plotting $\frac{\sigma_1}{(\lambda_1 - \frac{1}{\lambda_1^2})}$ against $\frac{1}{\lambda_1}$ should yield a line of slope $2C_2$, and an intercept with value $2(C_1 + C_2)$ on the vertical axis where $\frac{1}{\lambda} = 1$. Thus more details about stress coefficients can be obtained using this formula. A large increase in modulus at high elongation; is illustrated by figure 4.9 for natural rubber in the Mooney-Rivlin representation. This increase in modulus is generally observed in crystallizable networks with chemical cross-linking that undergo strain-induced crystallization.

At temperatures of 21°C and 50°C and at two different strain rates (0.039, and 2.34 min^{-1}), the loading curves for small deformation up to $\lambda = 2.5$ are inclined. However, the intersections and inclinations are different. At least, however, the existence of this inclined line means, that in the loading case the stress coefficients are constants. This means, since C_1 and C_2 are functions of ξ and that the degree of crystallinity does not change during loading in this deformation interval (up to $\lambda = 2.5$).

Qualitatively, this effect can be understood as follows: For loading crystallites of the folded chain type (lamellae) are destroyed at small deformation, and then many of the chain segments will become exposed to deformation stress. For larger deformation, crystallites of extended type are formed. According to Avrami [10, 11, 12] nucleation and growth in uniaxial extension are linear with time. As deformation proceeds, a departure from linearity will arise and an upturn of the loading curve will occur as a result of deformation-induced crystallization.

To validate this view, Kuhn's model is included in our statistical model as a special case, if we assume, that no state quantity depends on crystallinity and. If possibly existing crystallinity ξ_o does not change at all, then linear horizontal lines will be achieved as shown in figures 5.12, 5.13 and represented by dashed line. This can be compared to our model where formation of crystallinity with deformation is included. Thus, inclined lines will be achieved from our statistical model for the Mooney stress. For unloading, hysteresis is observed, due to further formation and transformation of crystallinity as it has been found and discussed for stress-strain curves. Hysteresis decreases with an increase of temperature, and with the decrease in strain rate as shown in figures 5.12, 5.13.

At high temperature (i.e. $80°C$), loading and unloading curves are compatible and only a very small hysteresis at the beginning of unloading is observed, as shown in figure 5.14.

(a)

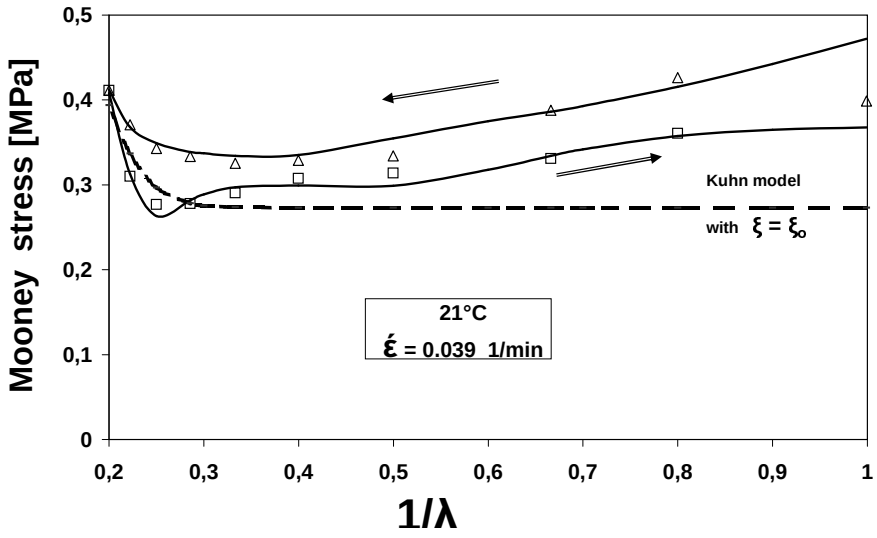

(b)

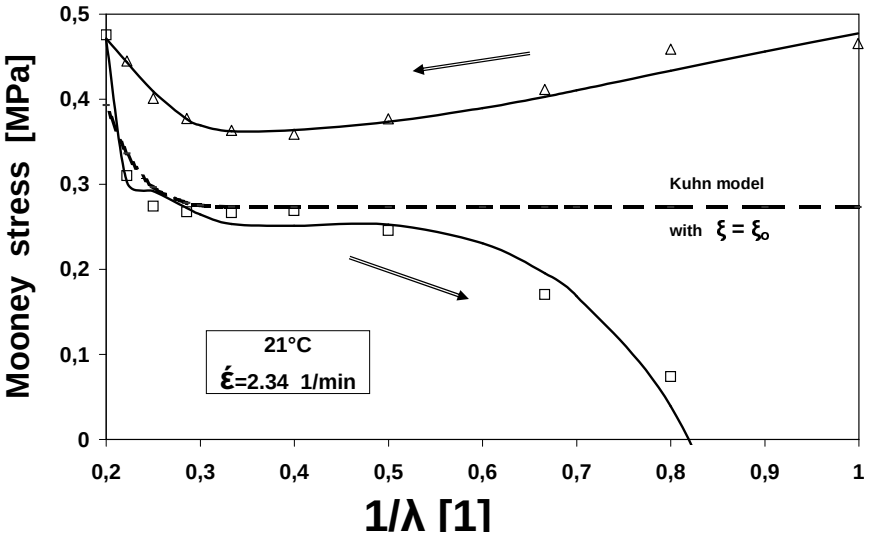

Figure 5.12: Mooney-representation for uniaxial loading-unloading of polyisoprene rubber at 21°C (theoretical results are represented by solid the line, the experimental results by points , while the dashed line is Kuhn's model when no change in crystallinity is assumed in our statistical model) for, (a) low strain rate = 0.039 (min^{-1}) and, (b) high strain rate = 2.34 (min^{-1}).

(a)

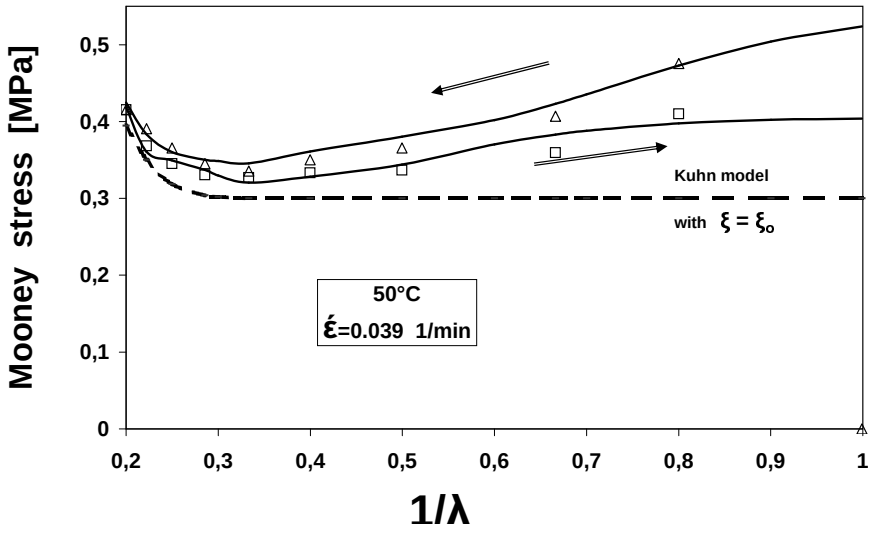

(b)

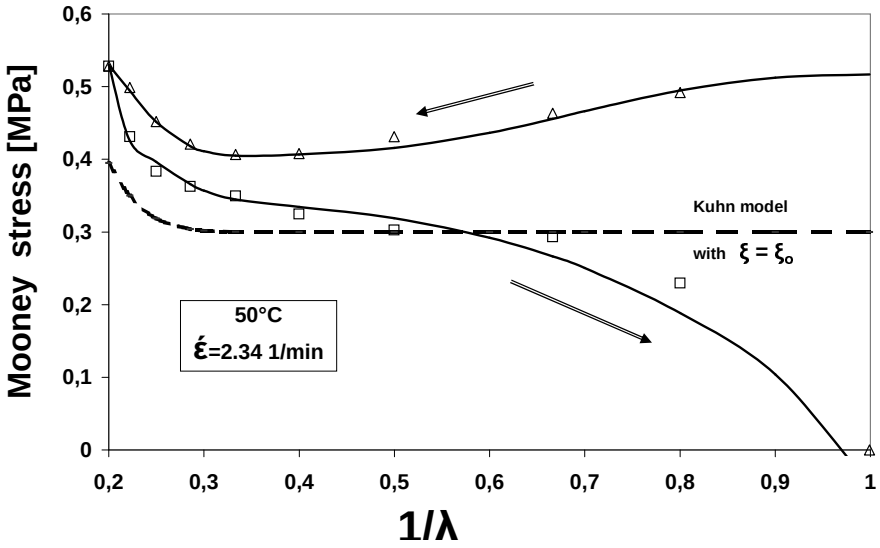

Figure 5.13: Mooney-representation for uniaxial loading-unloading of polyisoprene rubber at 50°C (theoretical results are represented by the solid line, the experimental results by points , while the dashed line is Kuhn's model when no change in crystallinity is assumed in our statistical model) for, (a) low strain rate = 0.039 (min^{-1}) and, (b) high strain rate = 2.34 (min^{-1}).

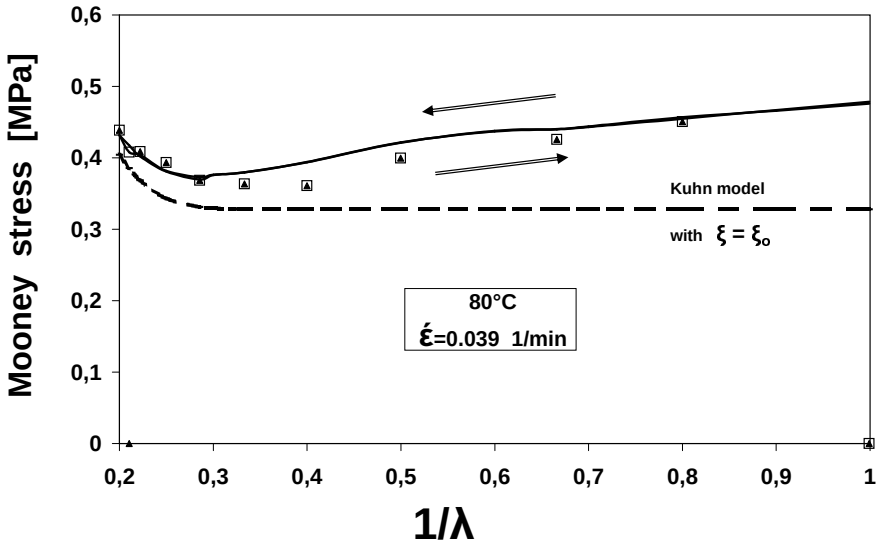

Figure 5.14: Mooney-representation for uniaxial loading-unloading of polyisoprene rubber at 80°C (theoretical results are represented by the solid line, the experimental results by points , while the dashed line is Kuhn's model when no change in crystallinity is assumed in our statistical model) for low strain rate = 0.039 (min^{-1}).

5.2.1.5 Volume change

According to equation (3.6), for a semi-crystalline polymer, the equilibrium volume increases first with deformation since a destruction of lamellae (spherulite) occurs initially and a decrease in volume is obtained for large deformation due to the formation of extended crystallites or orientation of both amorphous chains and destroyed lamellae parts. A linear relationship between volume change and strain was found up to large extension ratios. On the basis of an affine deformation, one calculates a dependence which is proportional to $\lambda - 1$ [25, 16, 30].

As shown in figure 5.15 strain rates have a drastic impact on volume change at certain temperatures. In our statistical theory, according to equation (3.6), a good approximation is achieved to predict the change of volume due to deformation-induced crystallization.

(a)

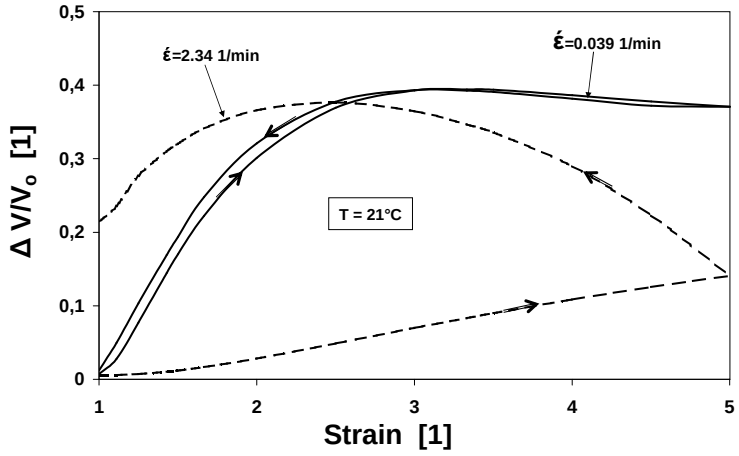

(b)

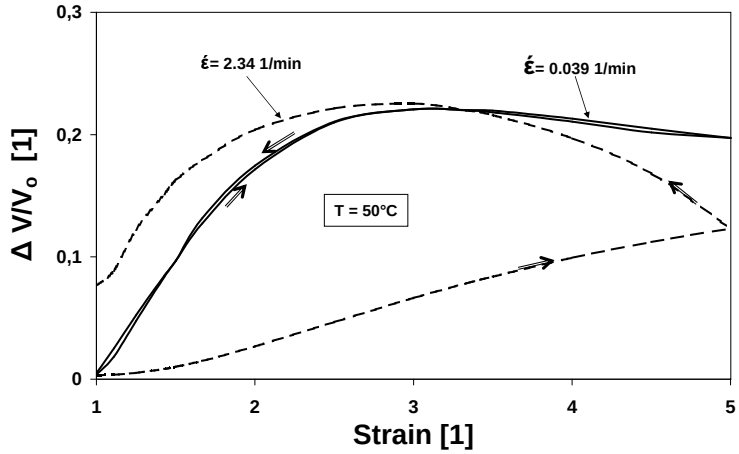

(c)

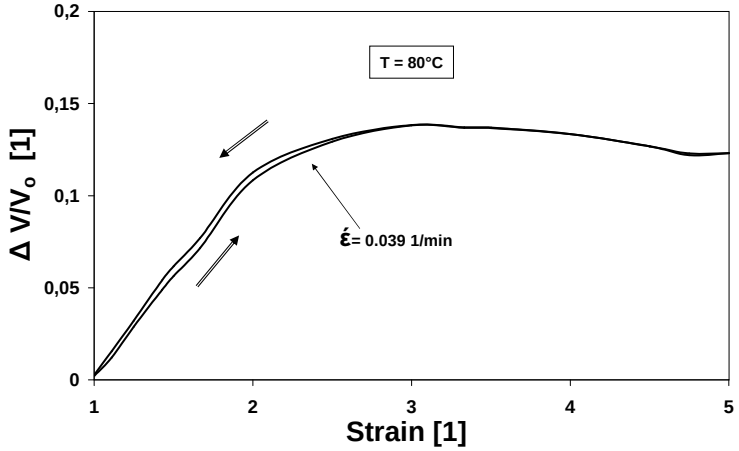

Figure 5.15: Change of volume, model results, at different strain rates for, (a) 21°C, (b) 50°C and, (c) 80°C.

5.2.2 Polyolefin thermoplastic elastomers

Thermoplastic elastomers differ from the usual cross-linked elastomers in so far as the cross-links are not covalent bonds but physical links, e.g. consisting of crystallized chain segments. These can be molten by heating, thus allowing thermoplastic processing [18].

The two polyolefin elastomers, that have been used in this study, are copolymers of ethylene-butene with two different degrees of crystallinity as shown in table 5.7.

Table 5.7: Physical and chemical properties of the thermoplastic ethylene-butene copolymer

Copolymer type	Density [g/cm^3]	% Total Crystallinity	T_m [°C]	T_g [°C]
ENX-7256	0.885	21.5	70	-48
ENX-7086	0.902	32.4	94	-39

Ethylene-butene copolymers have the chemical structure as shown in figure 5.16. ENX-7256 has a unique broader molecular weight distribution with higher branching levels that offers excellent clarity, processing and performance in foams and extrusion applications such as tubing, profiles, wire and cable insulations. ENX-7086 has much higher levels of long chain branching than other commercially available polyolefin elastomers. It is suited for blow molding, extrusion and thermoforming applications where high level of shear thinning and high melt strength may be required.

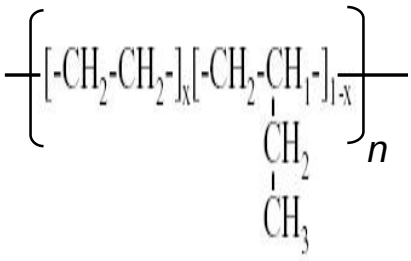

Figure 5.16: Chemical structure of ethylene-butene copolymer.

5.2.2.1 Crystallization results for the model

This difference in crystallinities may be recalled from the copolymer crystallization theories that the co-units present in a copolymer may either be completely rejected from the crystal (*exclusion*) or uniformly included as an equilibrium requirement (*inclusion*) [21, 23, 59, 60, 2, 3].

Flory's prediction is that all branches longer than methyl are excluded from the crystal lattice [33, 4]. Thus, ethyl and butyl side chains are excluded from the crystal lattice. Therefore, the morphology in more branched copolymers may involve *fringed-micelle*like crystals.

Deformation-induced crystallization in polyethylene-polybutene copolymers depends on temperature and strain rate in a similar way as does polyisoprene rubber, although the molecular rearrangements taking place are different. In the early stages of drawing an unoriented crystalline polymer, spherulites become

(a)

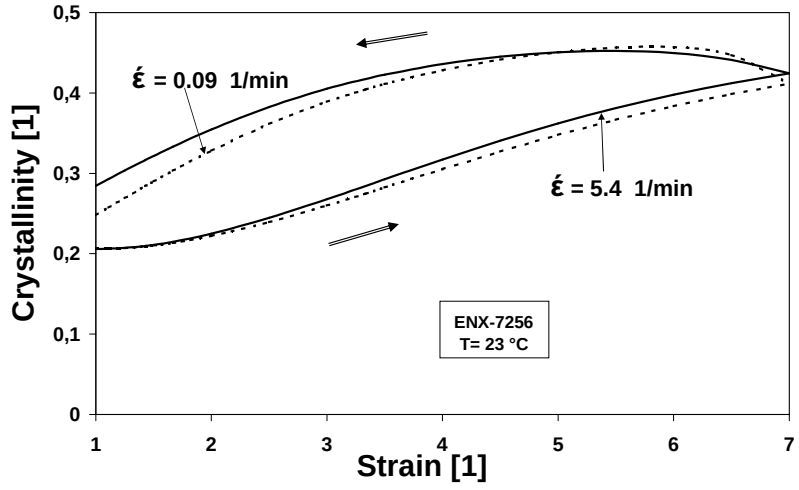

(b)

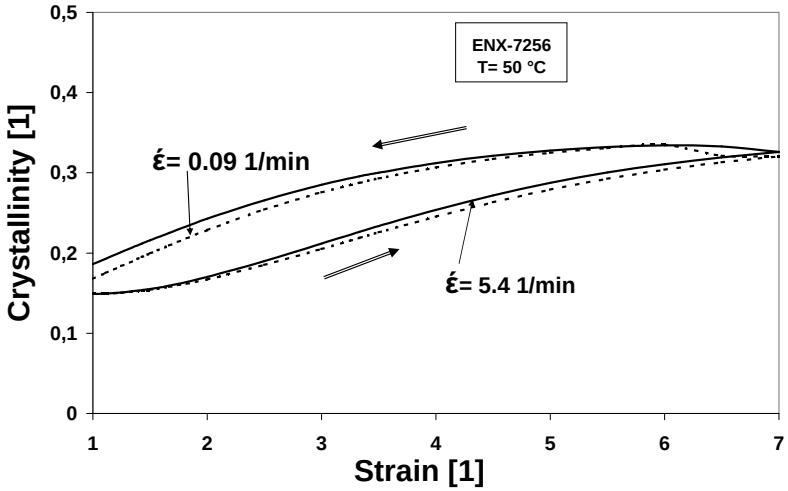

Figure 5.17: Theoretical crystallization of ENX-7256 at different strain rates for two temperatures of, (a) at 23°C, and (b) at 50°C.

elongated in the draw direction. Then, chain slipping occurs within the lamellae *(chain-folded crystals)* and the lamellae break up into small crystallites connected to each other by uncrystallized tie molecules.[58].

Due to this fact, crystallization is kept constant up to $\lambda_1 = 2$ since breaking the lamellae enhances the reorientation of these small broken crystallites in the drawing direction. This is obviously shown in figures 5.17 and 5.18 during the loading stretching process.

(a)

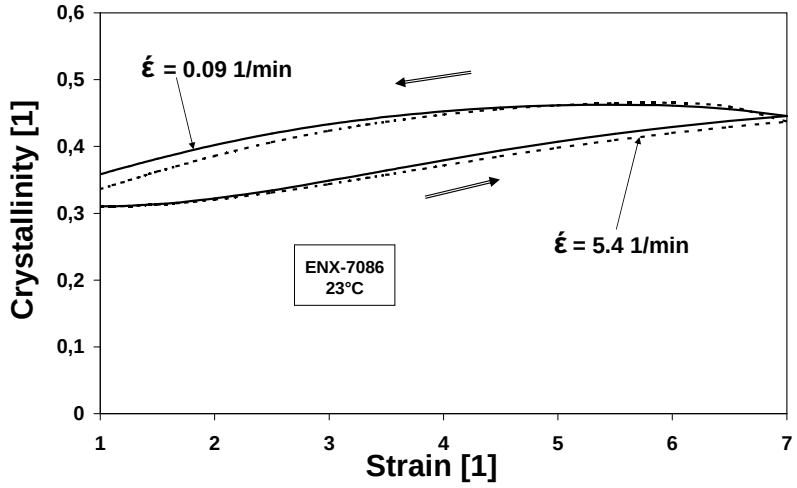

(b)

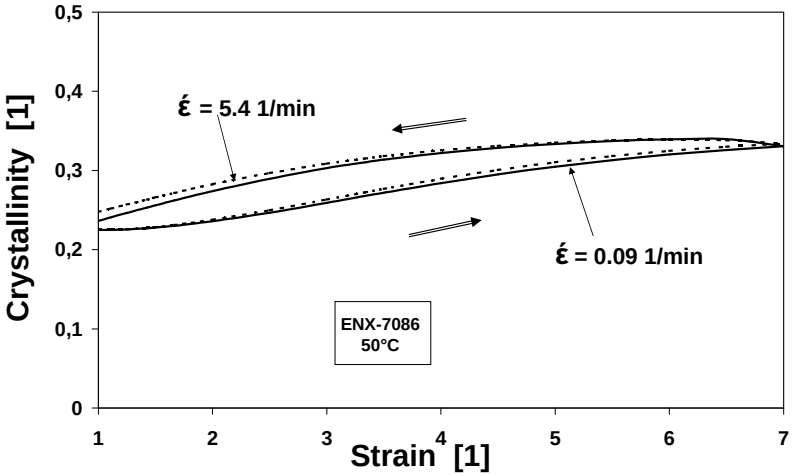

Figure 5.18: Theoretical crystallization of ENX-7086 at different strain rates for two temperatures of, (a) at 23°C, and (b) at 50°C.

The same figures show the effect of strain rate on the evolution of crystallinity as a function of the deformation. In fact, it is clear that both materials do not show drastic changes of crystallinity caused by changing strain rates at a certain temperature during the loading process. This is clearly shown in figures 5.17 and 5.18 for both copolymers.

The effect of temperature on crystallization is an important factor. An increase in temperature accelerates thermally activated processes and reduces relaxation times. Consequently, the hysteresis between the loading and unloading process is reduced.

5.2.2.2 Experimental part

We are indebted to *Rieter* Automative Germany GmbH for providing us with ethylene-butene copolymer materials. Also another acknowledgment is to German Polymer Institute *DKI*-Darmstadt for their highly appreciated cooperation and help with the preparations of samples and running of the tensile loading-unloading experiments.

For the preparation for the experiments, two ethylene−butene copolymers (ENX-7086, ENX-7256) were dried under vacuum at 80°C, extruded by twin microextruder, and pressed to form a thin sheet by the following sequence: heating 1 min at 1 bar and 150°C, pressing 2 min at 36 bar and 150°C , and cooling 2 min at 36 bar and 23°C. Then the samples were cut into a certain form (1.5 mm thickness, 27.7 mm length, and 4 mm width) from the pressed sheet using a standard cutting machine. A tensile machine (Zwick-020TH2A) was equipped with an environmental chamber that was used for performing the loading and unloading tests. To correct for shrinkage at high temperatures (50°C), sample length correction was used for deformation of the samples under constant temperature and humidity. Each sample was drawn up to $\lambda_1 = 7$ at two different temperatures, 23°C and 50°C, and two different deformation speeds, 2.5 mm/min and 150 mm/min.

5.2.2.3 Uniaxial stress-strain results

Since these ethylene-butene copolymers have a degree of crystallinity in the undeformed state of the order of 20-30%, deviation from rubbery behaviour is well expected at least in the small deformation region. Copolymer preparations with a density of less than 0.9 gcm^{-3} show increasingly fringed micelles as the dominant but not exclusive crystal morphology and exhibit mechanical and thermal properties that are not found in standard polyethylene [13, 14].

Crystallization of copolymers is predominately by branching statistics. However, in homopolymers it is largely influenced by the chain length and its distri-

bution, the extent of entanglement of chains in the melt and the undercooling. It was observed that the lamellar thickness at a selected crystallization temperature increases linearly with decreasing comonomer content (this is fully discussed in chapter two).

So far we considered the stress-strain response of amorphous chains (with low degree of crystallinity at the origin) that crystallize in the course of deformation. Stress-induced orientation reduces the energy barrier between the amorphous and crystalline state, permitting crystallization at temperatures where none would occur in the unoriented state.

Induction of crystallinity levels in the undrawn polymer can result in a brittle behaviour that is difficult to draw. In general, increasing crystallinity in any unoriented state increases the stress required for deformation, and shifts the stress-strain response towards brittle deformation.

Some copolymers with high levels of unoriented crystallinity can, however, be readily drawn. An unoriented, semicrystalline copolymer generally consists of lamellae structures. Chains fold back at the surface of each lamella.

The stress-strain response of a semicrystalline chain depends on temperature and strain rate in a similar way as do amorphous chains e.g. in polyisoprene rubber (negligible degree of crystallinity at the reference state). In the early stages of drawing an unoriented semi-crystallized chain, stress concentrates initially on spherulite which becomes elongated in the draw direction [32, 15], and in the region of $\lambda = 2 - 2.5$; chain tilting and slipping occur within the lamellae of the chain-folded crystals.

Necks begin to form in regions of stress concentration or *in a region where there are fewer molecular entanglement*. This leads to dramatic local orientation of the amorphous chain, and dramatic local deformation of the spherulites and lamellae in the crystallized portion of the chain.

Eventually, the plastic deformation of the spherulites induces the breaking of the lamellae into small crystallites connected to each other by conformational tie segments. Spherulite deformation under uniaxial tension has been studied. Results indicate that the first deformation events occur near the center [73, 74]. However, other researches showed, that the deformation starts from the equatorial regime and proceeds towards the polar regime of the spherulites [61].

Although stress-strain response is temperature and strain rate dependent, different results can be identified theoretically and experimentally for the two materials based on their difference in the degree of crystallinity in the undeformed

(a)

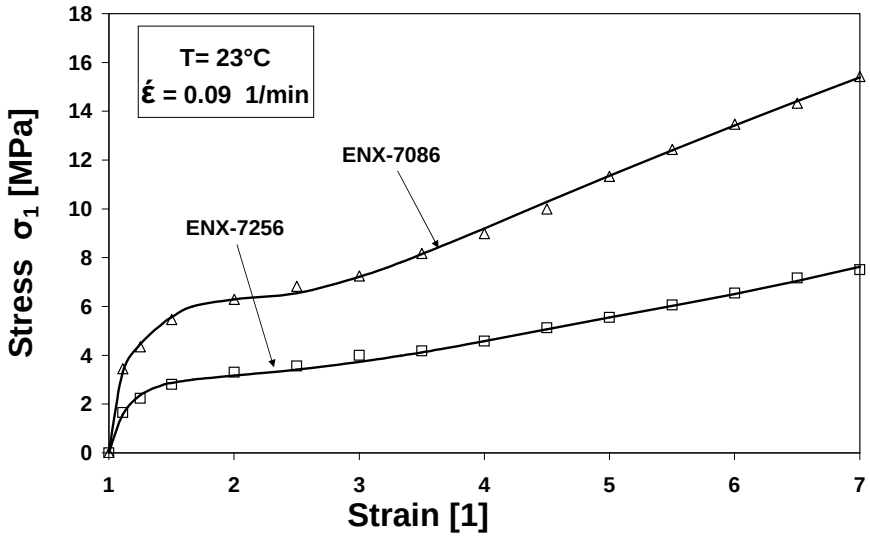

(b)

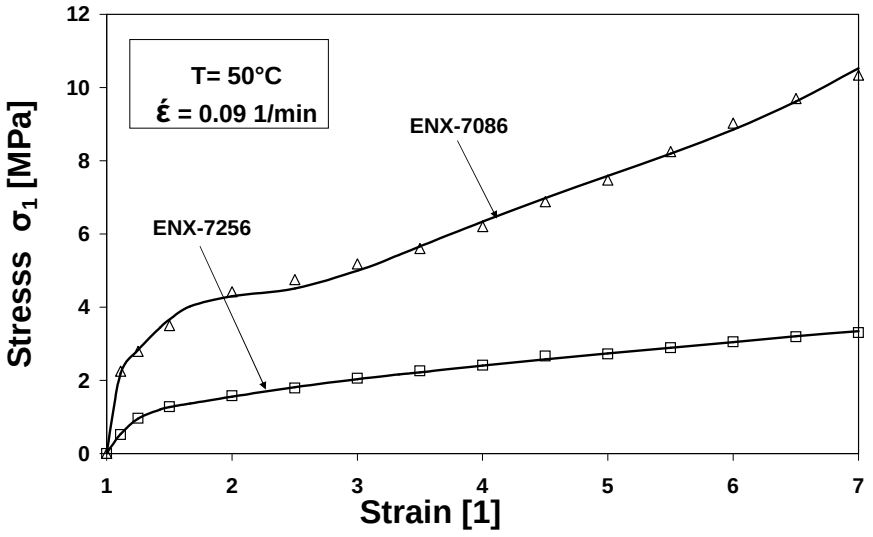

Figure 5.19: Effect of temperature on stress-strain loading curves at 0.09 (min^{-1}) strain rate for, (a) at 23°C and, (b) at 50°C. (Theoretical results are represented by the solid line, while the experimental results by points).

origin state.

ENX-7086 has a total degree of crystallinity at the reference state of $\xi_R = 0.332$, while ENX-7256 has $\xi_R = 0.221$. As a result one observes within a certain temperature range and regardless of the range of strain rate: The higher the reference crystallinity is the higher is also the mechanical energy required to break up and reorient the crystals. This is clear from figure 5.19; ENX-7086 ($\xi_R = 0.332$) has higher stress values compared to ENX-7256 ($\xi_R = 0.221$).

Since the reference crystallinity decreases with temperature, so the reference crystallinity equally decreases at high temperatures (i.e. $50°C$) and due to that, the stress required initially will be less than that at room temperature (i.e. $23°C$). However, the number of segments that are sitting in the crystalline lamellae state will be less and the required mechanical energy to break up the lamellae will decrease. This is obviously shown in figure 5.20.

The effect of the strain rate is not so conspicuous as it is in polyisoprene rubber. For example, at a certain temperature, increasing the strain rate increases the initial stress required to deform the lamellae domain. However a slight difference in stress value is found in the deformation range $\lambda = 2 - 7$ as shown in figure 5.21.

For the hysteresis, different loading-unloading processes have been performed to investigate the effect of temperature and strain rate on hysteresis.

As expected, the hysteresis decreases with increasing temperature for both materials, ENX-7086 and ENX-7256. It is found that further crystallization formation proceeds during undeforming causing pseudo plastic residual deformation (strain residuals) as shown in figure 5.22.

The effect of strain rates on the hysteresis is shown for both materials in figure 5.22. Increasing the strain rate will increase the hysteresis as well.

Three ENX-7256 ($\xi_R = 0.221$) samples were deformed up to three maximum different deformation ratios ($\lambda_f = 5, 6, 7$) after which they were unloaded. This was done to explain the behaviour of the material. As shown in figure 5.23 the three loading curves are compatible with certain ranges while each sample has a certain different residual strain after completing the unloading process. Residual strains for these, are caused by different crystallizations during unloading.

Doubts that hysteresis might have occurred due to some breakage and destruction of the sample's structure can be removed once the samples with certain residual lengths are heated. Then a full shape recovery is achieved for all samples (the sample regains its original dimensions as in the reference state).

(a)

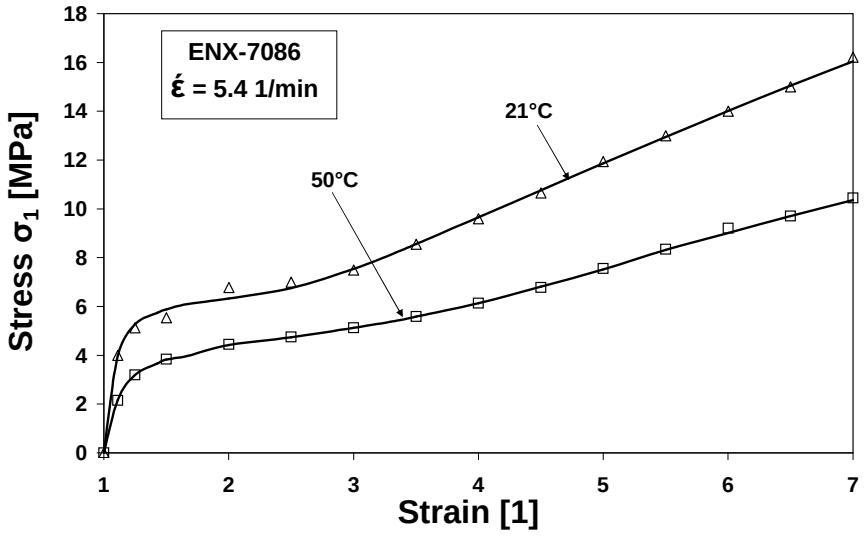

(b)

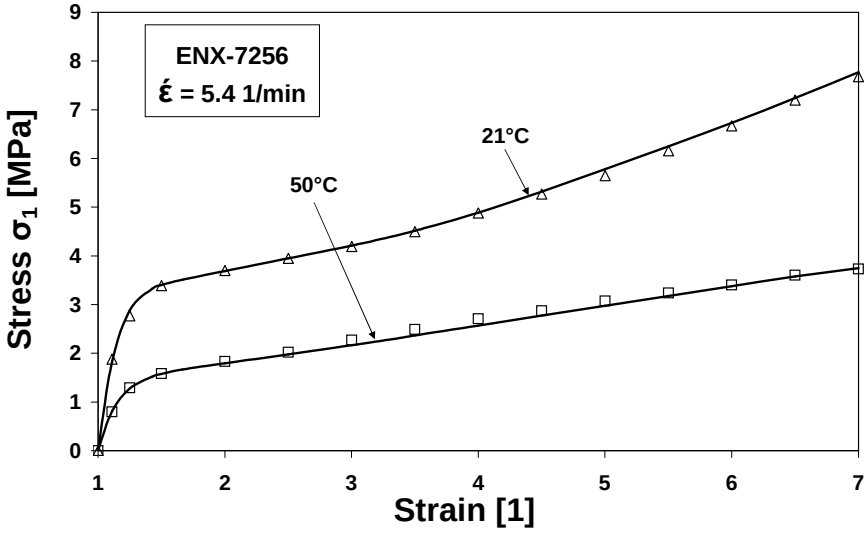

Figure 5.20: Stress-strain curves at 5.4 (min^{-1}) strain rates for, (a) ENX-7086 and, (b) ENX-7256 (theoretical results are represented by the solid line, while the experimental results by points).

(a)

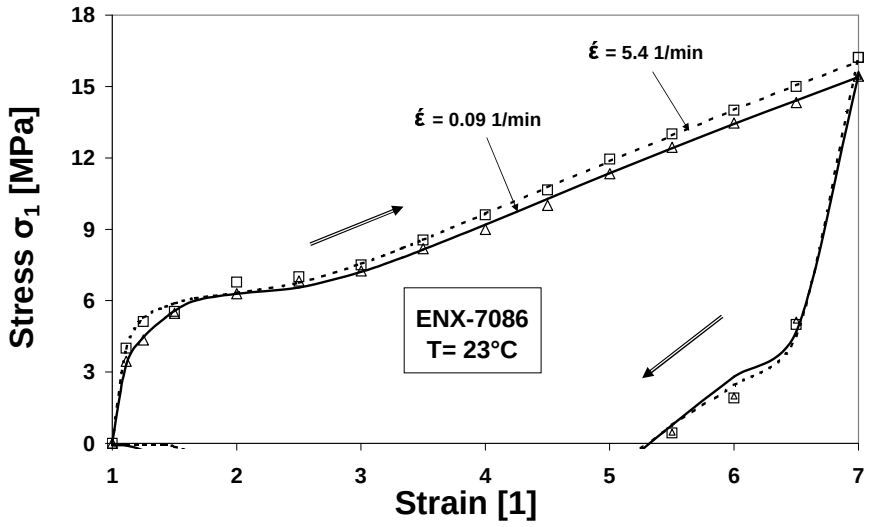

(b)

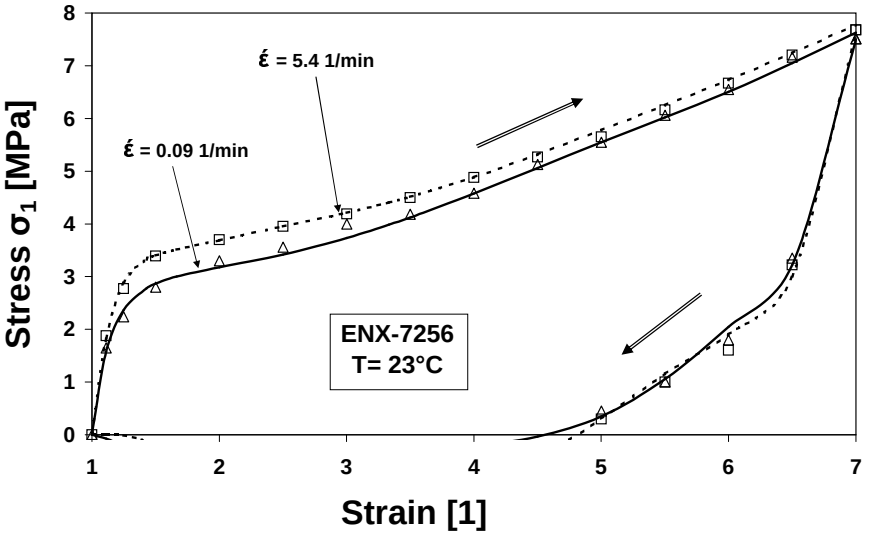

Figure 5.21: Effect of strain rate on stress-strain curves at 23°C for, (a) ENX-7086 and, (b) ENX-7256 (theoretical results are represented by solid and dashed lines, while the experimental results by points. Arrows indicate load path direction).

(a)

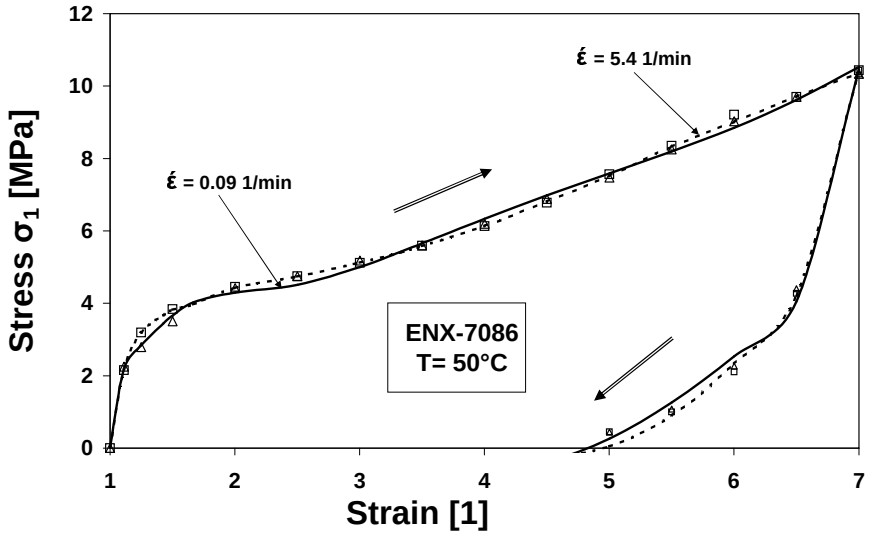

(b)

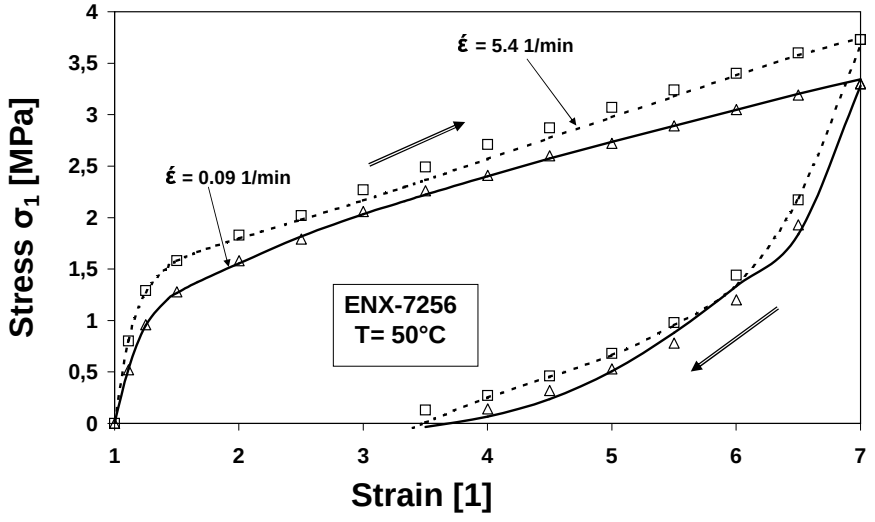

Figure 5.22: Effect of strain rate on stress-strain curves at 50°C for, (a) for ENX-7086 and, (b) for ENX-7256 (theoretical results are represented by solid and dashed lines, while the experimental results by points. Arrows indicate load path direction).

(a)

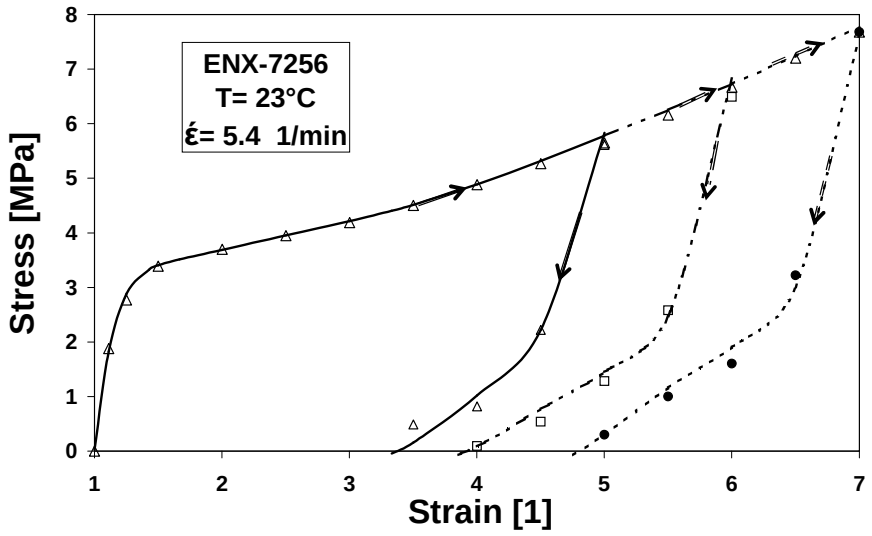

(b)

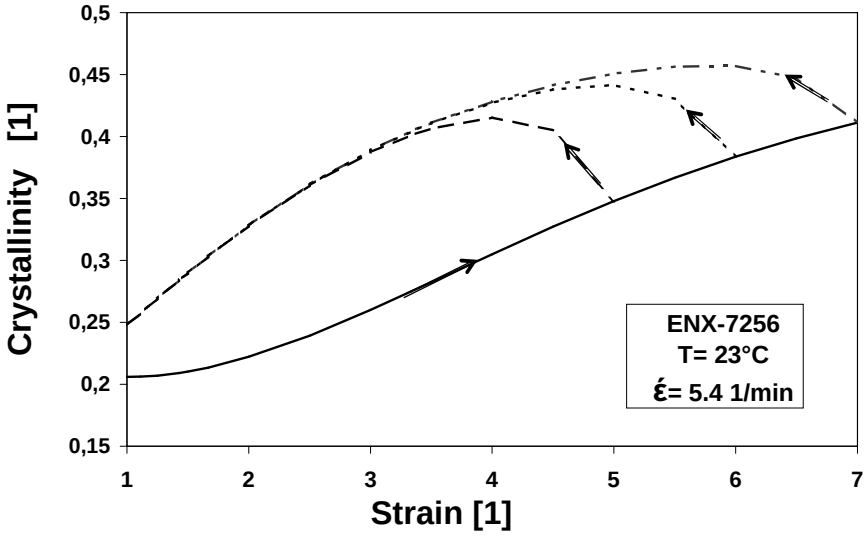

Figure 5.23: Three deformation cycles at three maximum strains for ENX-7256 at 23°C and 5.4 min^{-1} strain rate: (a) stress-strain curves (b) crystallinity-strain curves (theoretical results are represented by solid and dashed lines, while the experimental results by points. Arrows indicate load path direction).

5.2.2.4 Mooney representations

For crystallizable networks, there is frequently a downturn in the reduced stress prior to its upturn [20, 50].

Mooney-Rivlin representations of the stress-strain curves do not show the upturn in the isotherm up to this value of the deformation ratio, $\lambda_1 = 7$. However, the initiation of strain-induced crystallization is evidenced by the departure of the isotherm from linearity.

We believe if the sample had been deformed up to $\lambda_1 = 9 - 10$, then an upturn in the isotherm would be obtained. The following figures show Mooney-Rivlin representations for crystallizable chains of these two copolymer elastomers ENX-7086 and ENX-7256. This is shown in figures 5.24, 5.25, 5.26 and 5.27.

(a)

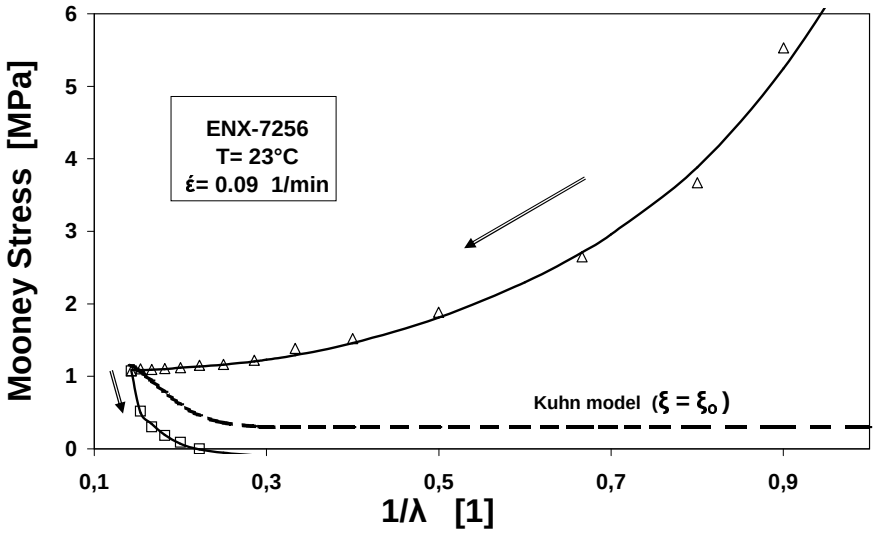

(b)

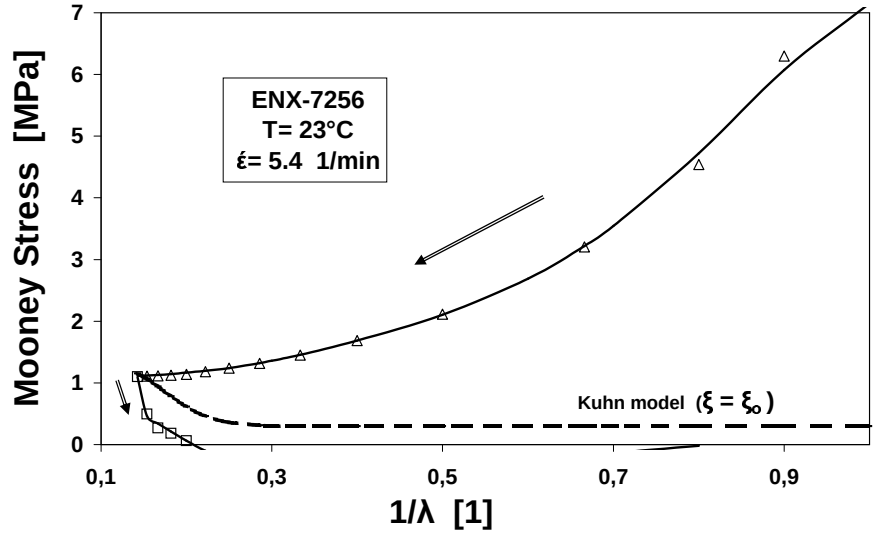

Figure 5.24: Mooney-representation of stress-strain for ENX-7256 at 23°C for, (a) low strain rate = 0.09 (min^{-1}) and, (b) high strain rate = 5.4 (min^{-1}) (theoretical results are represented by the solid line, the experimental results by points , while the dashed line is Kuhn's model when no change in crystallinity is assumed in our statistical model. Arrows indicate load path direction).

(a)

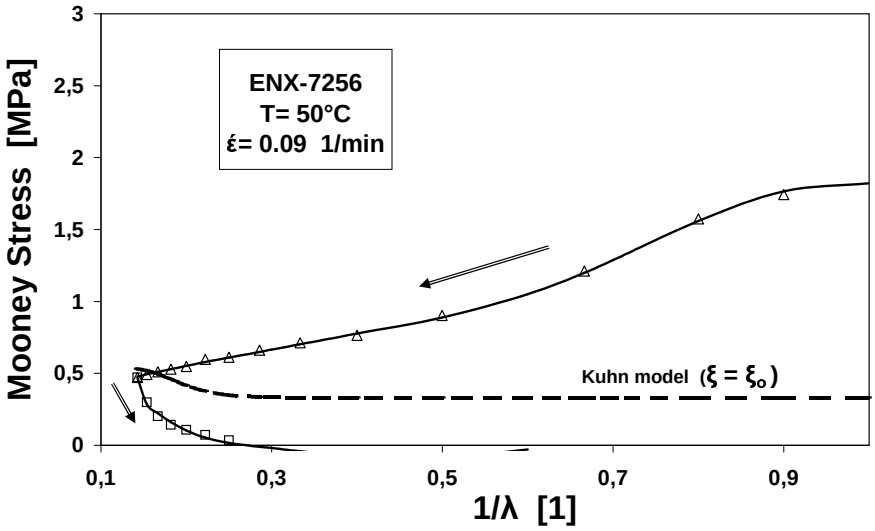

(b)

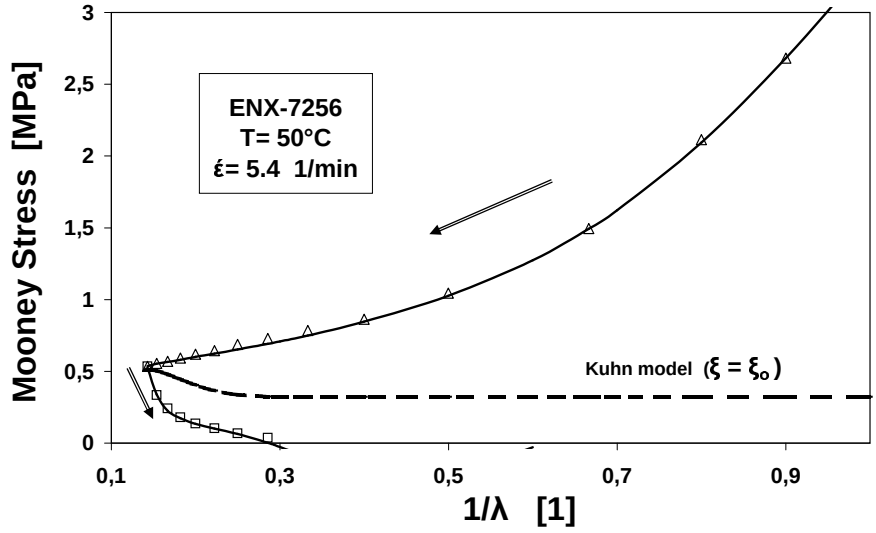

Figure 5.25: Mooney-representation stress-strain for ENX-7256 at 50°C for, (a) low strain rate = 0.09 (min^{-1}) and, (b) high strain rate = 5.4 (min^{-1}) (theoretical results are represented by the solid line, the experimental results by points , while the dashed line is Kuhn's model when no change in crystallinity is assumed in our statistical mode. Arrows indicate load path directionl).

(a)

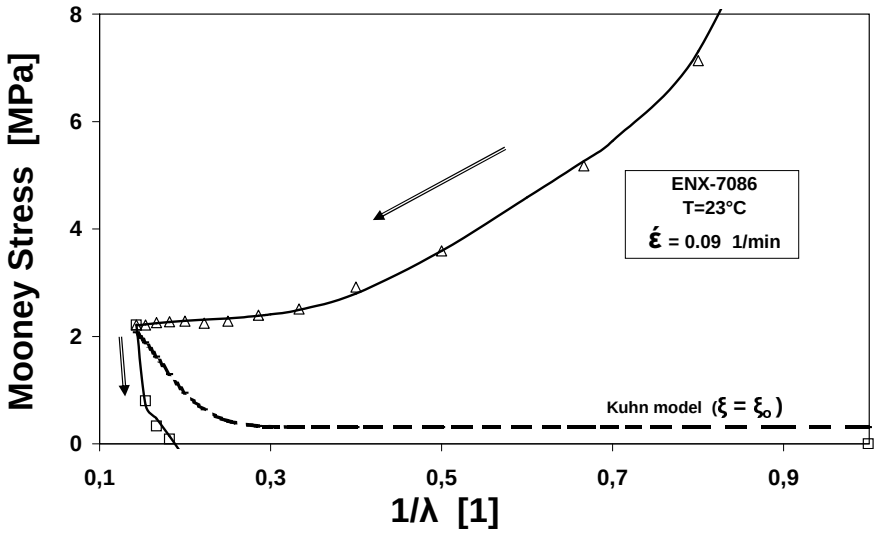

(b)

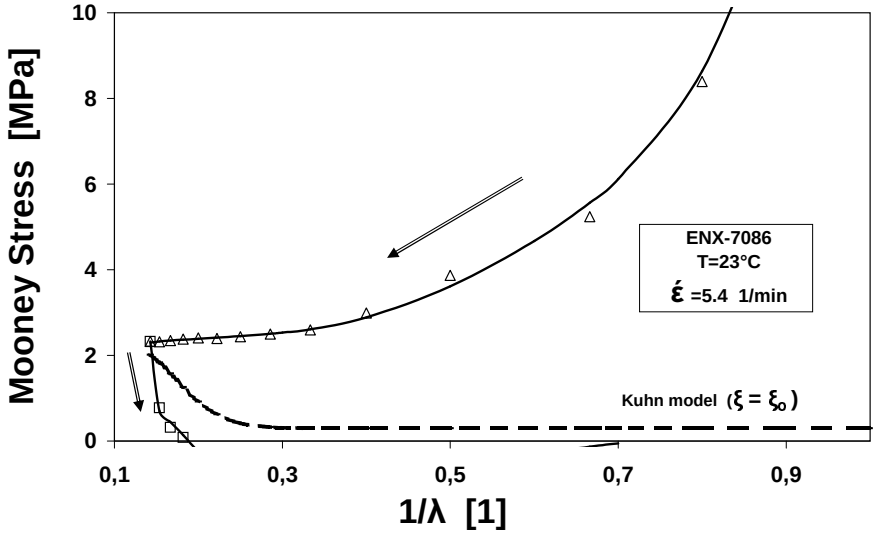

Figure 5.26: Mooney-representation of stress-strain for ENX-7086 at 23°C for, (a) low strain rate = 0.09 (min^{-1}) and, (b) high strain rate = 5.4 (min^{-1}) (theoretical results are represented by the solid line, the experimental results by points , while the dashed line is Kuhn's model when no change in crystallinity is assumed in our statistical model. Arrows indicate load path direction).

(a)

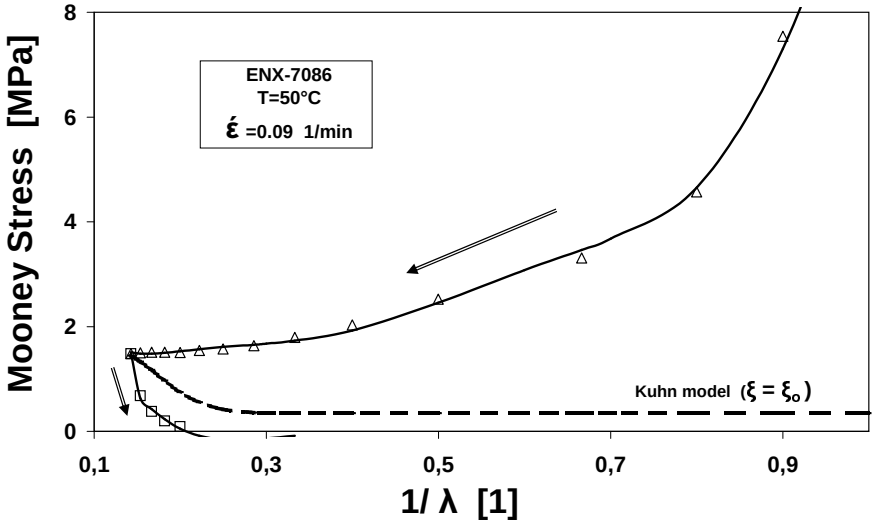

(b)

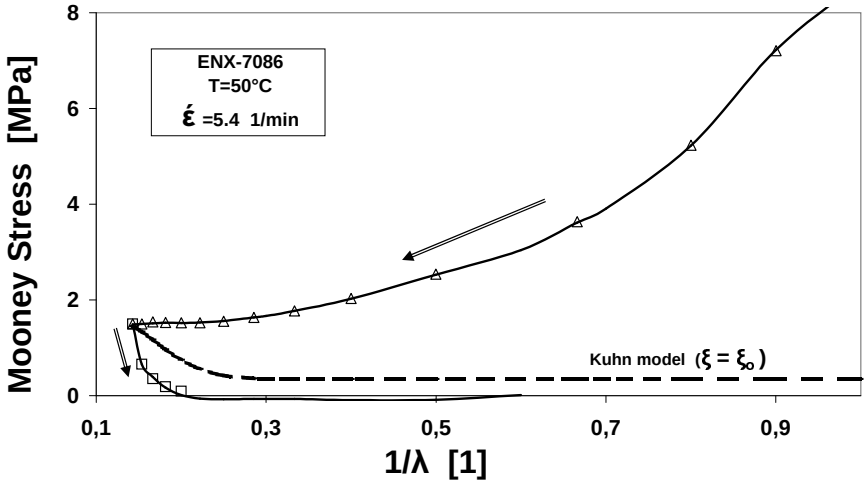

Figure 5.27: Mooney-representation of stress-strain for ENX-7086 at 50°C for, (a) low strain rate = 0.09 (min^{-1}) and, (b) high strain rate = 5.4 (min^{-1}) (theoretical results are represented by the solid line, the experimental results by points , while the dashed line is Kuhn's model when no change in crystallinity is assumed in our statistical model. Arrows indicate load path direction).

Chapter 6

Conclusions and Recommendations

6.1 Conclusions

An overview about the thermodynamics of rubber-like high polymers is obtained and simplified by employing some approximations and internal constraints. Uniaxial extension at constant temperature and constant external pressure is discussed in the thermodynamic constitutive theory. Continuum theory is inadequate to explicitly show the dependence of stress coefficients on the degree of crystallinity.

The crystallization formulation, which is based on irreversible thermodynamics, is adopted to describe the crystallization induced by deformation at different ranges of the temperature and strain rates and for uniaxial loading-unloading processes. Relaxation behaviour and its effect on crystallization kinetics has been explained in the context of the formulation of limiting cases.

The crystallization during stretching is less than that during unloading retraction processes. The important portion of crystallites, that are induced by deformation, are extended-chain crystallites that develop during the loading process, while during unloading other secondary crystallite types (folded-chain crystallites, shish-kebab structure) are formed.

Strain induced crystallization has been successfully modeled by the statistical approach in which the shortcomings of Flory's theory have been corrected. A modified Gaussian distribution is employed for chains of finite lengths to describe the end-to-end vector distribution function. The contribution of the chain to crystallinity based on affine deformation of the network of finite chain lengths

has been fully described. The dependence of stress coefficients $C_\alpha(\alpha = 1, 2)$ on the degree of crystallinity has been derived within the statistical framework. A good approximation is achieved to predict the change of volume due to the deformation-induced crystallization phenomena.

Stress-strain curves and their Mooney representations are introduced in our theory and compared to the experimental data. Stress-strain curves show high upturn with significant hysteresis. Hysteresis loops are attributed to the formation of deformation induced crystallites and their transformation.

Pseudo-plastic residual deformation is observed in the unloading retraction process as a result of the formation of the shish-kebab structures due to stress relaxation. This is obvious at high strain rates and low temperature (i.e. above the glass transition temperature). Hysteresis loops and inelastic deformation do not show up at infinitely quick or infinitely sluggish loading-unloading processes.

The upturn in the Mooney representation curves at high deformation ratios is clearly shown in polyisoprene rubber experiments. However, for ethylene-butene copolymer experiments, the initiation of strain induced crystallization is evidenced by departure of the isotherm from linearity. The modeled results are compared to experiments and fair agreement is found.

Ethylene-butene copolymer behaviour deviates from rubbery behaviour at least in the small deformation region, since they have a certain degree of crystallinity in the undeformed state. Although their stress-strain response is temperature and strain dependent in a similar way as amorphous chains e.g. polyisoprene rubber, different results have been identified theoretically and experimentally based on their difference in the degree of crystallinity in the undeformed original state.

6.2 Recommendations

From the theoretical and experimental works undertaken in this study, some recommendations can be made. It is imperative to do the further:

Our model parameters, of which some were obtained by different curve-fitting techniques, are by no means unique. Different fitting techniques will lead to equally valid results.

Extension of the theory for biaxial and triaxial stress are required to meet some industrial processes such as blow molding. This will be a complicated mission, but with the recent numerical softwares nothing is impossible. All-side compression can be included.

In-situ study of deformation-induced crystallization inside the polymer structure with enlargement of the temperature range and extension of the strain rate ranges will allow to meet the conditions for achieving tougher fibers in the fiber spinning process.

Our statistical model allows further to predict the heat effect for loading of rubbery samples. Deformation experiments should be performed inside a deformation calorimeter to study heat effects and the crystalline binding energy. Besides loading also unloading should be studied. [6, 7, 17, 19]

Appendix A

Table A.1: Parameter a: Values of adjustable constants during unloading process for polyisoprene rubber:

T[°C]	$\dot{\epsilon}$ [min^{-1}]	a_o	a_1	a_2	a_3	a_4	a_5
21	0.039	5.6740	-1.9490	0.4850	-0.0412	-2.4574	8.473×10^{-13}
21	2.340	-3.5450	0.9460	-0.2490	0.0263	2.1090	-1.623×10^{-12}
50	0.039	3.96843	-1.0537	0.2007	- 0.0119	2.6702	-3.905×10^{-13}
50	2.340	-3.4050	0.6340	-0.1602	0.0173	2.3570	-1.670×10^{-12}
80	0.039	-0.6490	0.3308	-0.077	0.0069	0.5020	-6.283×10^{-14}

Table A.2: Parameter a: Values of adjustable constants during unloading process for ENX-7256 elastomer:

T [°C]	$\dot{\epsilon}$ [min^{-1}]	a_o	a_1	a_2	a_3	a_4	a_5
21	0.09	1.4790	-0.5740	0.1220	-0.0077	-0.3370	-1.011×10^{-22}
21	5.40	-1.0872	-0.0463	0.0137	-0.0002	1.2130	-1.011×10^{-22}
50	0.09	1.9815	-0.7783	0.1638	-0.0109	-0.3180	-8.920×10^{-23}
50	5.40	6.4008	-1.725	0.3287	-0.0208	-2.6570	-1.412×10^{-22}

Table A.3: Parameter a: Values of adjustable constants during unloading process for ENX-7086 elastomer:

T [°C]	$\dot{\epsilon}$ [min^{-1}]	a_o	a_1	a_2	a_3	a_4	a_5
21	0.039	0.4650	-0.0598	-0.0063	0.0020	0.2026	-2.700×10^{-22}
21	2.340	-0.7140	0.1339	-0.0446	0.0050	0.9742	-3.350×10^{-22}
50	0.039	3.0470	-0.8500	0.17210	-0.0100	-0.9580	-2.440×10^{-22}
50	2.340	6.2010	-1.7700	0.3640	-0.0230	-2.5100	-2.150×10^{-22}

Appendix B

Table B.1: N_{force}: Values of adjustable constants during loading process for polyisoprene rubber:

T [°C]	$\dot{\epsilon}$ [min^{-1}]	b_o	b_1	b_2	b_3	b_4	b_5
21	0.039	-13.1890	87.3690	-41.5650	8.3930	-0.6110	04.41
21	2.340	10.5900	49.9100	-22.1000	4.2480	-0.2980	-99.00
50	0.039	26.2251	47.3980	25.9200	5.6220	-0.4260	-545.32
50	2.340	54.0045	-02.8210	00.9250	-0.0720	-0.0030	-485.09
80	0.039	27.1387	32.131	-13.492	2.3590	-0.1490	-959.78

Table B.2: N_{force}: Values of adjustable constants during loading process for ENX−7256 elastomer:

T [°C]	$\dot{\epsilon}$ [min^{-1}]	b_o	b_1	b_2	b_3	b_4	b_5
21	0.09	-03.8753	07.6210	0.4370	0.256	-0.041	-013.730
21	5.40	5.69468	-03.0910	4.0500	-0.2590	-0.0130	-098.531
50	0.09	32.5786	-13.1900	6.9700	-0.8330	0.0260	-533.660
50	5.40	-07.4905	22.867	-5.7880	1.1470	-0.0840	-162.590

Table B.3: N_{force}: Values of adjustable constants during loading process for ENX−7086 elastomer:

T [°C]	$\dot{\epsilon}$ [min^{-1}]	b_o	b_1	b_2	b_3	b_4	b_5
21	0.09	-16.1380	17.2300	-2.7958	0.5860	-0.0451	167.99
21	5.40	-13.15	14.817	-2.2043	0.5017	-0.0394	103.24
50	0.09	-07.536	10.643	-0.0554	0.0149	-0.0114	095.63
50	5.40	-06.543	08.7738	0.3945	0.0862	-0.0183	039.98

Bibliography

[1] Abramowitz, U.; Stegun, I. A. *Handbook of Mathematical functions*, Dover Publ:New York, 1972.

[2] Alamo, R.; Domzy, R.; Mandelkern, L. *J. Phys. Chem.* 1984,**88**, 6587.

[3] Alamo, R.; Mandelkern, L. *Macromolecules* 1989,**22**, 1273.

[4] Alamo, R.; Mandelkern, L. *Thermochim. Acta.* 1994,**238**, 155.

[5] Alts, T. *Thermodynamik elastischer Körper mit thermo-kinematischen Zwangsbedingungen-fadenverstärkte Materialien* -, Universitätsbibliothek der TUB-Abt.Publ.:Berlin, 1979.

[6] Alts, T. *Progr. Colloid and Polymer Sci.* 1979,**66**,367.

[7] Alts, T. *Progr. Colloid and Polymer Sci.* 1980,**67**, 183.

[8] Alts, T. *Arch. Mech.* 1981,**33**,4, 523.

[9] Anthony, R.L.; Caston, R.H.; Guth E. *J. Phys. Chem.* 1942,**46**, 826.

[10] Avrami, M. *J. Chem. Phys.* 1939,**7**, 1103.

[11] Avrami, M. *J. Chem. Phys.* 1940,**8**, 212.

[12] Avrami, M. *J. Chem. Phys.* 1941,**9**, 177.

[13] Bensason, S.; Minik, J.; Moet, A.; Chum, S.; Hiltner, A.; Baer, E. *J: Applied Polym. Sci.* 1996,**34**, 1301.

[14] Bensason, S.; Stepanov, S.; Chum, S.; Hiltner, A.; Baer E. *Macromolecules* 1997,**30**, 2436.

[15] Branov, V. G.; Gasparyan, K. A. *J. Polym. Sci. A-2* 1970,**8**, 1015.

[16] Christensen, R. G.; Hoeve, A. J. *J. Polym. Sci.* 1970,**8**, 1503.

[17] Dick, W.; Müller, F. H. *Kolloid-Z* 1960,**172**, 1.

[18] Ehrenstein, W. G. *Polymeric Materials Structure-Properties-Applications*, Carl Hanser Verlag:Munich, 2001.

[19] Eisele, U. *Kautschuk und Gummi Kunstoffe* 1972,**25**, 347.

[20] Erman, B.; Mark, E. J. *Structures and Properties of Rubberlike Networks* , Oxford University Press, Inc.:New York, 1997.

[21] Flory, P. J. *J. Chem. Phys.* 1947,**15**, 397.

[22] Flory, P. J.*Principles of Polymer Chemistry*, Cornell University Press:New York,, 1953.

[23] Flory, P. J. *Trans. Faraday Soc.* 1955,**51**, 848.

[24] Flory, P. J. *J. Am. Chem. Soc.* 1962,**17**, 3,223.

[25] Flory, P. J. *Trans. Faraday Soc.* 1961,**57**, 829.

[26] Gent, A. N. *Trans. Faraday Soc.* 1954,**50**, 521.

[27] Gent, A. N. *J. Polym. Sci. A* 1966,**4**, 447

[28] Gough, J. *Mem. Lit. Philos. London* 1805,**1**, 288.

[29] Göritz, D.; Kiss, M. *Rubb. Chem. Tech.* 1973,**251**, 892.

[30] Göritz, D.; Kiss, M. *Rubb. Chem. Tech.* 1986,**59**, 40.

[31] Göritz, D. *Colloid and Polym. Sci.* 1982,**260**, 193.

[32] Hay, I. L.; Keller, A. *Kolloid Z* 1965,**204**, 43.

[33] Hoffman, J. D.; Weeks, J. J. *J. Chem. Phys.* 1965,**42**, 4301.

[34] Joule, J. P. *Philos. Trans. Roy. Soc. London* 1859,**91**, 149.

[35] Kar, K. K.; Bhowmick, A. K. *J. Applied Polym. Sci.* 1997,**64**, 1541.

[36] Kar, K. K.; Bhowmick, A. K. *J. Applied Polym. Sci.* 1997,**65**, 1429.

[37] Keller, A. *Phil. Mag.* 1957,**2**, 1171.

[38] Keller, A. *Rep. Prog. Phys.* 1968,**31**, 623.

[39] Keller, A.; Machin, M. J. *J. Macromol. Sci. Phys.* 1967,**1**, 41.

[40] Kim, H.; Mandelkern, L. *J. Polym. Sci.* 1968,**A2**, 181.

[41] Kuhn, W. *Kolloid-Z* 1936,**76**, 258.

[42] Kuhn, W. *J. Polym. Sci.* 1946,**1**, 380.

[43] Liu, I-Shi *Arch. Rat. Mech. Anal.* 1972,**46**, 131.

[44] Lohmander, B.; Rittsten, U. S. *Kungl. Fysiogr. Saällsk. i Lund Förh* 1958,**28**, 45.

[45] Luch, D.; Yeh, G.S. *J. Appl. Phys.* 1972,**43**, 4326.

[46] Luch, D.; Yeh, G.S. *J. Macromol. Sci. Phys.* 1973,**B7**, 121.

[47] Mandelkern, J. *Crystallization of Polymers*, McGraw Hill Book Company:New York, ,1964.

[48] Mandelkern, J. *An Introduction to Macromolecules*, Springer-Verlag:New York, 1983.

[49] Mandelkern, J. *The Crystalline State in Physical Properties of Polymers*, Ed.,J.E. Mark, ACS Washington D.C., 1984.

[50] Mark, E. J.; Erman, B. *Rubberlike Elasticity: A molecular Primer* ,John Wiley Sons, Inc.:Canada, 1988.

[51] Meyer, H. K.; Ferri, C. *Helv. Chim. Acta* 1935,**18**, 570.

[52] Mooney, M. *J. Appl. Phys.* 1940,**11**, 582.

[53] Mukherjee, D. P. *Rubber Chem. Technol.* 1974,**47**, 1234.

[54] Müller, I. *Thermodynamik-Grundlagen der Material-Theorie*, Düsseldorf: Bertelsmann Universitätverlag, 1973.

[55] Rivlin, R. S. *Philos. Trans. Roy. Soc.* 1949,**A242**, 173.

[56] Rivlin, R. S.; Saunders, D. W. *Philos. Trans. Roy. Soc. London* 1951,**A243**, 251.

[57] Rosser, J. B. *Theory and Application of* $\int_0^z \exp(-x^2)\,dx$ *and* $\int_0^z \exp(-P^2Y^2)dy \int_0^y \exp(x^2)\,dx$, Mapleton House, Brooklyn:N.Y., 1948.

[58] Salem D.R. *Structure Formation in Polymeric Fibers*, Carl Hanser Verlag, Munich., 2001.

[59] Sanchez, I. C.M; Eby, R. K. *Macromolecules* 1975,**8**, 638.

[60] Sanchez, I. C.; Eby, R. K. *J. Res. Natl. Bur. Std-A Phys. Chem.* 1973,**77A**, 353.

[61] Schultz, J. *Polym. Mater. Sci.*,Prentice Hall, Englewood Cliffs:NJ, 1974.

[62] Semegen, S. T. *Encycolopedia of Science and Technology* 1987,**12**, 360.

[63] Semegen, S. T. *Encycolopedia of Science and Technology* 1987,**12**, 374.

[64] Smith, G. F. *Arch. Rat. Mech. Anal.* 1965,**18**, 282.

[65] Stevenson, A. *J. Polym. Sci. Phys.* 1983,**21**, 553.

[66] Stevenson, A. *Polymer* 1986,**27**, 1211.

[67] Suzuki, A.; Oikawa, H.; Murakami, K. L. *J. Macromol. Sci. Phys.* 1985,**B23**, 535.

[68] Toki, S.; Fujimaki, T.; Okuyama, M. *Polymer* 2000,**41**, 5423.

[69] Toki, S.; Hsiao, B.S.; Sics, I.; Ran, S.; Liu, L. *Polymer* 2003,**44**, 6003.

[70] Treloar, L.R.G. *The Physics of Rubber Elasticity*,**3rd ed**. Oxford:Clarendon, 1975.

[71] Truesdell, C.; Toupin, R. *The Classical Field Theories*, Springer-Verlag, 1960.

[72] Ulrich, E. *Introduction to Polymer Physics*, Springer-Verlag, 1990.

[73] Weynant, E.; Haudin, J. M.; G'Sell, C. *J. Mater. Sci.* 1980,**15**, 2677.

[74] Weynant, E.; Haudin, J. M.; G'Sell, C. *J. Mater. Sci.* 1982,**17**, 1017.

[75] Wood, L. A. *Rubber Chem. Technol.* 1966,**39**, 132.

[76] Yeh, G. S. Y. *Rubber Chem. Technol.* 1977,**50**, 863.

CURRICULUM VITAE

PERSONAL INFORMATIONS

Name:	Motasem N. H. Saidan
Addresse:	Heinheimerstrasse 86, D-64289 Darmstadt
Date of birth:	Dec 31,1974
Place of birth:	Sahab - Jordan
Nationality:	Jordanian
Marital status:	Single

EDUCATION

01/2002 - 01/2005	PhD in Engineering Technical University of Darmstadt, Darmstadt, Germany
09/1998 - 08/2001	M.Sc in Chemical Engineering University of Jordan, Amman, Jordan
09/1993 - 06/1998	B.Sc in Chemical Engineering University of Jordan, Amman, Jordan.
0/81992 - 08/1993	High school certificate, academic branch Sahab Secondary School, Sahab, Jordan

PROFESSIONAL EXPERIENCES

10/2002 - 01/2005	Research assistant German Polymer Institute-DKI, Darmstadt, Germany
07/2001 - 01/2002	Polymer laboratories supervising engineer Al-Balqa'a Applied University, Salt, Jordan
07/1998 - 08/2000	Design and sales engineer Irshidat Co. for water Treatment, Amman, Jordan
07/1997 - 09/1997	Training engineer Public Power Corporation, Ptolemais, Greece.